January 2010

Quantitative Phosphoproteomics through β-Elimination and Michael Addition with Natural Abundance and Stable Isotope Labeled Thiocholine

Meng Chen
Washington University in St. Louis

WASHINGTON UNVERSITY IN ST. LOUIS

Department of Chemistry

Dissertation Examination Committee

Richard W. Gross, Chair

Michael L. Gross

Christopher M. Jenkins

Sandor J. Kovacs

Kevin D. Moeller

Jacob Schaefer

Quantitative Phosphoproteomics through β-Elimination and Michael Addition with Natural Abundance and Stable Isotope Labeled Thiocholine

By

Meng Chen

A dissertation presented to the
Graduate School of Arts and Sciences
of Washington University in
partial fulfillment of the requirements for the degree of
Doctor of Philosophy

December 2010

Saint Louis, Missouri

ABSTRACT OF THE DISSERTATION

Quantitative Phosphoproteomics through β-Elimination and Michael Addition with Natural Abundance and Stable Isotope Labeled Thiocholine

by

Meng Chen

Doctor of Philosophy in Chemistry

Washington University in St. Louis, 2010

Professor Richard W. Gross, Chairperson

The reversible covalent phosphorylation of cellular proteins is widely believed to be the most important mechanism for the regulation of multiple signal transduction pathways in cell growth, division, and death by acting as a molecular switch at multiple nodes in metabolic networks. In this dissertation, first, a novel mass spectrometric strategy is reported that exploited the unique chemical properties of thiocholine that was introduced into protein phosphosites through alkaline β-elimination and Michael addition (BEMA), allowing the specific detection, identification and quantitation of phosphorylated serine/threonine containing peptides. Through replacement of the phosphate with thiocholine as the Michael donor, this strategy resulted in a marked increase in ionization sensitivity during ESI accompanied by enhanced peptide sequence coverage during CID. Moreover, the definitive localization of phosphorylated residues is greatly facilitated through the generation of diagnostic triads of fragment ions resulting from peptide bond cleavage and further neutral loss of either trimethylamine (-59 Da) or thiocholine thiolate (-119 Da) during CID in tandem mass spectrometric analyses such as MS^2 and MS^3. Synthesis of stable isotope labeled thiocholine enabled the quantitation of

protein phosphorylation with high precision by ratiometric comparisons. The utility of this approach was demonstrated in an intact cell system through identification of the endogenous phosphorylation sites in iPLA$_2$β during heterologous expression in Sf-9 cells. A total of 12 unique phosphopeptides and 19 phosphorylation sites were identified with the developed strategy whereas the conventional approach identified only five peptides and six phosphorylation sites. Lastly, the BEMA strategy was applied to *in vivo* tissue system for the quantitative analysis of the murine myocardial mitochondrial phosphoproteome following cardiac ischemia. A total of 36 phosphopeptides from 35 mitochondrial proteins with 50 phosphosites (37 of which were previously unknown), were identified.

Collectively, we have demonstrated β-elimination of phosphate and subsequent Michael addition (BEMA) with natural abundance and stable isotope labeled thiocholine is an effective strategy for *in vivo* quantitative phosphoproteomics of both cell-based and tissue-based systems.

ACKNOWLEDGEMENTS

First, I would like to express my sincere gratefulness to my advisor, Dr. Richard W. Gross for his support, guidance and encouragement throughout the course of my Ph.D. research. Without his inspiring wisdom and endless enthusiasm the completion of this dissertation wouldn't have been possible. It has been such a unique experience which I will cherish for the rest of my life.

I would like to convey my special thanks to Dr. Michael L. Gross and Dr. Kevin D. Moeller for providing invaluable help and advices for this work. I also want to thank other members of my dissertation committee: Dr. Jacob Schaefer, Dr. Sandor J. Kovacs and Dr. Christopher M. Jenkins for their comments and suggestions.

I would like to thank the following individuals either current or part members of the Gross' lab for their tremendous help and friendship which gave this lab a feeling of warmth like family: Xiong Su, Jingyue Yang, Jackie Snider, Christopher Jenkins, Sung Ho Moon, Ari Cedars, Omar El Ghazzawy, Harold Sims, Kui Yang, David Mancuso, Shaoping Guan, Wei Yan, Wei Shen, Michael Kiebish, Hui Jiang, Andee Pacheco, Debbie Warsmer, John Kelly, Beverly Gibson, Xianlin Han, Hua Cheng, Zhongdan Zhao, Youchun Zeng, Gang Sun.

I would like to thank the Department of Chemistry for providing the opportunity and financial support for me to pursue my Ph.D. here in St. Louis. I want to thank all the staff members, especially Dr. Edwin Hiss for his help through the years.

And I would like to take this opportunity to thank my parents, Chufan Chen and Guiling Qin, my sister, Qi Chen, and my brother, Lei Chen for their love, support and the

faith they always have in me, especially when I was going through some of the toughest times in my life. I also want to thank my parents-in-law, Siguang Yu and Yanhong Wu for their care and support.

Last but certainly not least, I would like to dedicate my thesis to my best friend, love, soul mate, beautiful wife, Han Yu who is always there for me, believing in me wholeheartedly and gives me love, hope, courage and strength. Without her, I simply couldn't have accomplished this thesis.

TABLE OF CONTENTS

CHAPTER 3

Identification of Endogenous Phosphorylation Sites of iPLA$_2$β from Sf-9 Cells with and Without Thiocholine Modification

CHAPTER 4

Quantitative Analysis of Alterations in the Myocardial Mitochondrial Phosphoproteome Induced by Cardiac Ischemia Assessed Using β-Elimination and Michael Addition with Light and Heavy Thiocholine

CHAPTER 5

Appendix

LIST OF SCHEMES

LIST OF TABLES

LIST OF FIGURES

ABBREVIATIONS

ATP	adenosine-5'-triphosphate
BEMA	β-elimination and subsequent Michael addition
α-CHCA	α-cyano-4-hydroxycinnamic acid
CE	capillary electrophoresis
CI	chemical ionization
CID	collision induced dissocation
$cPLA_2s$	cytosolic phospholipases A_2
2,5-DHB	2,5-dihydroxybenzoic acid
DMSO	dimethyl sulfoxide
DNA	deoxyribonucleic acid
DTNB	5,5‘-dithiobis(2-nitrobenzoic acid)
DTT	dithiothreitol
ECD	electron capture dissociation
EI	electron ionization
ESI	electrospray ionization
ETC	electron transport chain
ETD	electron transfer dissociation
FA	formic acid
FAB	fast atom/ion bombardment
FDR	false discovery rate
FT-ICR	Fourier transform-ion cyclotron resonance
GC	gas chromatography

HPLC	high-performance liquid chromatography
HPLC-ESI-MS^2/MS^3	high-performance liquid chromatography-electrospray ionization tandem with mass spectrometry
IMAC	immobilized metal affinity chromatography
$iPLA_2\beta$	calcium-independent phospholipase $A_2\beta$
iTRAQ	isobaric tags for relative and absolute quantitation
LTQ-Orbitrap	linear ion trap in tandem with Orbitrap
MALDI	matrix-assisted laser desorption ionization
MALDI-TOF/TOF	matrix-assisted laser desorption ionization tandem with time of flight
mRNA	messenger ribonucleic acid
MS	mass spectrometry
MS^2	tandem mass spectrometry MS/MS
MS^3	tandem mass spectrometry MS/MS/MS
MWCO	molecular-weight cutoff
NMR	nuclear magnetic resonance
PEP	posterior error probability
PITC	phenyl isothiocyanate
PKA	protein kinase A
pS/pT	phosphorylated serine/threonine
PTC	phenyl thiocarbamyl
PTH	phenyl thiohydantoins
PTM	posttranslational modification

SA	sinapic acid
SCX	strong cation exchange chromatography
SDS-PAGE	sodium dodecyl sulfate polyacrylamide gel electrophoresis
SF-9 cells	spodoptera frugiperda cells
SILAC	stable isotope labeling with amino acids in cell culture
SIMS	secondary ion mass spectrometry
SNL	signature neutral loss
$sPLA_2s$	secretory phospholipases A_2
SVM	support vector machine
TCH	Thiocholine
TFA	trifluoroacetic acid
TOF	time-of-flight
XIC	extracted ion chromatography

CHAPTER 1

INTRODUCTION

Posttranslational modifications (PTMs) of proteins are covalent transformations of terminal residues or side chains of the polypeptide backbone that occur after protein synthesis from mRNA, encoding each protein's primary sequence [1]. The chemical repertoire of protein functional diversity is greatly expanded through the addition of specific functional groups (e.g., phosphorylation, acetylation, glycosylation) that confer novel chemical properties to the primary amino acid sequence encoded by the mRNA transcribed from DNA. These PTMs serve multiple functions to facilitate enzyme-substrate recognition, catalytic efficiency, and the subcellular localization of the protein and the cadre of associated proteins that allow adaptive responses to cellular perturbations [2-5]. Currently, more than 200 different PTMs have been discovered located at tens of thousands of individual sites; they greatly expand the chemical diversity encoded by each organism's genomic structure [6].

Protein phosphorylation is the addition of a phosphate group to the side chain of an amino acid residue through esterification. This process is catalyzed by a class of enzyme,

called protein kinases. Phosphorylation is typically a reversible post translational modification because cells contain numerous phosphatases that can reversibly remove the phosphate moiety [7]. Collectively, the reversible cycle of phosphorylation and dephosphorylation is a central determinant of cellular metabolic flux through exploiting the differential catalytic or regulatory properties of the modified entity. Phosphorylation has historically been considered to be the most ubiquitous and important post translational modification of proteins; phosphorylation facilitates multiple changes in cellular regulation and signaling thereby promoting key chemical alterations that lead to effective adaptive regulation. In the human genome, about 2% of the encoded proteins are dedicated to maintaining the appropriate phosphorylation state of targeted proteins through the actions of a wide array of protein kinases and phosphatases [8-9]. Moreover, approximately 30% of all known proteins in cells are rapidly and reversibly phosphorylated to various extents during pathophysiologic perturbations to facilitate cellular adaptation [10-12].

Although phosphorylation has been demonstrated to occur on the hydroxyl group of serine, threonine, tyrosine, the carboxylic moiety of aspartic acid and glutamic acid [13]; the thiol group of cystine [14] or on basic amino acid residues such as arginine, lysine and histidine [15-16]; reversible phosphorylations on serine, threonine and tyrosine residues are of the greatest importance and collectively account for almost 99% of the protein phosphorylation in eukaryotic cells [17]. Variations in the phosphorylation state of proteins, often accompanied by changes in their tertiary structures, lead to alterations in their

enzymatic activities and provide essential clues to the molecular mechanisms mediating cellular activation after receptor stimulation or cellular adaptations reflecting fluctuations in the nutritional state, cellular environment and metabolic history of the cell [18]. The reversible covalent phosphorylation of cellular proteins is widely believed to be the most important mechanism for the regulation of multiple signal transduction pathways in cell growth, division, and death by acting as a molecular on/off switch at multiple nodes in metabolic networks [19-21].

Therefore, comprehensive protein-phosphorylation studies that identify the phosphosites and the level of phosphorylation have been conducted, leading to the growth of a new field termed “Phosphoproteomics”. More specifically, the total chemical characterization of phosphoproteins includes the detection, identification and quantitation of component phosphopeptides as well as the localization of the exact residues that are phosphorylated and the patterns of phosphorylation that are manifest in each protein.

Historically, labeling of proteins with radioactive phosphate (^{32}P) has typically been recognized as one of the “gold standards” for the detection of phosphorylated proteins and the identification of changes in protein phosphorylation. In this approach, ^{32}P is introduced into phosphoproteins to enable detection usually by scintillation counting or autoradiography. This technique was first introduced by Rall and Sutherland in 1956 [22]. There are generally two categories of ^{32}P radiolabeling: *in vivo* (within the living) and *in vitro* (within the glass) involving different approaches. In living systems, the ^{32}P labeled orthophosphate is transported across cells and converted into [γ-^{32}P]-ATP that serves as the

phosphate donor. The radioactive ^{32}P orthophosphate can be delivered either in cell culture experiments (by inclusion into the media), through perfusion in isolated organ systems or by introduction into live animals, and by other more specialized methods. Next, radiolabeled phosphates are transferred to amino acid targets (typically hydroxyl) by various endogenous protein kinases [23-24]. In contrast, *in vitro* systems require [γ-^{32}P]-ATP and the addition of exogenous protein kinases that are suitable for substrate protein or peptides contained in the target systems [25]. In both cases, ^{32}P labeled proteins are typically separated by sodium dodecyl sulfate polyacrylamide gel electrophoresis (SDS-PAGE) according to their electrophoretic mobilities, which are a function of their respective molecular weights. Traditionally these radiolabeled phosphoproteins are fixed in the gel prior to detection by autoradiography. Comparative quantitation of protein phosphorylation is achievable through the ratiometric comparisons of protein mass and ^{32}P radioactivity as revealed by Cerenkov radioactivity counting of excised bands [26].

Radiolabeling is a very sensitive method in terms of the detection of phosphoproteins. There are, however, several disadvantages associated with it. First, large amounts of ^{32}P are required to detect the phosphorylation of low abundance proteins owing to isotopic dilution from endogenous unlabelled ATPs; second, the success of labeling depends on the relative rate of phosphorylation and dephosphorylation as well as the incubation time; third, phosphosite localization requires mutagenesis, currently making it extremely difficult for phosphosite determination in individual proteins and rendering the large scale high throughput analysis of the phosphoproteome through this approach an intractable problem

[17, 27].

Fluorescence labeling is a sensitive nonradioactive alternative to ^{32}P radiolabeling with a detection limit at the nanogram level [28]. The fluorophore, which is a functional group that can absorb energy of a specific wavelength (absorption spectrum) and re-emit the energy at a different but specific wavelength (emission spectrum) to identify a molecule of interest that is either covalently [29] or non-covalently [30] introduced into phosphoproteins. Fluorescence labeling has been traditionally coupled with SDS-PAGE where proteins are separated, stained, detected and quantitated with fluorescence spectroscopy [31].

Phosphoproteins can also be detected by using immunoblotting methods [32], which employ high-quality antibodies derived specifically for phosphorylated serine, threonine and tyrosine residues. This technique will be discussed later in the enrichment of phosphopeptides.

The strategies discussed above only provide an indication of the presence of phosphoproteins and not information on the specific location or the extent of phosphorylation of specific residues at each phosphosite. In early studies, Edman degradation was the classic technique to locate the site of the phosphorylated amino acid residues and could yield semi-quantitative results when coupled with HPLC. This technique of stepwise degradation was first introduced by Pehr Edman in 1950 [33] who demonstrated that phenyl thiohydantoins (PTH) derived from amino acid could be used to cleave sequentially amino acids from the N-terminus of a protein or peptide. The strategy

was later named “Edman Degradation”, in his honor, and was used for decades to sequence proteins and peptides. Under the mild alkaline conditions of this method, the N-terminus of a peptide chain reacts with phenyl isothiocyanate (PITC) to form a phenylthiocarbamyl (PTC) derivative. Next, the first peptide bond from the N-terminus is cleaved under acidic conditions to give rise to a thiazolinone amino acid derivative. This thiazolinone derivative is isolated and transformed into the more stable isomer 3-phenyl-2-thiohydantoin (PTH)-amino acid derivative, which can be identified and quantitated by HPLC through comparing its elution profile with that of the standard PTH-amino acid derivative. The shortened peptide subsequently undergoes additional cycles of this series of reactions. Thus, by the identification of each individual PTH-amino acid derivative, the sequence of the peptide is established from the N-terminus. Further, phosphorylated serines, threonines and tyrosines can be located within the peptides.

Even under favorable conditions, Edman degradation can sequence a polypeptide chain that contains only 30 to 50 amino acids owing to the deteriorating overall yield after each cycle of reactions. Thus, useful information typically can only be obtained for only 15-20 residues [34]. It also requires pure peptides or proteins for unambiguous localization of each amino acid. Other limitations include modest sensitivity at the picomole level and time-consuming reaction and analysis processes [17]. Although automation is achievable through the development of automatic sequenators [35], many N-termini of proteins are blocked, precluding Edman degradation of these residues.

Unlike the techniques mentioned above, mass spectrometry (MS) is a

multi-dimensional technique that is extremely sensitive, amenable to high-throughput analyses, and can integrate protein phosphorylation detection, localization and quantitation in a single experiment. Accordingly, mass spectrometry has become the state-of-the-art technology for global phosphoproteomics in large part owing to the rapid advances in the development of instrumentation, bioinformatics platforms, and application paradigms that have revolutionized the field of MS during the past decade.

For MS studies, typically three major steps are employed in the analysis of a sample: 1) The generation of the ions in the ion source; 2) The selection and separation of the ions in the mass analyzer; 3) The detection and visualization of the ions by the ion detector that is coupled with data acquisition and analysis programs.

In the ion source, energy is transferred to the sample molecules, facilitating the molecules to escape from its original phase, either liquid or solid, into the gas phase. Neutral sample molecules are turned into charged ions through different mechanisms, such as protonation/deprotonation, electron rejection/capture or adduct formation, usually involving gas-phase reactions during the ionization process. Ion sources fall into two main categories, liquid-phase sources and solid-phase sources, based on the different phases of the samples and their surrounding matrices.

Traditional ion sources include Electron Ionization (EI) [36-37], Chemical Ionization (CI) [38], Fast Atom/Ion Bombardment (FAB) [39], Secondary Ion Mass Spectrometry (SIMS) [40-41] and other derivatives of these processes. However, these ion sources are not suitable for large biomolecules, such as proteins and peptides; because

either insufficient energy is provided for sample vaporization or sublimation, or excessive amounts of energy are applied that often result in extensive fragmentation and the loss of information from the intact analytes of interest. The development of Electrospray Ionization (ESI) [42] and Matrix-assisted Laser Desorption Ionization (MALDI) [43] has revolutionized the analysis of a wide variety of molecules, which has been recognized through the award of Nobel Prizes in Chemistry in 2002 to John Fenn and Koichi Tanaka. During electrospray, a strong electric field is applied to the solvent-containing analytes of interest; these are passed through a heated capillary and dispersed into gas phase to form a charged fine aerosol. The organic solvents, such as methanol, isopropanol and acetonitrile are quickly vaporized under inert gas, such as nitrogen, shrinking the sizes of droplets which in turn increases the droplet surface charge density and causes the droplets to divide owing to a stronger coulombic force than the cohesion force. Subsequently, the droplets go through shrinking cycles, and gas-phase ions are eventually formed either through desorption from the charged droplet surface [44] or until the droplet contains a single charged analyte molecule [45]. During the ionization process in MALDI, pulses of intense laser are shot onto a thin solid mixture of matrix molecules and analytes. These matrix molecules, such as alpha-cyano-4-hydroxycinnamic acid (α-CHCA), sinapic acid (SA) and 2,5-dihydroxy benzoic acid (2,5-DHB), strongly absorb laser wavelengths and transfer the energy absorbed from the laser shot to the analytes, causing the sublimation of matrix molecules and the formation of a matrix plume where analyte molecules are ionized through gas-phase proton transfer [46].

After the ions are formed, they are transferred to the mass analyzer and separated according to their mass-to-charge ratio (*m/z*) through different schemes. A magnetic sector analyzer separates ions according to their respective momentums [47]; a quadruple analyzer determines *m/z* according to ion stability path [48]; kinetic energy is measured and differences are compensated by using an electrostatic sector analyzer [49]; a time-of-flight (TOF) analyzer measures ion flight time (i.e., velocity) [50]; whereas a quadruple ion trap [51], a Fourier transform-ion cyclotron resonance (FT-ICR) [52] and an Orbitrap analyzer all rely on ion orbital frequencies and restoring potentials to determine *m/z* [53]. Different mass analyzers can be coupled together to form hybrid instruments that access the advantages of each individual analyzer, such as accurate mass analyses that are routinely performed today using time-of-flight (TOF), Fourier transform ion cyclotron (FT-ICR) and Orbitrap mass analyzers.

Another important function of coupled or hybrid instrumentation is to perform tandem mass spectrometry (MS/MS, or MS^2) on the ions of interest. The first step is to obtain the information regarding the ions of interest through scanning with one mass analyzer. Then an ion of interest (precursor ion) is selected by the first mass analyzer, fragmented through gas-phase collisions with air or other inert gases in the collision cell, which may also be a mass analyzer [54]. The fragment ions, or product ions, resulting from the collision are subsequently analyzed by a second mass analyzer to reveal the structural information of the analyte [55]. Ion trap analyzers are capable of performing tandem mass spectrometric analyses independently, in time rather than in space, but their mass accuracy

is limited especially by current technology [51].

To achieve better sensitivity when analyzing complex samples, MS is often coupled with a separation technique, such as gas chromatography (GC) [56-57], high-performance liquid chromatography (HPLC) [58] or capillary electrophoresis (CE) [59-60]. The analytes are separated according to their different physical or chemical properties, and they are either directly introduced into the mass spectrometer for analysis (on-line) or collected and analyzed off-line.

Despite possessing advantages such as high sensitivity, high-throughput, high tolerance of sample impurity and the ability to carry out the detection, identification, localization and quantitation of phosphorylation sites simultaneously, mass spectrometric procedures for the analysis of protein phosphorylation still have considerable limitations owing to the intrinsic chemical properties of phosphorylated proteins. Peptides containing phosphorylated serine/threonine (pS/pT) residues rapidly undergo neutral loss of phosphoric acid (H_3PO_4) through cyclo-elimination occurring in low-energy collision-induced dissociation (CID); this reaction leads to loss of sequence coverage [61]. In addition, typical signaling proteins undergo reversible phosphorylation and are often present in extremely low abundance. Furthermore, protein phosphorylation patterns, which are of great biological significance, are heterogeneous and extremely difficult to determine. Phosphorylated peptides generally have poor ionization efficiencies in the positive ion mode due to the acidity of the phosphate group and ion suppression [17]. Therefore, various methods are available to improve the analysis of the phosphoproteome from

different perspectives.

Precursor-ion scanning utilizes the signature fragment ion of phosphate (PO_3^-, *m/z* = 79) from phosphopeptides during CID in the negative-ion mode [62-63]. This scanning mode is highly effective for the identification of phosphopeptides. Nonetheless, the exact location of the phosphorylated residue cannot be determined in these studies using the negative-ion mode. Phosphosite localization usually requires a separate sample run under acidic conditions in the more sensitive positive-ion mode. Another scanning mode that takes advantage of the neutral loss of phosphoric acid is neutral-loss triggered in an MS^3 experiment with an ion trap mass analyzer [64-65]. As mentioned above, the neutral loss of H_3PO_4 will prevent the cleavage of the peptide bond in CID. However, data-dependent MS^3 was employed to analyze further fragment ions that are 98 Da less than the precursor ions to reveal sequence information. Multistage activation utilizes a similar approach to induce the fragmentation of precursor ions and the target fragment ions resulting from the neutral loss of phosphoric acid in one single experiment [66-67]. This effectively combines product-ion spectra from MS^2 and MS^3 into a single spectrum. The actual utility of both neutral-loss triggered MS^3 and multistage activation in large-scale phosphoproteome analysis is debatable compared to utilizing a high-mass accuracy instrument employing conventional strategies [68].

The above-mentioned neutral loss of H_3PO_4 is associated with commonly employed collision induced dissociation (CID). In CID, peptide fragmentation depends on the protonation of the peptide-bond nitrogen and an increase in vibrational energy that a

peptide gains through the collision with inert gas (e.g., helium, argon) that allows it to traverse the energy barrier required for the cleavage of a peptide bond. Thus, the fragmentation behavior of a peptide in CID depends on its specific sequence and the posttranslational modifications (PTMs) [61]. Other fragmentation methods can circumvent the unwanted neutral loss of phosphate; these include electron-capture dissociation (ECD) [69] and electron-transfer dissociation (ETD) [61]. In ECD, proteins and peptides that are bearing multiple positive charges from the protonation process during electrospray react with electrons in a Fourier transform ion cyclotron resonance (FT-ICR) mass spectrometer causing fragmentation of the peptide backbone in a series of radical-induced reactions that are independent of the nature of the amino acid residues, leaving the PTMs intact [70-71]. However, the utility of ECD is somewhat limited because that it can only be coupled with FT-ICR, which is more expensive to build and maintain than any other mass spectrometer since the storage of the electron requires static electric and magnetic fields [72]. On the other hand, in the recently developed method of ETD, an electron is transferred to a peptide through the gas-phase reaction between the peptide molecule and an anionic compound that serves as an electron carrier. The electron carrier usually has a very low electron-affinity; it is often an anion that can easily lose the extra electron; an example neutral is anthracene. Similar to ECD, ETD leads to the generation of c and z fragment ions instead of the b and y ions that form in CID, and the phosphate group on the amino acid residue remains intact [73-74]. ETD can be coupled with routine mass spectrometers such as quadruple ion trap and linear ion trap, expanding its utility in phosphoproteomics.

However, doubly charged peptides generally have poorer sequence coverage than do high-charge peptides in ETD because they undergo non-dissociative electron transfer [75] and, thus, must usually be coupled with traditional CID for improved results [76-77].

Because the abundance of phosphoproteins is low, efforts have been focused on the development of enrichment strategies. Immunoblotting is a very sensitive method for the detection of phosphoproteins as discussed earlier. Similarly, antibodies have been utilized to enrich phosphorylated proteins and peptides found in a complex mixture. Although antibodies are available specifically for phosphorylated serines, threonines and tyrosines [78-80], those for phosphorylated serines and threonines are less effective than those for phosphorylated tyrosines. Numerous studies on phosphorylated tyrosine residues involved in signal transduction pathways show, through enrichment by immunoprecipitation and subsequent analysis, improved signal to noise ratio. [81-82].

Immobilized metal affinity chromatography (IMAC) is used to enrich phosphopeptides based on the affinity interaction between the phosphate group and metal ions (e.g., Fe^{3+}, Ga^{3+}) that are immobilized on a stationary phase [83-84]. For improved selectivity of IMAC, methyl esterification was adapted to reduce the undesirable binding of acidic/electron rich residues [85]. However, the identification of phosphopeptides is complicated by incomplete and or nonspecific methyl esterification [86]. Other enrichment strategies, such as utilizing titanium dioxide (TiO_2) [87] and zirconium dioxide (ZrO_2) [88] have shown better specificity towards phosphopeptides. Titanium dioxide is the most commonly employed enrichment resin. This strategy is based on the affinity between the

phosphate group and titanium dioxide through formation of a bridging bidentate surface complex [89]. It can be used offline in the form of a micro-column [86], or coupled with traditional HPLC columns in an online multidimensional liquid chromatography setting [90]. Strong cation exchange chromatography (SCX) is another widely used enrichment method that does not have specificity for phosphopeptides compared to other enrichment strategies but can considerably reduce sample complexity. The reduction in sample complexity results from the early elution of phosphorylated peptides owing to their low charge state in acidic conditions. The majority of the tryptic peptides are doubly (+2) or triply (+3) charged under these conditions and, thus, elute later than their phosphopeptide counterparts. Strong cation exchange chromatography is usually utilized in tandem with other enrichment or separation techniques, such as TiO_2 or reverse-phase (RP) chromatography either offline [91] or online [92].

Because phosphorylated tyrosines comprise only approximately 0.1% of the total phosphorylation present in proteins and can be effectively enriched through immunoprecipitation with commercially available antibodies as mentioned above, focus has been centered on improved strategies for analysis of phosphorylated serines (~90%) and threonines (~10%). Chemically replacing the phosphate on serine or threonine with other functional groups via alkaline induced β-elimination and subsequent Michael Addition (BEMA) is one such approach that was first introduced by Myers et al in 1986 [93]. Phosphorylated tyrosines are stable under alkaline conditions becuase the β-proton is on the benzene moiety and is not readily eliminated [27]. The major limitation of this

strategy is the non-specific β-elimination reaction that occurs on other residues besides phosphorylated serine and threonine. Residues such as alkylated cysteines, O-glycosylated serines and threonines as well as non-phosphorylated serines and threonines undergo β-elimination and generate the same product residues of dehydroalanine or β-methyldehydroalanine as phosphoserine and phosphothreonine, respectively, and, therefore, non-specific loss cannot be differentiated from a genuine phosphosite [94]. This was solved by the introduction of catalytic specificity through the use of a bivalent metal hydroxide. More specifically, through employing barium hydroxide ($Ba(OH)_2$) as the catalyst for the β-elimination of the phosphate group, β-elimination of alkylated cysteines or O-glycosylated serines and threonines occur two orders of magnitude more slowly than β-elimination from pS/pT and non-phosphorylated serine and threonine residues are unaffected [95].

The BEMA strategy not only eliminates the unfavorable neutral loss of H_3PO_4 but also increases the ionization ability of the phosphorylated peptides by removing the acidic phosphoric acid side chain. Furthermore, various functional groups can be incorporated into the phosphopeptides to act as molecular handles to achieve different goals. Affinity pairs can be applied in the BEMA reaction, in which one is attached to the side chain (e.g. biotin) while the other serves as stationary phase for the enrichment, such as avidin [96]. Alternatively, a perfluorinated tag and fluorous solid phase extraction columns can be employed [97]. The functional group could also serve as a resource for characteristic fragment ions in tandem mass spectrometry analysis, such as using

2-dimethylamino-ethanethiol as the Michael donor followed by hydrogen peroxide oxidation to generate a thioester ethanesulfoxide derivative that generates a characteristic fragment ion in the low-energy CID mode [98]. The utilization of cysteamine as the nucleophile in BEMA can even convert the formally phosphorylated peptides into a substrate of trypsin so that phosphorylation information is obtained at the time of enzymatic proteolysis [99]. The utility of the BEMA strategy is further extended through stable isotope labeled Michael donors, which together with their natural abundance counterparts, enable comparative quantitative phosphoproteome analysis [100-102].

Stable isotope labeling with amino acids in cell culture (SILAC) is a common strategy for comparative quantitative phosphoproteomics [103-105]. SILAC utilizes cells grown in separate media conditions to label cellular proteins with light (natural abundance) and heavy (isotope labeled) amino acids. Then the proteins from two different cell culture conditions are mixed together at a normalized total protein content, trypsinized, separated using HPLC and analyzed by mass spectrometry. The same phosphopeptides labeled with light and heavy amino acids will elute from the HPLC column at the same time, and their peak intensity ratio indicates the different extents of phosphorylation of this peptide in two different cell states. Thus, the quantitation information is obtained at the molecular ion level. However, the obvious limitation of SILAC is that it cannot be used to conduct quantitative phosphoproteome analysis in tissue samples; these analyses are more likely to reveal the biological significance of changes in protein phosphorylation in living animals.

Isobaric tags for relative and absolute quantitation (iTRAQ) is also a useful labeling

technique for multiplexed quantitative phosphoproteomics [106-107]. Peptides digested from the proteins of up to four different biological states are modified with different isobaric tags at their N-termini. The same phosphopeptides from different states are indistinguishable from one another in a molecular ion scan because they possess the same *m/z*. However, during the tandem mass spectrometric analysis, the isobaric tags can produce different reporter fragment ions in the low-mass region (*m/z* = 114-117). Therefore, by comparing the relative abundances of the reporter ions, the phosphorylation change of this peptide is revealed. iTRAQ can be used in the analysis of tissue samples because the modifications are at peptide level. However, given that the quantitation is achieved at the MS^2 level, the sensitivity of this strategy is limited and could lead to large run-to-run deviations and, thus, poor reproducibility.

With the insight to develop a BEMA based technology with a molecular handle that possesses strong nucleophilicity, the ability to increase peptide ionization efficiency and a unique structure that would produce characteristic fragment in tandem mass spectrometric analysis, we demonstrate in the first part of this thesis, the development of a novel strategy employing the unique chemical properties of the quaternary amine present in thiocholine (2-mercapto-*N*,*N*,*N*-trimethyl-ethanaminium) in conjunction with alkaline β-elimination and Michael addition (BEMA) reactions for the specific detection, identification and quantitation of phosphorylated serine/threonine-containing peptides. Through replacement of the phosphate with thiocholine, the negative charge on the phosphopeptide is switched to a quaternary amine containing a permanent positive charge (Scheme 1.1). This strategy

results in a markedly increased ionization sensitivity during ESI (with a sub-500 amol/μL detection limit) accompanied by the enhanced production of informative peptidic fragment ions during CID that affords increased sequence coverage. Moreover, the definitive localization of phosphorylated residues is greatly facilitated through the generation of diagnostic triads of fragmentation ions resulting from peptide bond cleavage and further neutral loss of either trimethylamine (-59 Da) or thiocholine thiolate (-119Da) during CID in MS^2 and MS^3 experiments (Scheme 1.2). Synthesis of stable isotope labeled thiocholine enabled the quantitation of protein phosphorylation with high precision using ratiometric comparisons of heavy and light thiocholine (Scheme 1.3).

The second part of this thesis describes the application of the developed BEMA strategy for the identification of endogenous phosphorylation sites of the hexahistidine tagged calcium-independent phospholipase $A_2\beta$ ($iPLA_2\beta$) heterologously expressed in Sf9 cells. In parallel, traditional direct analysis of phosphopeptides with data-dependent acquisition MS^2 and neutral loss of phosphoric acid triggered MS^3 was also used to analyze $iPLA_2\beta$ phosphorylation. The two methods were compared and evaluated to show that the BEMA strategy was substantially more effective in the identification of phosphopeptides and localization of phosphosites with better ion scores as well as higher sequence coverage than the traditional direct analysis. 3-D structure modeling of the $iPLA_2\beta$ protein was also generated with I-TASSER [108-110] to reveal the spacial relations between the phosphorylated residues and the catalytic site of the enzyme.

The third part of this thesis identifies the quantitative alterations in the myocardial

mitochondrial phosphoproteome induced by cardiac ischemia was studied by using mass spectrometry with the developed strategy, β-elimination of phosphate and subsequent Michael addition (BEMA), with natural abundance thiocholine and stable isotope labeled thiocholine. In addition to increased ionization efficiency, sensitivity and improved identification through characteristic diagnostic triads in MS^2 and MS^3 levels enabled by BEMA strategy, a highly selective phosphopeptide enrichment technique using titanium dioxide resin (TiO_2) was incorporated prior to the BEMA reactions to reduce sample complexity and improve reaction yields for phosphopeptides [87]. The MASCOT search engine was used to conduct all database searches [111]. The results generated by MASCOT were re-scored by Percolator [112-113], a program that utilizes a semi-supervised machine learning algorithm called support vector machine (SVM) to compare true and false positives, for improved phosphopeptides identification.

In this study, the phosphoproteome of mitochondria obtained from isolated Langendorff-perfused mouse hearts that underwent global ischemia was investigated. The comparative quantitation of phosphorylation changes as a result of ischemia was achieved by comparing the phosphopeptides modified by heavy thiocholine from mitochondria of ischemic hearts to those modified by light thiocholine from control hearts that were perfused normally. We identified 141 phosphopeptides from 133 unique proteins with 227 phosphorylated sites from 6 independent biological replicates generated from 24 perfused mouse hearts (12 control-perfused, 12 global ischemic), including 36 phosphopeptides from 35 mitochondrial proteins with 50 phosphosites and 37 new mitochondrial

phosphosites that have not been reported previously. This study has demonstrated that β-elimination of phosphate and subsequent Michael addition (BEMA) using light and heavy thiocholine together with a TiO_2 phosphopeptide enrichment method and a Percolator re-scoring algorithm represents a very effective mass-spectrometry based strategy for comparative quantitative phosphoproteome analysis of *in vivo* tissue-based systems.

References

(1) Uy, R.; Wold, F. *Science* **1977**, *198*, 890-896.

(2) Yang, X. J.; Seto, E. *Mol Cell* **2008**, *31*, 449-461.

(3) Vosseller, K.; Wells, L.; Hart, G. W. *Biochimie* **2001**, *83*, 575-581.

(4) Schmid, D. G.; von der Mulbe, F. D.; Fleckenstein, B.; Weinschenk, T.; Jung, G. *Anal Chem* **2001**, *73*, 6008-6013.

(5) Thornton, J. M. *J Mol Biol* **1981**, *151*, 261-287.

(6) Krishna, R.; Wold, F. *Protein Structure: A Practical Approach*, 2 ed.; Oxford University Press, USA, 1997.

(7) Cohen, P. *Nat. Cell Biol.* **2002**, *4*, E127-130.

(8) Manning, G.; Whyte, D. B.; Martinez, R.; Hunter, T.; Sudarsanam, S. *Science* **2002**, *298*, 1912-1934.

(9) Venter, J. C.; Adams, M. D.; Myers, E. W. *Science* **2001**, *291*, 1304-1351.

(10) Krebs, E. G. *Philos. Trans. R. Soc. Lond. B. Biol. Sci.* **1983**, *302*, 3-11.

(11) Pyerin, W.; Taniguchi, H. *Embo J* **1989**, *8*, 3003-3010.

(12) Zolnierowicz, S.; Bollen, M. *EMBO J.* **2000**, *19*, 483-488.

(13) Kennelly, P. J.; Potts, M. *J Bacteriol* **1996**, *178*, 4759-4764.

(14) Meins, M.; Jeno, P.; Muller, D.; Richter, W. J.; Rosenbusch, J. P.; Erni, B. *J Biol Chem* **1993**, *268*, 11604-11609.

(15) Shibagaki, Y.; Gotoh, H.; Kato, M.; Mizumoto, K. *J Biochem* **1995**, *118*,

1303-1309.

(16) Kuba, M.; Ohmori, H.; Kumon, A. *Eur J Biochem* **1992**, *208*, 747-752.

(17) Mann, M.; Ong, S. E.; Gronborg, M.; Steen, H.; Jensen, O. N.; Pandey, A. *Trends Biotechnol.* **2002**, *20*, 261-268.

(18) Martinez, A.; Haavik, J.; Flatmark, T.; Arrondo, J. L.; Muga, A. *J Biol Chem* **1996**, *271*, 19737-19742.

(19) Hunter, T. *Cell* **2000**, *100*, 113-127.

(20) Ashcroft, M.; Kubbutat, M. H.; Vousden, K. H. *Mol Cell Biol* **1999**, *19*, 1751-1758.

(21) Olsen, J. V.; Blagoev, B.; Gnad, F.; Macek, B.; Kumar, C.; Mortensen, P.; Mann, M. *Cell* **2006**, *127*, 635-648.

(22) Rall, T. W.; Sutherland, E. W.; Wosilait, W. D. *J Biol Chem* **1956**, *218*, 483-495.

(23) Wegener, A. D.; Simmerman, H. K.; Lindemann, J. P.; Jones, L. R. *J Biol Chem* **1989**, *264*, 11468-11474.

(24) Kiss, E.; Edes, I.; Sato, Y.; Luo, W.; Liggett, S. B.; Kranias, E. G. *Am J Physiol* **1997**, *272*, H785-790.

(25) Hopper, R. K.; Carroll, S.; Aponte, A. M.; Johnson, D. T.; French, S.; Shen, R. F.; Witzmann, F. A.; Harris, R. A.; Balaban, R. S. *Biochemistry* **2006**, *45*, 2524-2536.

(26) Cooper, J. A.; Sefton, B. M.; Hunter, T. *Methods Enzymol* **1983**, *99*, 387-402.

(27) Yan, J. X.; Packer, N. H.; Gooley, A. A.; Williams, K. L. *J Chromatogr A* **1998**, *808*, 23-41.

(28) Steinberg, T. H.; Agnew, B. J.; Gee, K. R.; Leung, W. Y.; Goodman, T.;

Schulenberg, B.; Hendrickson, J.; Beechem, J. M.; Haugland, R. P.; Patton, W. F. *Proteomics* **2003**, *3*, 1128-1144.

(29) Wang, P. G.; Giese, R. W. *Analytical Chemistry* **1993**, *65*, 3518-3520.

(30) Schulenberg, B.; Arnold, B.; Patton, W. F. *Proteomics* **2003**, *3*, 1196-1205.

(31) Martin, K.; Steinberg, T. H.; Cooley, L. A.; Gee, K. R.; Beechem, J. M.; Patton, W. F. *Proteomics* **2003**, *3*, 1244-1255.

(32) Kaufmann, H.; Bailey, J. E.; Fussenegger, M. *Proteomics* **2001**, *1*, 194-199.

(33) Edman, P. *Acta Chem. Scand* **1950**, *4*, 277.

(34) Laursen, R. A. *Eur J Biochem* **1971**, *20*, 89-102.

(35) Niall, H. D. *Methods Enzymol* **1973**, *27*, 942-1010.

(36) Bleakney, W. *Phys. Rev.* **1929**, *34*, 157-160.

(37) Nier, A. O. *Rev Sci Instrum* **1947**, *18*, 398-411.

(38) Harrison, A. G. *Chemical Ionization Mass Spectrometry*; CRC Press, Boca Raton, FL, 1983.

(39) Barber, M.; Bordoli, R. S.; Garner, G. V.; Gordon, D. B.; Sedgwick, R. D.; Tetler, L. W.; Tyler, A. N. *Biochem J* **1981**, *197*, 401-404.

(40) Van Vaeck, L.; Adriaens, A.; Gijbels, R. *Mass Spectrometry Reviews* **1999**, *18*, 1-47.

(41) Adriaens, A.; Van Vaeck, L.; Adams, F. *Mass Spectrometry Reviews* **1999**, *18*, 48-81.

(42) Fenn, J. B.; Mann, M.; Meng, C. K.; Wong, S. F.; Whitehouse, C. M. *Science* **1989**,

246, 64-71.

(43) Karas, M.; Hillenkamp, F. *Anal Chem* **1988**, *60*, 2299-2301.

(44) Kebarle, P.; Tang, L. *Analytical Chemistry* **1993**, *65*, A972-A986.

(45) Dole, M.; Mack, L. L.; Hines, R. L.; Mobley, R. C.; Ferguson, L. D.; Alice, M. B. *Journal of Chemical Physics* **1968**, *49*, 2240-2249.

(46) Zenobi, R.; Knochenmuss, R. *Mass Spectrom. Rev.* **1998**, *17*, 337-366.

(47) Mattauch, J.; Herzog, R. *Z. Physik* **1934**, 786.

(48) Ferguson, R. E.; McKulloh, K. E. *J. Chem. Phys.* **1965**, *42*, 100.

(49) Johnson, E. G.; Nier, A. O. *Phys. Rev.* **1953**, *91*, 10.

(50) Guilhaus, M. *Journal of Mass Spectrometry* **1995**, *30*, 1519-1532.

(51) March, R. E. *Journal of Mass Spectrometry* **1997**, *32*, 351-369.

(52) Marshall, A. G.; Hendrickson, C. L.; Jackson, G. S. *Mass Spectrometry Reviews* **1998**, *17*, 1-35.

(53) Hu, Q.; Noll, R. J.; Li, H.; Makarov, A.; Hardman, M.; Graham Cooks, R. *J Mass Spectrom* **2005**, *40*, 430-443.

(54) Medzihradszky, K. F.; Campbell, J. M.; Baldwin, M. A.; Falick, A. M.; Juhasz, P.; Vestal, M. L.; Burlingame, A. L. *Anal Chem* **2000**, *72*, 552-558.

(55) McLafferty, F. W. *Tandem Mass Spectrometry*; Wiler, New York, 1983.

(56) Kitson, F. G.; Larson, B. S.; McEwen, C. N. *Gas Chromatography and Mass Spectrometry: a Practical Guide*; Academic Press, New York 1996, 1996.

(57) McMaster, M. C.; McMaster, C. *GC/MS: a Practical User's Guide*; Wiley, New

York 1998, 1998.

(58) Ardrey, R. E. *LC-MS: an Introduction*; VCH, New York 1999, 1999.

(59) Niessen, W. M. A.; Tjaden, U. R.; Vandergreef, J. *Journal of Chromatography* **1993**, *636*, 3-19.

(60) Issaq, H. J.; Janini, G. M.; Chan, K. C.; el Rassi, Z. *Adv Chromatogr* **1995**, *35*, 101-169.

(61) Syka, J. E.; Coon, J. J.; Schroeder, M. J.; Shabanowitz, J.; Hunt, D. F. *Proc. Natl. Acad. Sci. U. S. A.* **2004**, *101*, 9528-9533.

(62) Carr, S. A.; Huddleston, M. J.; Annan, R. S. *Anal Biochem* **1996**, *239*, 180-192.

(63) Annan, R. S.; Huddleston, M. J.; Verma, R.; Deshaies, R. J.; Carr, S. A. *Anal Chem* **2001**, *73*, 393-404.

(64) Beausoleil, S. A.; Jedrychowski, M.; Schwartz, D.; Elias, J. E.; Villen, J.; Li, J.; Cohn, M. A.; Cantley, L. C.; Gygi, S. P. *Proc Natl Acad Sci U S A* **2004**, *101*, 12130-12135.

(65) Ulintz, P. J.; Bodenmiller, B.; Andrews, P. C.; Aebersold, R.; Nesvizhskii, A. I. *Mol Cell Proteomics* **2008**, *7*, 71-87.

(66) Schroeder, M. J.; Shabanowitz, J.; Schwartz, J. C.; Hunt, D. F.; Coon, J. J. *Anal Chem* **2004**, *76*, 3590-3598.

(67) Chi, A.; Huttenhower, C.; Geer, L. Y.; Coon, J. J.; Syka, J. E.; Bai, D. L.; Shabanowitz, J.; Burke, D. J.; Troyanskaya, O. G.; Hunt, D. F. *Proc Natl Acad Sci U S A* **2007**, *104*, 2193-2198.

(68) Villen, J.; Beausoleil, S. A.; Gygi, S. P. *Proteomics* **2008**, *8*, 4444-4452.

(69) Zubarev, R. A.; Kelleher, N. L.; McLafferty, F. W. *Journal of the American Chemical Society* **1998**, *120*, 3265-3266.

(70) Shi, S. D.; Hemling, M. E.; Carr, S. A.; Horn, D. M.; Lindh, I.; McLafferty, F. W. *Anal Chem* **2001**, *73*, 19-22.

(71) Zubarev, R. A.; Horn, D. M.; Fridriksson, E. K.; Kelleher, N. L.; Kruger, N. A.; Lewis, M. A.; Carpenter, B. K.; McLafferty, F. W. *Anal Chem* **2000**, *72*, 563-573.

(72) Mann, M.; Jensen, O. N. *Nat Biotechnol* **2003**, *21*, 255-261.

(73) Aebersold, R.; Goodlett, D. R. *Chem Rev* **2001**, *101*, 269-295.

(74) Leinenbach, A.; Hartmer, R.; Lubeck, M.; Kneissl, B.; Elnakady, Y. A.; Baessmann, C.; Muller, R.; Huber, C. G. *J Proteome Res* **2009**, *8*, 4350-4361.

(75) Horn, D. M.; Ge, Y.; McLafferty, F. W. *Anal Chem* **2000**, *72*, 4778-4784.

(76) Swaney, D. L.; McAlister, G. C.; Wirtala, M.; Schwartz, J. C.; Syka, J. E.; Coon, J. J. *Anal Chem* **2007**, *79*, 477-485.

(77) Good, D. M.; Wirtala, M.; McAlister, G. C.; Coon, J. J. *Mol Cell Proteomics* **2007**, *6*, 1942-1951.

(78) Otvos, L., Jr.; Feiner, L.; Lang, E.; Szendrei, G. I.; Goedert, M.; Lee, V. M. *J Neurosci Res* **1994**, *39*, 669-673.

(79) Zhao, J. Y.; Kuang, J.; Adlakha, R. C.; Rao, P. N. *FEBS Lett* **1989**, *249*, 389-395.

(80) Flick, M. B.; Sapi, E.; Perrotta, P. L.; Maher, M. G.; Halaban, R.; Carter, D.; Kacinski, B. M. *Oncogene* **1997**, *14*, 2553-2561.

(81) Snyder, G. L.; Girault, J. A.; Chen, J. Y.; Czernik, A. J.; Kebabian, J. W.; Nathanson, J. A.; Greengard, P. *J Neurosci* **1992**, *12*, 3071-3083.

(82) Steen, H.; Kuster, B.; Fernandez, M.; Pandey, A.; Mann, M. *J Biol Chem* **2002**, *277*, 1031-1039.

(83) Andersson, L.; Porath, J. *Anal. Biochem.* **1986**, *154*, 250-254.

(84) Posewitz, M. C.; Tempst, P. *Anal. Chem.* **1999**, *71*, 2883-2892.

(85) Ficarro, S. B.; McCleland, M. L.; Stukenberg, P. T.; Burke, D. J.; Ross, M. M.; Shabanowitz, J.; Hunt, D. F.; White, F. M. *Nat. Biotechnol.* **2002**, *20*, 301-305.

(86) Mazanek, M.; Mituloviae, G.; Herzog, F.; Stingl, C.; Hutchins, J. R.; Peters, J. M.; Mechtler, K. *Nat. Protoc.* **2007**, *2*, 1059-1069.

(87) Larsen, M. R.; Thingholm, T. E.; Jensen, O. N.; Roepstorff, P.; Jorgensen, T. J. *Mol. Cell. Proteomics* **2005**, *4*, 873-886.

(88) Kweon, H. K.; Hakansson, K. *J. Proteome Res.* **2008**, *7*, 749-755.

(89) Connor, P. A.; McQuillan, A. J. *Langmuir* **1999**, *15*, 2916-2921.

(90) Pinkse, M. W.; Mohammed, S.; Gouw, J. W.; van Breukelen, B.; Vos, H. R.; Heck, A. J. *J Proteome Res* **2008**, *7*, 687-697.

(91) Zanivan, S.; Gnad, F.; Wickstrom, S. A.; Geiger, T.; Macek, B.; Cox, J.; Fassler, R.; Mann, M. *J. Proteome Res.* **2008**, *7*, 5314-5326.

(92) Peng, J.; Elias, J. E.; Thoreen, C. C.; Licklider, L. J.; Gygi, S. P. *J Proteome Res* **2003**, *2*, 43-50.

(93) Meyer, H. E.; Hoffmann-Posorske, E.; Korte, H.; Heilmeyer, L. M., Jr. *FEBS Lett.*

1986, *204*, 61-66.

(94) Wells, L.; Vosseller, K.; Cole, R. N.; Cronshaw, J. M.; Matunis, M. J.; Hart, G. W. *Mol. Cell. Proteomics* **2002**, *1*, 791-804.

(95) Byford, M. F. *Biochem. J.* **1991**, *280 (Pt 1)*, 261-265.

(96) Oda, Y.; Nagasu, T.; Chait, B. T. *Nat. Biotechnol.* **2001**, *19*, 379-382.

(97) Brittain, S. M.; Ficarro, S. B.; Brock, A.; Peters, E. C. *Nat. Biotechnol.* **2005**, *23*, 463-468.

(98) Steen, H.; Mann, M. *J. Am. Soc. Mass Spectrom.* **2002**, *13*, 996-1003.

(99) Knight, Z. A.; Schilling, B.; Row, R. H.; Kenski, D. M.; Gibson, B. W.; Shokat, K. M. *Nat. Biotechnol.* **2003**, *21*, 1047-1054.

(100) Weckwerth, W.; Willmitzer, L.; Fiehn, O. *Rapid Commun Mass Spectrom* **2000**, *14*, 1677-1681.

(101) Amoresano, A.; Marino, G.; Cirulli, C.; Quemeneur, E. *Eur J Mass Spectrom (Chichester, Eng)* **2004**, *10*, 401-412.

(102) Vosseller, K.; Hansen, K. C.; Chalkley, R. J.; Trinidad, J. C.; Wells, L.; Hart, G. W.; Burlingame, A. L. *Proteomics* **2005**, *5*, 388-398.

(103) Ong, S. E.; Blagoev, B.; Kratchmarova, I.; Kristensen, D. B.; Steen, H.; Pandey, A.; Mann, M. *Mol Cell Proteomics* **2002**, *1*, 376-386.

(104) Larive, R. M.; Urbach, S.; Poncet, J.; Jouin, P.; Mascre, G.; Sahuquet, A.; Mangeat, P. H.; Coopman, P. J.; Bettache, N. *Oncogene* **2009**, *28*, 2337-2347.

(105) Rinschen, M. M.; Yu, M. J.; Wang, G.; Boja, E. S.; Hoffert, J. D.; Pisitkun, T.;

Knepper, M. A. *Proc Natl Acad Sci U S A* **2010**, *107*, 3882-3887.

(106) Ross, P. L.; Huang, Y. N.; Marchese, J. N.; Williamson, B.; Parker, K.; Hattan, S.; Khainovski, N.; Pillai, S.; Dey, S.; Daniels, S.; Purkayastha, S.; Juhasz, P.; Martin, S.; Bartlet-Jones, M.; He, F.; Jacobson, A.; Pappin, D. J. *Mol Cell Proteomics* **2004**, *3*, 1154-1169.

(107) Reinl, T.; Nimtz, M.; Hundertmark, C.; Johl, T.; Keri, G.; Wehland, J.; Daub, H.; Jansch, L. *Mol Cell Proteomics* **2009**, *8*, 2778-2795.

(108) Zhang, Y. *BMC Bioinf.* **2008**, *9*, 40.

(109) Zhang, Y. *Proteins* **2009**, *77 Suppl 9*, 100-113.

(110) Roy, A.; Kucukural, A.; Zhang, Y. *Nat. Protoc.* **2010**, *5*, 725-738.

(111) Perkins, D. N.; Pappin, D. J. C.; Creasy, D. M.; Cottrell, J. S. *Electrophoresis* **1999**, *20*, 3551-3567.

(112) Kall, L.; Canterbury, J. D.; Weston, J.; Noble, W. S.; MacCoss, M. J. *Nat Methods* **2007**, *4*, 923-925.

(113) Brosch, M.; Yu, L.; Hubbard, T.; Choudhary, J. *J Proteome Res* **2009**, *8*, 3176-3181.

Schemes

Scheme 1.1 Chemical modification of phosphoserine and phosphothreonine containing peptides via β-elimination in the presence of $Ba(OH)_2$ and Michael Addition with thiocholine as the Michael donor.

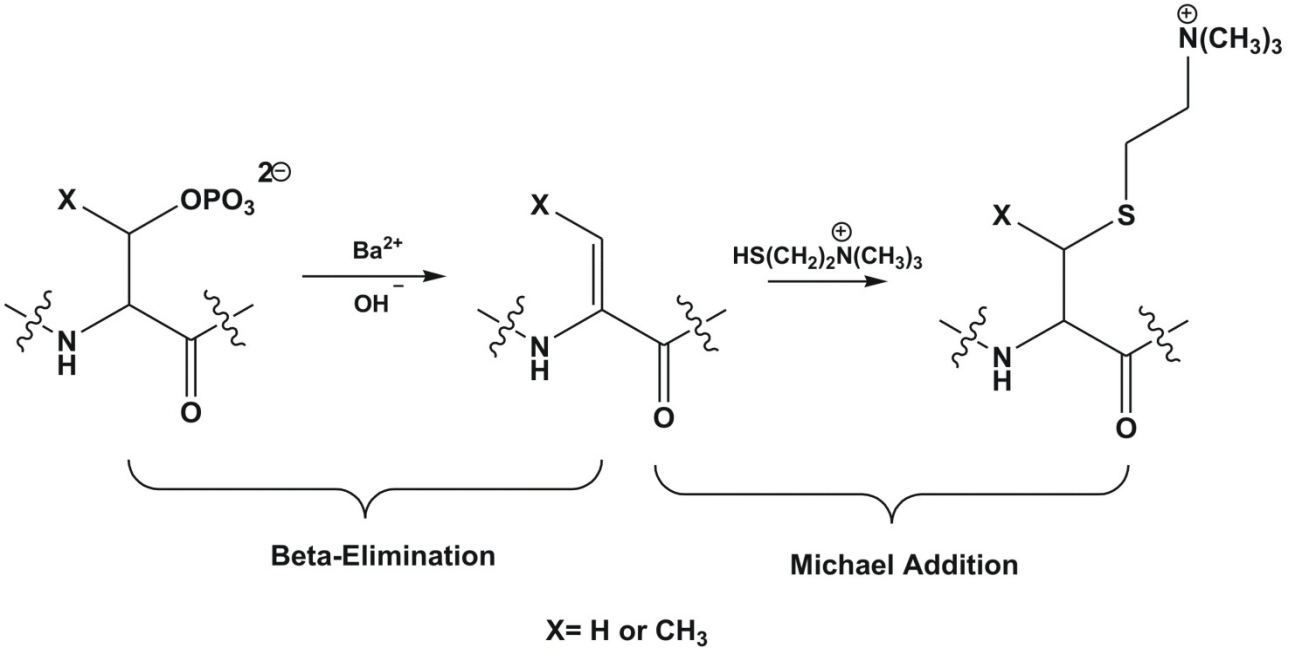

Scheme 1.2 Collision induced dissociation (CID) resulting in the neutral loss of either (A) trimethylamine (m = 59 Da) or (B) the thiocholine thiolate (m = 119 Da) from the thiocholine peptide adduct.

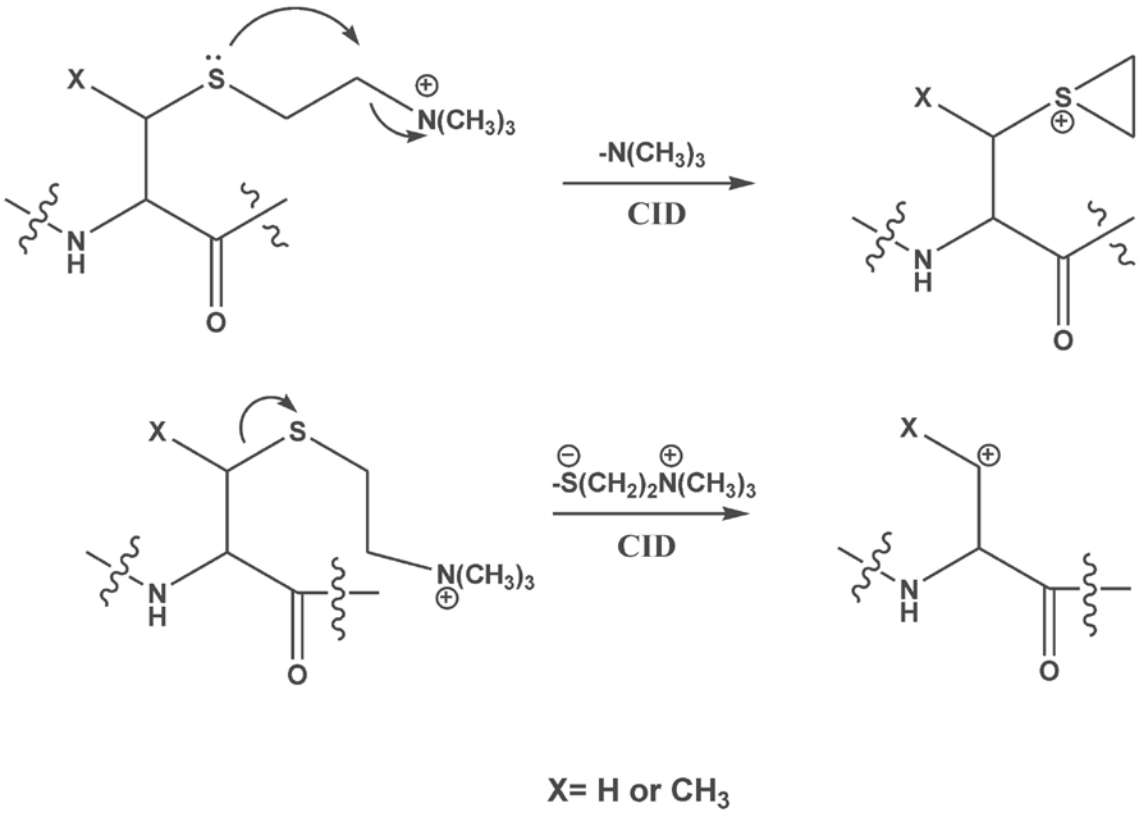

Scheme 1.3

A. Synthesis of thiocholine through acidic hydrolysis of S-acetylthiocholine (72% yield).

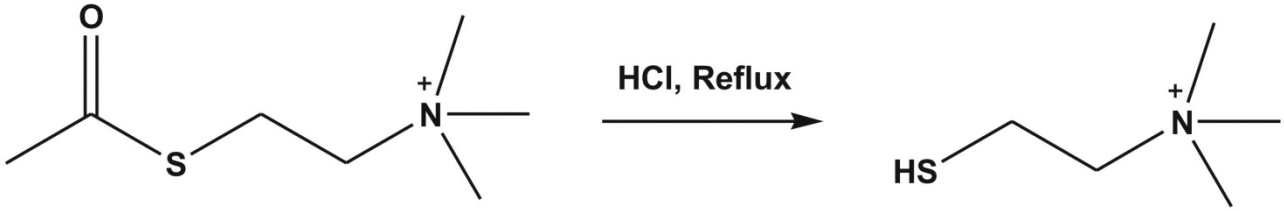

B. Synthesis of thiocholine-$^{13}C,d_3$. The thiol group of 2-(dimethylamino)ethanethiol was protected by thioesterification with acetic anhydride prior to the addition of methyl-$^{13}C,d_3$. The final product was obtained through acidic hydrolysis (50% yield).

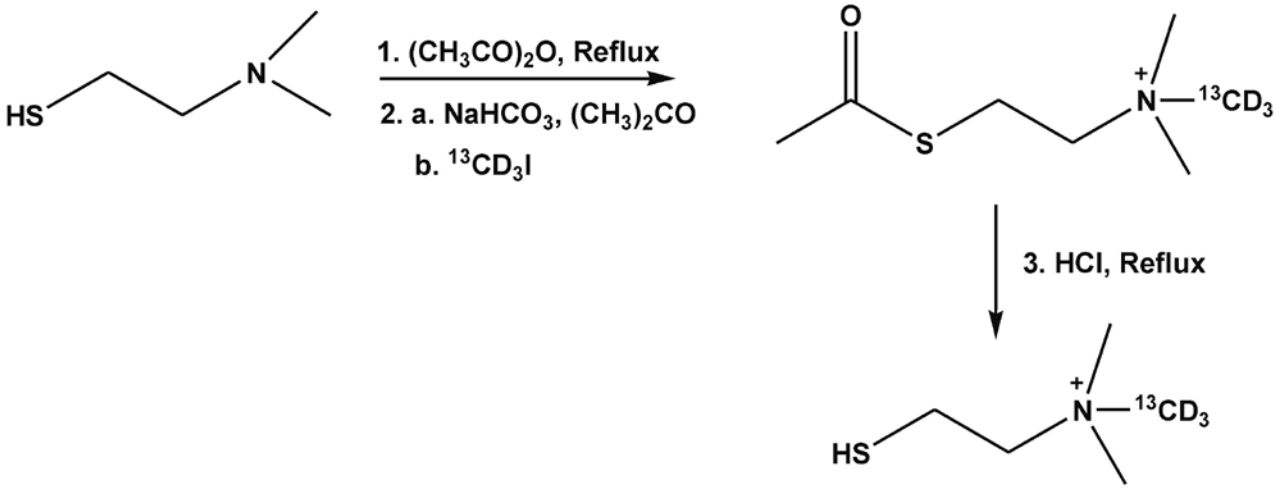

CHAPTER 2

Facile Identification and Quantitation of Protein Phosphorylation via β-Elimination and Michael Addition with Natural Abundance and Stable Isotope Labeled Thiocholine

2.1 Abstract

Herein, we employ the unique chemical properties of the quaternary amine present in thiocholine (2-mercapto-*N*,*N*,*N*-trimethyl-ethanaminium) in conjunction with alkaline β-elimination and Michael addition (BEMA) reactions for the specific detection, identification and quantitation of phosphorylated serine/threonine-containing peptides. Through replacement of the phosphate with thiocholine, the negative charge on the phosphopeptide is switched to a quaternary amine containing a permanent positive charge. This strategy resulted in a marked increase in ionization sensitivity during ESI (sub-500 amol/μL detection limit) accompanied by a markedly enhanced production of informative peptidic fragment ions during CID that dramatically increase sequence coverage. Moreover, the definitive localization of phosphorylated residues is greatly facilitated through the generation of diagnostic triads of fragmentation ions resulting from peptide bond cleavage and further neutral loss of either trimethylamine (-59 Da) or thiocholine thiolate (-119 Da) during CID in MS^2 and MS^3experiments. Synthesis of stable isotope

labeled thiocholine enabled the quantitation of protein phosphorylation with high precision by ratiometric comparisons using heavy and light thiocholine. Collectively, this study demonstrates a sensitive and efficient strategy for mapping of phosphopeptides by BEMA using thiocholine through the production of a diagnostic repertoire of unique fragment ions during LC-MS^2/MS^3 analyses, facilitating phosphosite identification and quantitative phosphoproteomics.

2.2 Introduction

In the human genome, about 2% of the encoded proteins are dedicated to maintaining the appropriate phosphorylation state of targeted proteins through the actions of a wide variety of protein kinases and phosphatases [1-2]. Moreover, approximately 30% of all known proteins in cells are rapidly and reversibly phosphorylated to various extents during physiologic or pathophysiologic processes, making phosphorylation one of the most common post-translational modifications (PTMs) of proteins [3]. Although phosphorylation can occur on many amino acid residues (e.g., aspartic acid, glutamic acid, arginine and etc), reversible phosphorylations of serine, threonine and tyrosine collectively account for almost 99% of the protein phosphorylation in cells. The reversible covalent phosphorylation of cellular proteins is widely believed to be the most important mechanism for the regulation of multiple signal transduction pathways [4-6].

The intrinsic chemical properties of phosphorylated peptides render the detection, identification of the phosphorylation sites, and quantitation of alterations in phosphorylation state a challenging problem in proteomics [7-8]. Peptides containing phosphorylated serine/threonine (pS/pT) rapidly undergo neutral loss of phosphoric acid through cyclo-elimination during low-energy CID, and this leads to the loss of peptide sequence coverage. Typical signaling proteins are present in extremely low abundance. While the phosphorylation patterns of these signaling proteins are of great biological significance; they are highly diversified and oftentimes extremely difficult to determine owing to the presence of multiple S or T residues. Moreover, phosphorylated peptides

generally have poor ionization efficiencies in the positive-ion mode owing to the acidity of the phosphate group and ion suppression [9-12].

Complementary approaches have been developed to overcome these difficulties. Enrichment using immobilized metal affinity chromatography (IMAC) after esterification of carboxylates has been useful in many cases [13-15]. However, identification of phosphopeptides is complicated by polydispersity generated by potentially incomplete and nonspecific methyl esterification [16]. Other enrichment strategies, such as use of titanium dioxide [17-18] and zirconium dioxide [19] have shown great efficiency, but these approaches are still hindered by the intrinsic chemical properties of the phosphate moiety that facilitates its neutral loss. The utility of electron transfer dissociation (ETD) in phosphopeptide analysis is becoming increasingly appreciated [12]. ETD generates c- and z-type ions in which the neutral loss of H_3PO_4 does not occur [20-21].

Finally, phosphorylated tyrosine comprises only about 0.1% of the total phosphorylation in proteins, and its enrichment and analysis can be effectively achieved through immunoprecipitation with high quality commercially available antibodies [22-23]. Accordingly, analytic efforts have focused on identification and quantitation of phosphorylated serine (~90%) and threonine (~10%) residues that account for the overwhelming majority of phosphorylation in cells. Chemical replacement of the phosphate on serine or threonine with other functional groups by β-elimination and subsequent Michael addition (BEMA) was first introduced by Meyers et al. in 1986 [24]. Since then, this strategy has been widely studied and applied effectively with different Michael donors in the enrichment, identification, quantitation of peptides containing

phosphoserine and phosphothreonine [25-27]. In prior work, Steen *et al.* demonstrated the efficacy of 2-dimethylamino-ethanethiol followed by hydrogen peroxide oxidation to generate thioester ethanesulfoxide derivatives that produced informative fragment ions during low-energy CID [28]. However, controlled oxidation with the generation of a single predominant reaction product is not straightforward. With cysteamine as the Michael donor, Knight *et al*. developed a strategy to cleave enzymatically proteins at their phosphorylation sites [29]. Although information on the phosphorylated proteins can be obtained through enzymatic proteolysis, lysine residues have to be quantitatively blocked through additional chemical reactions to ensure the exclusive cleavage at modification sites. During the development of our strategy, Li *et al*. used BEMA with several nucleophiles including thiocholine for the detection of phosphopeptides by Raman spectroscopy and mass spectrometry. However, prior mass spectrometric analyses were limited to detection of molecular ions in full MS scans without exploring the unique advantages of this strategy for covalent identification of specific phosphorylation sites through the enhanced generation of informative fragment ions in either the MS^2 or MS^3 modes [30].

In this study, we report a novel strategy for specific detection, identification and quantitation of pS/pT-containing peptides. Thiocholine is introduced into the peptide at the phosphorylation site via high-yield Ba^{2+} catalyzed β-elimination of phosphate and subsequent Michael addition (Scheme 1.1). Sample complexity is reduced through reductive alkylation of cysteines and development of optimized BEMA conditions for pS or pT individually. This charge-switch strategy with the thiocholine quaternary amine

results in a marked increase in ionization efficiency during ESI with detection levels in the sub 500 amol/μL range. The increased endogenous positive charge also engenders higher charge states of thiocholine-labeled tryptic peptides facilitating the production of peptidic fragment ions resulting in increased sequence coverage. Furthermore, phosphopeptide identification has been substantially improved by exploiting the facile neutral loss of trimethylamine (59 Da) and the thiocholine thiolate (119 Da) from the thiocholine adduct (Scheme 1.2). Thus, CID contains not only the b and y series of peptidic fragment ions but, in addition, a diagnostic array of fragment ions during MS^2 and MS^3 analyses. Finally, through the synthesis and use of stable isotope labeled thiocholine, quantitative analysis of alterations in the phosphorylation state of proteins during cellular perturbations can be performed through ratiometric comparisons of phosphopeptides containing stable isotope labeled thiocholine to those containing natural abundance thiocholine.

.

2.3 Materials and Methods

Materials

Phosphoprotein β-Casein and phosphopeptide FQpSEEQQQTEDELQDK were obtained from Sigma-Aldrich (St. Louis, MO), phosphopeptide DHTGFLpTEYVATR was obtained from BIOMOL (Plymouth Meeting, PA); POROS 20 R2 resin was purchased from ABI (Foster City, CA); Slide-A-Lyzer MINI Dialysis Unit, 7K MWCO was purchased from Pierce (Rockford, IL); Rapigest was purchased from Waters (Milford, MA); Protein Kinase A and trypsin were purchased from Promega (Madison, MI); α-cyano-4-hydroxycinnamic acid (α-CHCA) solution was obtained from Agilent (Santa Clara, CA). All solvents for mass spectrometric analyses were obtained from Honeywell Burdick&Jackson (Muskegon, MI). All other chemicals were obtained from Sigma-Aldrich (St. Louis, MO)

Synthesis of Thiocholine Chloride and Thiocholine-$^{13}C,d_3$ Chloride

Thiocholine chloride was prepared as previously described by Moss *et al*. with minor modifications [31]. Briefly, S-acetylthiocholine chloride, 1 g (5 mmol), was dissolved in 10 mL of nitrogen-purged Millipore-purified water, followed by addition of 3.5 mL concentrated HCl to give a solution of 3 *N* HCl. The solution was heated to 80 °C under nitrogen for 30 min and HCl was evaporated from the solution while drying under vacuum. The dried product was then triturated with anhydrous diethyl ether (3~5 mL) and absolute ethanol (3~5 mL). Additional anhydrous ether was added to precipitate the

product (10 mL) which was filtered and re-crystallized using hot anhydrous ethanol and anhydrous diethyl ether (0.56g, 3.6 mmol).{ ^{1}H NMR (D_2O) δ 2.75-2.85 (m, 2H, CH_2S), 3.0 (s, 9H, $N(CH_3)_3$), 3.35-3.45 (m, 2H, CH_2N)}(Appendix A).

Thiocholine-$^{13}C,d_3$ chloride was prepared similarly to thiocholine chloride, except that the precursor S-acetylthiocholine-(N,$^{13}C,d_3$) was synthesized according to Ouyang *et al*. [32]. Briefly, 2.82 g (20 mmol) 2-(dimethylamino)ethanethiol hydrochloride and 2.82 mL (30 mmol) acetic anhydride were mixed and refluxed for 10 min. The mixture was allowed to stand overnight and transferred to a mortar where the solid was triturated with ethyl ether (3-5 mL), the precipitate (2.9 g, 20 mmol)) was resuspended in 5 mL acetone and the pH was neutralized using $NaHCO_3$. Next, 5 g (25 mmol) of iodomethane-$^{13}C,d_3$ was added and incubated at room temperature under nitrogen for 48 h. Subsequently, thiocholine-$^{13}C,d_3$ chloride was obtained using the same hydrolysis method as that for the naturally occurring isotope described above (1.6 g, 10 mmol). {^{1}H NMR (D_2O) δ 2.75-2.85 (m, 2H, CH_2S), 2.97, 2.98 (d, 6H, $N(CH_3)_2$), 3.35-3.45 (m, 2H, CH_2N)})}(Appendix B).

The free thiol concentrations of both light and heavy thiocholine were determined using Ellman's assay [51]. Briefly, 40 mg 5,5'-dithiobis(2-nitrobenzoic acid) (DTNB) was added in 0.1 M phosphate buffer (pH 8.0) 10 mL. 0.1 mL of this prepared solution (Ellman's reagent) was mixed with 2 mL of 0.1 M phosphate buffer (pH 8.0) containing 0.1 mg of EDTA in a cuvette. The absorbance of the resultant solution was measured at 412 nm. Next 6 μL of light or heavy thiocholine chloride solution at the concentration of 0.03mmol/5mL (by weight) was added directly to the same cuvette and was incubated at

room temperature for 15 min. The absorbance of the resultant solution was measured at 412 nm. The concentration of free thiol in the cuvette was calculated using the equation ΔA (net change of absorbance) = ε_{412nm} x $C_{SH,}$ where ε_{412nm} = 13.6 cm^{-1} mM^{-1}. The results indicated a 98% free thiol content in the prepared thiocholine samples. The overall reaction yield for light thiocholine was 72% and 50% for heavy thiocholine chloride.

BEMA of Model Phosphopeptide FQpSEEQQQTEDELQDK with Thiocholine

The phosphopeptide FQpSEEQQQTEDELQDK was modified via BEMA with thiocholine according to the method of Shokat *et al*. with minor modifications [29]. Lyophilized FQpSEEQQQTEDELQDK was suspended in water to make a 40 pmol/µL stock solution. 12.5 µL of this stock solution was mixed with 9.5 µL DMSO and 3 µL absolute ethanol followed by the addition of 12.5 µL of freshly prepared saturated $Ba(OH)_2$. The reaction was incubated at room temperature under nitrogen for 1 h with gentle vortexing every 20 min. The final pH was 12~13. Next, 25 µL of 1 M thiocholine solution freshly prepared in water was directly added to the reaction. The reaction mixture was incubated at room temperature under nitrogen for 3 h at pH 8~9 and then terminated by the addition of 5 µL of 10% TFA.

BEMA of Model Phosphopeptide DHTGFLpTEYVATR with Thiocholine

Lyophilized DHTGFLpTEYVATR was suspended in water to make a 40 pmol/µL stock solution. 12.5 µL of this peptide stock solution was mixed with 9.5 µL DMSO and 3 µL absolute ethanol followed by the addition of 12.5 µL freshly prepared saturated $Ba(OH)_2$.

The reaction was incubated at room temperature under nitrogen for 3 h with gentle vortexing every 20 min. The final pH was 12~13. Next, the β-elimination reaction was terminated by addition of 5 μL of 10% TFA and the resulting solution was desalted with a POROS 20 R2 micro column. The purified peptide solution was dried and reconstituted in 50 μL of 0.5 M thiocholine solution freshly prepared in 0.1 M NaOH. The mixture was incubated at 50 C° under nitrogen for 5 h at pH 8~9. The reaction was terminated by the addition of 5 μL 10% TFA.

Phosphorylation of Calcium-independent Phospholipase $A_2\beta$ by Protein Kinase A

Purified $iPLA_2\beta(His)_6$ was obtained as previously described by Jenkins *et al*. [33]. The catalytic subunit of protein kinase A (400U) was incubated with 100 μg of purified $iPLA_2\beta(His)_6$ in 40 mM Tris-HCl buffer, pH 7.4 containing 20 mM magnesium acetate and 0.3 mM ATP for 1 h at 30°C. The resultant phosphorylated enzyme was dialyzed against 1L deionized water for 8 h using a Slide-A-Lyzer® MINI Dialysis Unit. The dialyzed $iPLA_2\beta$ sample was dried in a SpeedVac apparatus (Savant, Holbrook, NY) and reconstituted in 50 μL of 0.2% Rapigest in 50 mM NH_4HCO_3. Next, 2.5 μL of 100 mM DTT was added to a final concentration of 5 mM. The sample was then incubated at 60°C for 30 min before 6 μL 150 mM iodoacetamide was added to quench the reduction and initiate alkylation. The sample was incubated for an additional 30 min in the dark. Trypsin was added to the solution at an enzyme to protein ratio of 1:30 (w:w). The total volume of the sample solution was adjusted to 100 μL with 50 mM NH_4HCO_3. 500fmol/μL protein sample was incubated at 37 °C for 2 h then acidified with 10 μL 10%

TFA to lower the pH to < 2. The sample was again incubated at 37 °C for 30 min and centrifuged at 13,000 rpm to pellet the hydrolyzed Rapigest. The resultant supernatant was used for thiocholine modification.

BEMA of Trypsinized Calcium-independent Phospholipase $A_2\beta$ with Thiocholine

Trypsinized iPLA$_2$β samples were dried in a SpeedVac apparatus and reconstituted in 50 μL deionized water follow by the addition of 38 μL DMSO and 12 μL of absolute ethanol. The trypsinized protein solution was then divided into 2 equal aliquots of 50 μL that were separately modified with one of two protocols.

Protocol I: 25 μL of saturated $Ba(OH)_2$ was added to the sample and the reaction was incubated at room temperature under a nitrogen atmosphere for 1 h and gently vortexed every 20 min. The final pH of the reaction mixture was pH 12~13. 1M thiocholine was freshly prepared in water and 50 μL was directly added to each reaction. This reaction was incubated at room temperature for 3 h at pH 8-9 and then terminated by the addition of 10 μL 10% TFA.

Protocol II: 25 μL of saturated $Ba(OH)_2$ was added to the sample and the reaction was incubated at room temperature under a nitrogen atmosphere for 3 h and gently vortexed every 20 min. The final pH was 12-13. Next, the β-elimination was terminated by addition of 10 μL of 10% TFA and the resulting solution was desalted with a POROS 20 R2 micro column. The purified peptide solution was dried and reconstituted in 50 μL of 0.5 M thiocholine solution freshly prepared in 0.1 M NaOH. This reaction was incubated at 50C° under nitrogen for 5 h at pH 8-9. The reaction was terminated by the addition of

5 μL 10% TFA.

Comparative Quantitation of Phosphoproteins using Natural Abundance Thiocholine and Thiocholine-$^{13}C,d_3$ with the Model Protein β-Casein

50 μL 1 mg/mL β-Casein solution prepared in water was mixed with 50 μL 0.2% Rapigest in 100 mM NH_4CO_3. The protein sample was subjected to in-solution tryptic digestion as described above. The resulting trypsinized β-Casein was concentrated with a SpeedVac to ~50 μL and divided to 2 equal aliquots. Aliquot 1 was subject to BEMA with natural abundance thiocholine as the Michael donor while aliquot 2 was modified with stable isotope labeled thiocholine-$^{13}C,d_3$ both using *Protocol I* for iPLA$_2$β covalent modification as described above. Modified trypsinized β-Casein in aliquots 1 and 2 were then mixed in selected ratios (v:v; aliquot 1: aliquot 2, or light: heavy): five independent replicates at 1:1 and three independent replicates at 1:2, 1:3, 1:4, 4:1, 3:1 and 2:1 ratios respectively were performed. Experimental ratios from mass spectrometric analyses were compared to expected ratios to evaluate the reproducibility and linearity of the method.

Sample Purification

All samples subject to mass spectrometric analysis were desalted with POROS 20 R2 micro columns according to the procedure by Thingholm *et al*. [34]. Briefly, a POROS 20 R2 micro column was assembled by stamping out a small plug of C8 material from a 3 M Empore C8 extraction disk using a HPLC syringe needle and placing this plug in the constricted end of a GELoader tip. Next, POROS R2 beads that were suspended 50%

acetonitrile at 5mg/200 µL were packed in the GELoader tip by pressing air through the micro column using an Eppendorf syringe. The length of the packed POROS R2 resin was about 3-6 mm. Then the column was washed with 30 µL 50% acetonitrile and equilibrated with 30 µL 0.1% trifluoroacetic acid. Sample solution was then loaded onto the POROS R2 micro column. The sample was slowly passed through the micro column by pressing air through the using a Eppendorf syringe. The column was washed twice with 30 µL 0.1% trifluoroacetic acid and the bounded peptides were eluted first using 30 µL 70% acetonitrile with 0.05 % trifluoroacetic acid, then 5 µL 30% acetonitrile with 0.05% trifluoroacetic acid.

MALDI-TOF/TOF Mass Spectrometric Analyses

MALDI-TOF/TOF mass spectrometric analyses were performed using a 4800 MALDI-TOF/TOF Analyzer (Applied Biosystems, Foster City, CA). 1 µL of each peptide sample eluted from a POROS R2 micro column was mixed with 1µL α-CHCA solution and 0.5 µL of the mixture was spotted on an Opti-TOF 384 well plate. Mass spectra of all peptide samples were acquired in the positive ion mode by averaging 500 consecutive laser shots (50 shots per subspectrum with ten total subspectra) with default calibration. MS^2 analyses of the peptide samples were accomplished by collision-induced dissociation (CID) using air at medium pressure.

HPLC-ESI-MS^2/MS^3 Mass Spectrometric Analyses

Trypsinized protein and peptide samples desalted with POROS 20 R2 micro columns

were dried and reconstituted in 0.1% formic acid before injection and separation using a Surveyor HPLC system (Autosampler and Pump, ThermoFisher, San Jose, CA) equipped with a reverse-phase C18 PepMap100 Nano-LC column (75 μm I.D. x 15 cm, 3 μm, 100 angstrom; Dionex, Sunnyvale, CA). Flow rate was maintained at 220-280 nL/min. Samples eluting from the column were directed to the nanospray apparatus (i.e. NanoMate HD with LC coupler, Advion Bioscience Ltd., Ithaca, NY) and sprayed directly into an LTQ-Orbitrap mass spectrometer (ThermoFisher, San Jose, CA) at a spray voltage of 1.7 kV in the positive ion mode. Model peptides and trypsinized β-casein samples were eluted with a gradient from 100% A to 50% A, 50% B in 20 min (Buffer A: 90% water, 10% acetonitrile, 0.1% formic acid; Buffer B: 10% water, 90% acetonitrile, 0.1% formic acid, v:v) and were subject to data-dependent MS^2 analyses: full mass scans were acquired using an Orbitrap (300-1600 *m*/*z*, mass resolution = 30,000) followed by product-ion scans in the LTQ of the five most abundant ions. $iPLA_2\beta$ samples, modified by the two optimized protocols, were analyzed first in survey runs, which consisted of a 90-min gradient from 100% A to 50% A, 50% B and data-dependent MS^2 analyses: full mass scans in the Orbitrap (300-1600 *m*/*z*, mass resolution = 30,000) were followed by product-ion scans in the LTQ of the five most abundant ions. The ions of interest from the survey runs were then included in the parent mass list of the target runs. The target runs consisted of a 180-min gradient from 100% A to 75% A, 25% B (120 min), then to 50% A, 50% B (60 min) and data-dependent MS^2/MS^3 analyses: full mass scan in the Orbitrap (300-1600 *m*/*z*, mass resolution = 30,000) were followed by product-ion scans in the LTQ of the three most abundant ions from the parent mass list and the MS^3 scans in the LTQ

of the ten most abundant fragment ions following each of the three product-ion scans. The normalized collision energy for CID was set at 25 for all data-dependent scans.

Data Processing

The local MASCOT server was used to conduct all database searches. A single-protein (iPLA$_2$β) database was created by *in silico* trypsinolysis. Thiocholine and thiocholine-^{13}C,d$_3$ with neutral loss trimethylamine and thiolate were integrated into MASCOT for customized processing of the designed covalent modifications for serine and threonine residues at the MS^2 level. Carbamidomethylation (C) was set as the fixed modification for trypsinized iPLA$_2$β samples.

2.4 Results and Discussion

The chemical replacement of the phosphate on serine and threonine residues via β-elimination and Michael addition has been widely used for analyses of phosphopeptides. However, an efficient method that concomitantly yields high sensitivity, minimal side reactions and informative diagnostic ions suitable for quantitative analyses of both pS and pT-containing peptides in the phosphoproteome has remained elusive. Thiocholine was chosen as the Michael donor in this study because of the extraordinary sensitivity of the quaternary amine for ionization during ESI and its utility in creating diagnostic fragment ions resulting from the neutral loss of trimethylamine and the thiocholine thiolate. The syntheses of both thiocholine and stable isotope labeled thiocholine-$^{13}C,d_3$ are straightforward (Scheme 1.3). Model peptides containing either phosphoserine (FQpSEEQQQTEDELQDK) or phosphothreonine (DHTGFLpTEYVATR) were chosen to assure that reaction conditions were developed that facilitate assessment of either serine or threonine phosphorylation sites. For proteins, either the traditionally employed model protein β-Casein was used or phosphorylation of the signaling protein iPLA$_2$β by protein kinase A (PKA) was studied.

Optimization of BEMA Conditions and Ionization Efficiency

The overall reaction yield is an important factor for the success of the BEMA strategy. Given that the reaction rates of phosphorylated serine and threonine residues are quite different for either β-elimination or Michael addition owing to the electron-donating

effect of the β-methyl group of threonine residue (Appendix C), the reaction conditions were optimized for phosphorylated serines and threonines individually by using the model phosphopeptides FQpSEEQQQTEDELQDK and DHTGFLpTEYVATR. Through the use of $Ba(OH)_2$, a controlled high-yield conversion of FQpSEEQQQTEDELQDK to its corresponding dehydro-alanine derivative was accomplished within 40 min (Figure 2.1). The addition of thiocholine then resulted in the rapid (< 60 min) synthesis of the desired thiocholine adduct. Based upon integrated UV absorbance, these sequential transformations were accomplished in near quantitative yield (Figure 2.1). To ensure the completeness of the reaction for more complicated samples, the reaction times were set at 1 h and 3 h for β-elimination and Michael addition, respectively.

The mass spectrometric utility of this covalent conversion was demonstrated by a marked increase in ionization efficiency with ESI illustrated by the total ion current tracing obtained during reversed-phase chromatography after injection of identical amounts of the thiocholine-modified peptide and its non-modified phosphopeptide precursor. This remarkable increase in ionization efficiency is engendered by the replacement of acidic phosphate with quaternary amine bearing thiocholine that possesses an endogenous positive charge and is extraordinarily sensitive to ionization during the electrospray process (Figure 2.2-A). The detection limit of this method using ESI is at the attomole level (Figure 2.3). Using MALDI, a 3-fold increase in MS signal was present after derivatization as demonstrated by analysis of a sample containing equal amounts of phosphopeptide and thiocholine-modified phosphopeptide onto a MALDI plate using α-CHCA as matrix (Figure 2.2-B).

Phosphorylated threonines, possessing secondary hydroxyls, generally have slower reaction rates during both β-elimination and Michael addition in comparison to their primary hydroxyl counterparts [35]. Simply increasing the incubation temperature and/or incubation time results in increased formation of side products and is not productive [11, 36-37]. However, by purification of the dehydro-alanine intermediate from β-elimination and through the use of nitrogen protection, the overall reaction yield for Michael addition using the model peptide, DHTGFLpTEYVATR, has been greatly improved (Figure 2.4-2.6). These modification strategies individualized for pS or pT residues greatly maximize the effectiveness of BEMA for phosphoproteomics. Phosphorylated tyrosines are stable and are not altered under the alkaline conditions employed in this study [35].

Fragmentation of Thiocholine-modified Peptides

In addition to dramatically increasing ionization efficiency in ESI-MS, thiocholine derivatization exhibits the unique ability to generate diagnostic triads of informative fragment ions resulting from both the routine peptide bond cleavage and the facile neutral loss of either trimethylamine (59 Da) or thiocholine thiolate (119 Da) during CID in MS^2 and MS^3 scanning. This results in a greatly improved identification algorithm for target peptides. A representative ESI-product-ion spectrum of the triply charged molecular ion of the thiocholine-modified peptide FQS*EEQQQTEDELQDK is shown in Figure 2.7-A. Analysis of the fragmentation pattern demonstrated multiple informative b and y ions necessary for sequence identification. As shown in the expanded

spectrum, a representative peptidic fragment ion b_5^+ (*m/z* = 722.3) is accompanied by its neutral loss counterparts $b_5 - 59^+$ (*m/z* = 663.2) and $b_5 - 119^+$ (*m/z* = 603.2) after loss of trimethylamine or thiocholine thiolate, respectively (nomenclature of peptide fragment ions is presented in Appendix D). The concurrence of these diagnostic triads of fragment ions obtained through conventional CID represent key informative features that can further facilitate the identification of peptides and increase the confidence of assignment of the phosphorylated residue(s) on peptides containing multiple potential phosphorylation sites.. Furthermore, use of MS^3 for the thiocholine-containing ion y_{14}^{+2} (*m/z* = 904.4) demonstrated that neutral loss of trimethylamine is the dominant fragmentation pathway leading to a signature neutral loss product at *m/z* 875.1 (M - 59) (Figure 2.7-B). Thus, introduction of the thiocholine side chain and subsequent fragmentation resulted in the generation of suites of diagnostic triads of fragment ions in both MS^2 and MS^3 experiments that helped not only to enhance sequence coverage, but also to increase the confidence of the phosphopeptide identification and the specific location of the modified residue. Tandem mass spectrometric analyses of FQS*EEQQQTEDELQDK were also conducted on the singly charged molecular ion with MALDI and the doubly charged molecular ion with ESI. In MALDI experiments, the product-ion spectrum of the molecular ion at *m/z* 2082.62 (+) contains a dominant signature ion at *m/z* 2023.7 (+) (Figure 2.7-C). This ion resulted from the neutral loss of trimethylamine (59 Da) from the thiocholine side chain of the molecular ion with minimal sequence-informative b and y ions. The product-ion spectrum obtained with ESI of the doubly charged molecular ion showed a strong neutral loss peak from the

molecular ion at *m/z* 1012.5 (+2) (Figure 2.8). In MALDI, peptides are almost always singly charged [38]. With the low kinetic energy, singly charged thiocholine-containing peptides require higher collision energy to induce peptidic chain fragmentation relative to the neutral loss of trimethylamine. Therefore, the neutral loss is more prone to occur than the formation of b and y ions in low-energy CID, leading to a dominant neutral loss pattern. Similarly, in ESI, neutral loss represents a pathway that requires lower energy to induce fragmentation of the doubly charged parent ion. However, when the peptide is triply charged, with the higher vibrational energy derived from collisions at the increased kinetic energy gained during acceleration, peptide chain fragmentation becomes more favorable than the neutral loss of trimethylamine leading to the production of a sequence of informative b and y ions [39]. Although neutral loss of trimethylamine is no longer dominant in this case, it can still occur on thiocholine containing fragment ions, which together with the ions from neutral loss of thiocholine thiolate provides additional confirmatory sequence information and facilitates the assignment of phosphorylation sites. Moreover, as described above (Figure 2.7-B), neutral loss of trimethylamine becomes favorable again in MS^3, producing a signature neutral loss (SNL) peak during CID, which adds an additional dimension to the identification of peptide phosphosites. Although the majority of the tryptic peptides are doubly charged using ESI owing to basic amino acid residues on both N- and C- termini using conventional trypsinolysis, the modified phosphopeptides typically possess a charge state of 3 or higher due to the additional positive charge introduced by thiocholine. Through combining tryptic proteolysis with thiocholine modification, the majority of the thiocholine-modified

peptides will be triply charged or higher, thereby leading to a rich repertoire of diagnostic triads of peptidic fragment ions and ions from neutral loss of trimethylamine and the thiocholine thiolate for significant improvement in the identification of phosphorylation sites during ESI-MS^2 analyses. In addition, ions containing intact thiocholine side chains losing trimethylamine produce a signature neutral loss pattern in MS^3, greatly improving the confidence of the identification of phosphopeptides and the localization of the phosphorylated residue(s) in peptides containing more than one potential phosphosite or in the elucidation of phosphorylation patterns in cases where multiple sites are phosphorylated.

Identification of Protein Kinase A Phosphorylation Sites in Calcium-independent Phospholipase $A_2\beta$ ($iPLA_2\beta$)

$iPLA_2\beta$ is an important phospholipase in cellular signaling that contributes to diverse cellular processes including arachidonic acid release, insulin secretion, calcium signaling, and apoptosis [33, 40-42]. We used the developed method to identify *in vitro* PKA phosphorylation sites of $iPLA_2\beta$ to demonstrate the application of this method in a biologically relevant system. Prior to BEMA modification, the potential interference from free thiols must be eliminated [43]. Previously, perfomic acid oxidation was widely used to oxidize cysteine residues directly or convert cysteine disulfide bonds to cysteic acid residues [44-45]. However, although harsh oxidation may convert all cysteines to cysteic acid, it also leads to additional oxidation and an undesirable increase the chemical diversity and complexity of the sample [46-47]. Other potentially susceptible moieties

include alkylated cysteines, either endogenous or introduced by reductive alkylation, as well as O-glycosylated serines and threonines. These residues could cause ambiguities similar to an intact cysteine because they could also be converted to the same modified residues as pS/pT under alkaline conditions in the presence of strong nucleophiles [48-49]. However, using Ba^{2+} as the catalyst coupled with well-controlled reaction conditions, β-elimination of alkylated cysteines or O-glycosylated serines and threonines occurs at rates two orders of magnitude more slowly than β-elimination from pS/pT whereas unphosphorylated serine and threonine residues are unaffected [35]. Under the conditions employed in this study, reductive alkylation does not interfere with BEMA targeting of phosphopeptides, and, thus, many side products and potential ambiguities are avoided. The identification of peptide $C^{a}N^{d}$VMGPS*GFPIHTAMK in $iPLA_2\beta$ contains both alkylated cysteine and thiocholine-modified serine residues showing the compatibility of the routine reductive alkylation with Ba^{2+} catalyzed BEMA (Figure 2.9).

The fragmentation patterns and sequence coverage of the trypsin-generated phosphopeptides that were identified in the PKA phosphorylated $iPLA_2\beta$ with and without thiocholine modification are demonstrated for the peptide SSGAAPTYFRPNGR (582-595). The product-ion spectrum of the phosphopeptide p(SS)GAAPTYFRPN^{d}GR (Figure 2.10-B) exhibits a strong peak corresponding to the neutral loss of H_3PO_4 from the doubly charged molecular ion with key peptidic chain cleavage products y_{13} and b_1 at the Ser-Ser peptide bond missing from the spectrum precluding discrimination of phosphorylation at residues Ser582 or Ser583. In sharp contrast, the product-ion spectrum of SS*GAAPTYFRPN^{d}GR (Figure 2.10-A) shows an abundant diagnostic y_{13}^{+3}

ion at *m/z* 499.4 as well as its satellite neutral loss ions (shown in the expanded spectrum), which led to the unambiguous assignment of phosphorylation at residue Ser583. In low-energy CID, phosphopeptides are prone to lose a neutral phosphoric acid to form a five-member oxazole ring, which is a preferred fragmentation pathway for phosphopeptides [12]. The five-member ring prevents peptide bond cleavage at the site of phosphorylation and informative b and y ions resulting from that particular bond cleavage are missing, thus preventing conclusive identification of the phosphorylation site(s) in many cases. Therefore, although a phosphopeptide is easily identified through its neutral loss of 98 Da, the site of phosphorylation is often difficult to determine precisely by conventional means. In summary, replacing the phosphate with thiocholine prevents the cyclo-elimination of phosphoric acid in CID owing to the increased charge state of modified peptides thus improving sequence coverage and facilitating the unambiguous identification of the specific phosphorylated residue.

As shown in Table 1, 32 different phosphorylation sites were identified in iPLA$_2$β phosphorylated samples examined using the customized protocols optimized for either pS or pT. These phosphorylation sites originated from a total of 16 unique sequences. Figure 2.11-A shows the product-ion spectrum of triply charged peptide EIS*VADYTSHER (26-37). The spectrum consists of b and y ions with diagnostic triads of all thiocholine containing peptidic fragment ions. Shown in the expanded spectrum are representative diagnostic triads from y_{10}^{+2} and b_6^+ fragmentation ions resulting from peptide bond cleavage (*m/z* = 633.6 and 716.3) and further neutral loss of trimethylamine (-59 Da, *m/z* = 603.3 and 657.2) and the thiocholine thiolate (-119 Da, *m/z* = 574.1 and 597.2). The

characteristic neutral losses in MS^2 level are incorporated into MASCOT to contribute to the identification of the peptide and location of the phosphorylation site(s).

A promising future prospect of this approach is the use of this chemical property in a weighted scoring system for ion identification that uses these unique and predictable diagnostic triads of fragmentation ions from thiocholine-modified peptides to facilitate identification of phosphorylated peptides and phosphosites in singly and multiply phosphorylated peptides. Among the ions generated in MS^2 fragmentation, the ten most abundant ions were chosen to be further fragmented at the MS^3 level. Examination of the y_{10}^{+2} ion at *m/z* 633.6 (amongst the top ten ions selected) demonstrated that it also possesses the intact thiocholine side chain, which led to its signature neutral loss pattern in its MS^3 spectrum (Figure 2.11-B). The ion peak at *m/z* 604.0 corresponds to the neutral loss of trimethylamine from the precursor y_{10}^{+2} at *m/z* 633.6. From the example of the peptide EIS*VADYTSHER, it is clear that the thiocholine side chain enabled a unique tandem fragmentation pattern ideal for proteomic analyses, since sequencing of the peptide at the MS^2 level is not disrupted by the neutral losses of either trimethylamine or thiocholine thiolate but rather strengthened by the presence of diagnostic triads of fragment ions in conjunction with the signature neutral loss at MS^3 level. Collectively, these features serve to provide important structural information facilitating both the identification of the peptide as well as the location of the precursor ion to facilitate unambiguous identification of the phosphorylated residues. In the current study, nine out of 16 unique sequences demonstrated at least one ion with a signature neutral loss during MS^3 scanning underscoring the utility of the developed method. Although neutral-loss

information has been incorporated in MASCOT as part of the variable modification of thiocholine, MS^3 spectra with signature neutral loss patterns must be manually selected at the present time.

Comparative Quantitation of Phosphoproteins using Natural Abundance Thiocholine and Thiocholine-$^{13}C,d_3$ with Model Protein β-Casein

Comparative quantitation via BEMA with thiocholine and thiocholine-$^{13}C,d_3$ was evaluated with the model phosphoprotein β-casein to determine the reproducibility and linearity of the developed method. As described in experimental procedures, two equal aliquots of trypsinized β-casein were modified with either thiocholine or thiocholine-$^{13}C,d_3$. The light and heavy thiocholine containing peptides of β-casein were then mixed at different ratios (v:v) as follows;: five independent replicates at 1:1, three independent replicates at 1:2, 1:3, 1:4, 4:1, 3:1 and 2:1 respectively. The tryptic phosphopeptide FQpSEEQQQTEDELQDK was chosen to characterize the quantitation of the phosphorylation of β-casein. Thiocholine and thiocholine-$^{13}C,d_3$-modified peptides FQS*EEQQQTEDELQDK and FQS**EEQQQTEDELQDK were compared by their ion intensities at their prevailing charge state (+3) at the time of elution. The average adjusted experimental ratio of ion intensities for five replicates at 1:1 is 0.96 with a standard deviation of 0.02. Thus, this method shows comparable reliability to similar experiments employing isotope-coded affinity tags [50]. The full-mass spectrum from the XIC of two modified peptides at the time of the elution is shown in Figure 2.12 with the well recognized (M + 4) isotopologue pattern. The experimental ratios of peak intensities were

obtained for samples mixed in selected ratios and plotted against theoretical values to yield a correlation coefficient of $R^2 = 0.99$. Furthermore, there was no chromatographic shift between the light and heavy thiocholine-modified peptides (Figure 2.13). Overall, stable isotope ratiometric comparisons demonstrated the anticipated quantitative accuracy in both reproducibility and linearity using heavy and light thiocholine modification.

2.5 Conclusion and Perspective

We have demonstrated a strategy for the facile, sensitive and precise detection, identification and quantitation of serine/threonine phosphorylation in proteins. By introducing thiocholine into the target peptides, a powerful mass spectrometric methodology is added that greatly increases the sensitivity of phosphosite identification, enriches the repertoire of observable fragmentation ions from the production of a higher charge state, and provides diagnostic triads of fragment ions through signature neutral loss patterns. The development of an affinity purification method for quaternary amines such as those previously demonstrated using calixirenes [52] may greatly facilitate the large scale integrated use of this strategy in cellular systems.

2.6 References

(1) Manning, G.; Whyte, D. B.; Martinez, R.; Hunter, T.; Sudarsanam, S. *Science* **2002**, *298*, 1912-1934.

(2) Venter, J. C.; Adams, M. D.; Myers, E. W. *Science* **2001**, *291*, 1304-1351.

(3) Zolnierowicz, S.; Bollen, M. *EMBO J.* **2000**, *19*, 483-488.

(4) Krebs, E. G. *Philos. Trans. R. Soc. Lond. B. Biol. Sci.* **1983**, *302*, 3-11.

(5) Yan, J. X.; Packer, N. H.; Gooley, A. A.; Williams, K. L. *J. Chromatogr., A* **1998**, *808*, 23-41.

(6) Hunter, T. *Cell* **2000**, *100*, 113-127.

(7) Mann, M.; Ong, S. E.; Gronborg, M.; Steen, H.; Jensen, O. N.; Pandey, A. *Trends Biotechnol.* **2002**, *20*, 261-268.

(8) Steen, H.; Jebanathirajah, J. A.; Rush, J.; Morrice, N.; Kirschner, M. W. *Mol. Cell. Proteomics* **2006**, *5*, 172-181.

(9) Zhou, W.; Merrick, B. A.; Khaledi, M. G.; Tomer, K. B. *J. Am. Soc. Mass Spectrom.* **2000**, *11*, 273-282.

(10) Adamczyk, M.; Gebler, J. C.; Wu, J. *Rapid Commun. Mass Spectrom.* **2001**, *15*, 1481-1488.

(11) Li, W.; Boykins, R. A.; Backlund, P. S.; Wang, G.; Chen, H. C. *Anal. Chem.* **2002**, *74*, 5701-5710.

(12) Syka, J. E.; Coon, J. J.; Schroeder, M. J.; Shabanowitz, J.; Hunt, D. F. *Proc. Natl. Acad. Sci. U. S. A.* **2004**, *101*, 9528-9533.

(13) Andersson, L.; Porath, J. *Anal. Biochem.* **1986**, *154*, 250-254.

(14) Posewitz, M. C.; Tempst, P. *Anal. Chem.* **1999**, *71*, 2883-2892.

(15) Ficarro, S. B.; McCleland, M. L.; Stukenberg, P. T.; Burke, D. J.; Ross, M. M.; Shabanowitz, J.; Hunt, D. F.; White, F. M. *Nat. Biotechnol.* **2002**, *20*, 301-305.

(16) Mazanek, M.; Mituloviae, G.; Herzog, F.; Stingl, C.; Hutchins, J. R.; Peters, J. M.; Mechtler, K. *Nat. Protoc.* **2007**, *2*, 1059-1069.

(17) Larsen, M. R.; Thingholm, T. E.; Jensen, O. N.; Roepstorff, P.; Jorgensen, T. J. *Mol. Cell. Proteomics* **2005**, *4*, 873-886.

(18) Zanivan, S.; Gnad, F.; Wickstrom, S. A.; Geiger, T.; Macek, B.; Cox, J.; Fassler, R.; Mann, M. *J. Proteome Res.* **2008**, *7*, 5314-5326.

(19) Kweon, H. K.; Hakansson, K. *J. Proteome Res.* **2008**, *7*, 749-755.

(20) Chi, A.; Huttenhower, C.; Geer, L. Y.; Coon, J. J.; Syka, J. E.; Bai, D. L.; Shabanowitz, J.; Burke, D. J.; Troyanskaya, O. G.; Hunt, D. F. *Proc. Natl. Acad. Sci. U. S. A.* **2007**, *104*, 2193-2198.

(21) Gunawardena, H. P.; Emory, J. F.; McLuckey, S. A. *Anal. Chem.* **2006**, *78*, 3788-3793.

(22) Rosenblum, K.; Dudai, Y.; Richter-Levin, G. *Proc. Natl. Acad. Sci. U. S. A.* **1996**, *93*, 10457-10460.

(23) Pandey, A.; Podtelejnikov, A. V.; Blagoev, B.; Bustelo, X. R.; Mann, M.; Lodish, H. F. *Proc. Natl. Acad. Sci. U. S. A.* **2000**, *97*, 179-184.

(24) Meyer, H. E.; Hoffmann-Posorske, E.; Korte, H.; Heilmeyer, L. M., Jr. *FEBS Lett.* **1986**, *204*, 61-66.

(25) Oda, Y.; Nagasu, T.; Chait, B. T. *Nat. Biotechnol.* **2001**, *19*, 379-382.

(26) Zhou, H.; Watts, J. D.; Aebersold, R. *Nat. Biotechnol.* **2001**, *19*, 375-378.

(27) Brittain, S. M.; Ficarro, S. B.; Brock, A.; Peters, E. C. *Nat. Biotechnol.* **2005**, *23*, 463-468.

(28) Steen, H.; Mann, M. *J. Am. Soc. Mass Spectrom.* **2002**, *13*, 996-1003.

(29) Knight, Z. A.; Schilling, B.; Row, R. H.; Kenski, D. M.; Gibson, B. W.; Shokat, K. M. *Nat. Biotechnol.* **2003**, *21*, 1047-1054.

(30) Li, H.; Sundararajan, N. *J. Proteome Res.* **2007**, *6*, 2973-2977.

(31) Moss, R. A.; Bizzigotti, G. O.; Huang, C. *J. Am. Chem. Soc.* **1980**, *102*, 754-762.

(32) Ouyang, T.; Walt, D. R. *J. Org. Chem.* **1991**, *56*, 3752-3755.

(33) Jenkins, C. M.; Yan, W.; Mancuso, D. J.; Gross, R. W. *J. Biol. Chem.* **2006**, *281*, 15615-15624.

(34) Thingholm, T. E.; Jorgensen, T. J.; Jensen, O. N.; Larsen, M. R. *Nat. Protoc.* **2006**, *1*, 1929-1935.

(35) Byford, M. F. *Biochem. J.* **1991**, *280 (Pt 1)*, 261-265.

(36) Li, W.; Backlund, P. S.; Boykins, R. A.; Wang, G.; Chen, H. C. *Anal. Biochem.* **2003**, *323*, 94-102.

(37) Soderling, T. R.; Walsh, K. *J. Chromatogr.* **1982**, *253*, 243-251.

(38) Zenobi, R.; Knochenmuss, R. *Mass Spectrom. Rev.* **1998**, *17*, 337-366.

(39) Hoffmann, E. d.; Stroobant, V. *Mass Spectrometry: Principles and Applications, 2ed.*; Wiley: Chichester, 2002.

(40) Gross, R. W. *J. Lipid Mediators Cell Signalling* **1995**, *12*, 131-137.

(41) Mancuso, D. J.; Abendschein, D. R.; Jenkins, C. M.; Han, X.; Saffitz, J. E.; Schuessler, R. B.; Gross, R. W. *J. Biol. Chem.* **2003**, *278*, 22231-22236.

(42) Atsumi, G.; Murakami, M.; Kojima, K.; Hadano, A.; Tajima, M.; Kudo, I. *J. Biol. Chem.* **2000**, *275*, 18248-18258.

(43) Bohak, Z. *J. Biol. Chem.* **1964**, *239*, 2878-2887.

(44) Sanger, F. *Biochem. J.* **1949**, *44*, 126-128.

(45) Toennies, G.; Homiller, R. P. *Anal. Chem.* **1942**, *64*, 3054-3056.

(46) Chowdhury, S. K.; Eshraghi, J.; Wolfe, H.; Forde, D.; Hlavac, A. G.; Johnston, D. *Anal. Chem.* **1995**, *67*, 390-398.

(47) Finley, E. L.; Dillon, J.; Crouch, R. K.; Schey, K. L. *Protein Sci.* **1998**, *7*, 2391-2397.

(48) Wells, L.; Vosseller, K.; Cole, R. N.; Cronshaw, J. M.; Matunis, M. J.; Hart, G. W. *Mol. Cell. Proteomics* **2002**, *1*, 791-804.

(49) Vosseller, K.; Hansen, K. C.; Chalkley, R. J.; Trinidad, J. C.; Wells, L.; Hart, G. W.; Burlingame, A. L. *Proteomics* **2005**, *5*, 388-398.

(50) Gygi, S. P.; Rist, B.; Gerber, S. A.; Turecek, F.; Gelb, M. H.; Aebersold, R. *Nat. Biotechnol.* **1999**, *17*, 994-999.

(51) Whitesides, G. M.; Lilburn, J. E.; Szajewski, R. P. *J. Org. Chem.* **1977**, *42*, 332-338.

(52) Biros, S. M.; Ullrich, E. C.; Hof, F.; Trembleau, L.; Rebek, J., Jr. *J Am Chem Soc* **2004**, *126*, 2870-2876.

2.7 Table Legends

Table 2.1

Identification of phosphorylation sites in iPLA$_2$β phosphorylated by protein kinase A (PKA). Tryptic iPLA$_2$β peptides were modified by two different protocols optimized for either phosphoserine or phosphothreonine as described in the Materials and Methods section. The thiocholine-modified peptides were desalted, separated using reverse-phase nanobore HPLC and analyzed with an LTQ-Orbitrap system. Candidate peptides were identified using MASCOT with the designated thiocholine modification as well as common amino acid modifications as described in the Materials and Methods section.

16 unique sequences and 32 different phosphorylation sites were identified. "*" denotes phosphorylation sites; "$^{(*)}$" denotes that more than one phosphorylation site was identified in the same peptide. Those that were not concurrent are indicated by "/" whereas "+" indicates peptides that possessed multiple concurrent phosphorylation sites. Superscripts "^{ace}", "^{ac}", "^{d}" and "^{o}" denote the following modifications: acetylation (N-terminus), acetylation (K), deamidation (NQ) and oxidation (M), respectively. All cysteine residues were carbamidomethylated. Identified peptides with missed cleavages are listed together with the completely trypsinized peptides as indicated by bold bordered boxes. Peptides which yielded a signature neutral loss pattern in MS^3 are highlighted in bold.

Table 2.1

Sequence#	Sequence	Phosphorylation Site(s)	Δm (ppm)	Ion Score
1-23	MQFFGRLVN^{d}TLSSVTN^{d}LFS*N^{d}PFR	S13/S19	2.99	10.8
24-37	**VKEIS*VADYTS$^{(*)}$HER**	S28/S34	-1.79	38.7
24-37	**VKEIS*VADYTS*HER**	S28+S34	-1.69	23.7
26-37	**EIS*VADYTS$^{(*)}$HER**	S28/S34	-1.86	32.5
26-37	**EIS*VADYTS*HER**	S28+S34	-0.99	23.0
38-53	**VREEGQLILFQNAS*NR**	S51	-1.01	33.8
208-232	NAS*AGLNQVN^{d}KQGLTPLHLACQMGK	S210	2.87	5.7
246-261	**CN^{d}VMGPS*GFPIHT$^{(*)}$AMK**	S252/T258	-1.24	31.7
266-282	^{ace}GCAEM^{o}IISMDS*S*QIHS*K^{ac}	S276+S277+S281	-1.35	12.2
306-327	^{ace}RGCDVDST*S*AAGN^{d}T*ALHVAVM^{o}R	T313+S314+T319	0.45	4.6
307-327	GCDVDSTSAAGNT*ALHVAVM^{o}R	T319	1.29	12.2
393-405	**^{ace}ISK^{ac}Q^{d}LQ^{d}DLMPIS*R**	S404	3.91	7.4
396-405	QLQ^{d}DLMPIS*R	S404	-3.46	12.5
406-417	ARKPAFILS*S$^{(*)}$MR	S414/S415	-1.02	37.0
406-420	**ARKPAFILS*S$^{(*)}$MRDEK**	S414/S415	-2.00	9.3
408-417	**KPAFILS*S$^{(*)}$MR**	S414/S415	-1.76	32.0
408-420	**KPAFILS*S$^{(*)}$MRDEK**	S414/S415	-1.29	20.0
479-489	S*MAYMRGVYFR	S479	-5.00	13.6
492-511	**DEVFRGS*RPYESGPLEEFLK^{ac}**	S498	1.60	6.2
497-511	GS*RPYES*GPLEEFLK	S498+S503	-1.78	13.2
497-511	**GS*RPYES$^{(*)}$GPLEEFLK**	S498/S503	-0.28	54.5
513-524	EFGEHT*KM^{o}T$^{(*)}$DVK	T518/T521	-3.32	6.3
520-527	^{ace}MT$^{(*)}$DVK^{ac}KPK	T521	3.18	16.3
528-537	**VMLT*GTLS$^{(*)}$DR**	T531/S535	-1.84	28.0
528-537	VM^{o}LT*GTLS*DR	T531+T533	0.61	15.5
582-595	**SS*GAAPT$^{(*)}$YFRPN^{d}GR**	S583/T588	-0.89	39.9
632-643	^{ace}K^{ac}LS*IVVS$^{(*)}$LGT$^{(*)}$GR	S634/S638/T641	3.54	13.1
644-665	SPQVPVTCVDVFRPS*NPWELAK	S658	1.07	3.6
692-705	**^{ace}ARAWS*EM^{o}VGIQ^{d}YFR**	S696	2.56	4.5
694-705	**AWS*EMVGIQYFR**	S696	-1.95	22.1

2.8 Figure Legends

Figure 2.1 Optimization of β-elimination and Michael addition (BEMA) reaction conditions for phosphorylated serine containing peptides using the model peptide FQpSEEQQQTEDELQDK.

The model peptide FQpSEEQQQTEDELQDK was modified using BEMA with thiocholine as described in the Materials and Methods section. The β-elimination and Michael addition reactions were terminated at the indicated time intervals. The resultant reaction mixtures were separated on an HPLC reverse-phase column (C_{18}, 150 x 4.6mm) and the peptides were detected with a UV monitor at λ = 206 nm. The β-elimination reaction was complete within 40 mins and Michael addition was complete in approximately 60 min.

Figure 2.2 Comparison of the ionization efficiency of the phosphopeptide FQpSEEQQQTEDELQDK ▲() and its thiocholine-modified derivative FQS*EEQQQTEDELQDK (■).

The model peptide FQpSEEQQQTEDELQDK was modified via BEMA with thiocholine as described in the Materials and Methods section and an equivalent amount of the original unmodified phosphopeptide FQpSEEQQQTEDELQDK was added. The quantitative yields of the BEMA reactions were similar to those shown in Figure 1. "pS" indicates the phosphorylation site and "S*" indicates the thiocholine-modified site.

A. Separation of the peptide mixture using a reverse-phase C_{18} column and analysis

employing an ESI-LTQ-Orbitrap as described in the Materials and Methods section. The full-mass scan extracted ion chromatography (XIC) of ions at *m/z* 694.983 (+3) and 1031.417 (+2) with normalized ion intensities is presented. The ion at *m/z* 694.983 corresponds to the triply charged molecular ion (dominant charge state) of FQS*EEQQQTEDELQDK (■) and the ion at *m/z* 1031.417 corresponds to the doubly charged molecular ion (dominant charge state) of FQpSEEQQQTEDELQDK (▲). The XIC shows a marked increase in ionization efficiency of the peptide after thiocholine modification.

B. The full mass spectrum of the 1:1 peptide mixture obtained with a 4800 MALDI-TOF/TOF Analyzer with normalized ion intensity. The ion peak at *m/z* 2061.52 corresponds to the singly charged molecular ion of FQpSEEQQQTEDELQDK (▲) and the ion peak at *m/z* 2082.62 corresponds to the singly charged molecular ion of FQS*EEQQQTEDELQDK (■). A 3-fold increase in ionization efficiency of the peptide after thiocholine modification was observed with MALDI-MS.

Figure 2.3 Detection limit for the thiocholine-modified peptide FQS*EEQQQTEDELQDK.

Extracted ion chromatogram (XIC) and product-ion spectra were acquired with an LTQ-Orbitrap as described in the Materials and Methods section.

A. Extracted ion chromatogram of the thiocholine-modified model peptide FQS*EEQQQTEDELQDK at *m/z* 694.983 (+3) at the concentration of 500 amol/ul (Ion counts = 2.01E3).

B. The full mass spectrum of the thiocholine-modified model peptide FQS*EEQQQTEDELQDK at *m/z* 694.983 (+3) at the concentration of 500 amol/ul (Ion counts = 2.01E3, Signal-to-Noise = 4).

Figure 2.4 Optimization of β-elimination and Michael addition reaction conditions for the phosphorylated threonine containing peptide: DHTGFLpTEYVATR (i).

The β-elimination of DHTGFLpTEYVATR was terminated at the indicated time intervals. The resultant reaction mixtures were separated on an HPLC reverse-phase column (C18, 150x4.6mm) and the peptides were detected with a UV monitor at λ = 206 nm.

Figure 2.5 Optimization of β-elimination and Michael addition reaction conditions for the phosphorylated threonine containing peptide: DHTGFLpTEYVATR (ii).

The phosphothreonine containing peptide, DHTGFLpTEYVATR, was subject to 3h $Ba(OH)_2$ catalyzed β-elimination followed by overnight room-temperature incubation with thiocholine to effect Michael addition. The full mass spectrum of the resulting thiocholine addition product was acquired on a 4800 MALDI-TOF/TOF analyzer. The spectrum was remarkable for the predominance of the undesired oxidation of the histidine residue (denoted H^o) and N-terminal acetylation (denoted ^{ace}D) (*m/z* 1549.47). Only minimal amounts of the desired Michael adduct (*m/z* 1610.47) was observed under these conditions.

Figure 2.6 Optimization of β-elimination and Michael addition reaction conditions for the phosphorylated threonine containing peptide: DHTGFLpTEYVATR (iii).

The β-elimination and Michael addition of thiocholine to DHTGFLpTEYVATR were carried out under nitrogen and the intermediate products of β-elimination were purified with a POROS R2 micro-column as described in the Materials and Methods section before undergoing Michael addition at pH = 8-9. Extracted ion chromatogram (XIC) and product-ion spectra were acquired with an LTQ-Orbitrap as described in the Materials and Methods section.

A. Extracted ion chromatogram of the thiocholine-modified peptide DHTGFLT*EYVATR and its β-elimination product DHTGFLT^{de}EYVATR after 5h of incubation with thiocholine at room temperature demonstrated minimal thiocholine addition.

B. Extracted ion chromatogram of the thiocholine-modified peptide DHTGFLT*EYVATR and its β-elimination product DHTGFLT^{de}EYVATR after 5h of incubation with thiocholine at 50°C showing a significantly improved yield.

C./ D. The product-ion spectra of DHTGFLT*EYVATR of the two XIC peaks from Figure S3-B at RT = 21.96 min and 25.32 min. No substantial differences between the spectra were observed. The difference in retention times implies the formation of diastereomers during the Michael addition reaction.

E. The product-ion spectrum of the β-elimination product DHTGFLT^{de}EYVATR.

Figure 2.7 Fragmentation of the thiocholine-modified peptide FQS*EEQQQTEDELQDK.

A. The product-ion spectrum of the triply charged molecular ion of FQS*EEQQQTEDELQDK at *m/z* 694.983 was obtained with an ESI-LTQ-Orbitrap as described in the Materials and Methods section. The fragment ion resulting from the neutral loss of trimethylamine from the parent ion was not detected. Shown in the expanded spectrum is an example of the diagnostic triad consisting of the b_5^+ ion resulting from peptide bond cleavage (*m/z* = 722.3) and further neutral losses of trimethylamine (-59 Da, *m/z* = 663.2) or the thiocholine thiolate (-119 Da, *m/z* = 603.2). "S*" indicates the thiocholine-modified site.

B. The MS^3 spectrum of the y_{14}^{+2} ion at *m/z* 904.4 resulting from the fragmentation of the triply charged molecular ion of FQS*EEQQQTEDELQDK at *m/z* 694.983. The ion peak at *m/z* 875.1 corresponds to the doubly charged fragment ion generated from the neutral loss of trimethylamine from the parent ion y_{14}^{+2}.

C. The product-ion spectrum of the singly charged molecular ion of FQS*EEQQQTEDELQDK at *m/z* 2082.62, obtained with a 4800 MALDI-TOF/TOF Analyzer as described in the Materials and Methods section. The ion peak at *m/z* 2023.72 corresponds to the fragment ion resulting from the neutral loss of trimethylamine from the parent ion. Shown in the expanded spectrum are the low-abundance y ions.

Figure 2.8 The product-ion spectrum of the doubly charged molecular ion for the thiocholine-modified model peptide FQS*EEQQQTEDELQDK at *m/z* 1041.964, acquired with an LTQ-Orbitrap as described in the Materials and Methods section. The ion peak at *m/z* 1012.5 corresponds to the fragment ion generated from the neutral loss of trimethylamine from the parent ion.

Figure 2.9 The product-ion spectrum of the thiocholine-modified peptide $C^aN^dVMGPS*GFPIHTAMK$ at *m/z* 616.958, acquired with an LTQ-Orbitrap as described in the Materials and Methods section.

The identification of the PKA mediated phosphorylation of iPLA$_2$β at Ser252 following reductive alkylation and thiocholine modification demonstrates that the peptide contains both an alkylated cysteine and a thiocholine-modified serine, showing the compatibility of routine reductive alkylation with Ba^{2+} catalyzed BEMA.

Figure 2.10 Sequence coverage comparison between the thiocholine-modified peptide $SS*GAAPTYFRPN^dGR$ and the phosphopeptide $p(SS)GAAPTYFRPN^dGR$ identified in protein kinase A (PKA) phosphorylated calcium-independent phospholipase A$_2$β (iPLA$_2$β).

A. Identification of PKA mediated phosphorylation of iPLA$_2$β at Ser583 via thiocholine modification. $SS*GAAPTYFRPN^dGR$ was identified after *in vitro* PKA catalyzed phosphorylation of iPLA$_2$β with subsequent thiocholine modification as described in the Materials and Methods section. Spectra were acquired using an LTQ-Orbitrap equipped

with an electrospray ion source. The product-ion spectrum of the triply charged molecular ion (dominant charge state) at *m/z* 528.264 shows a dominant y_{13}^{+3} peak leading to unambiguous assignment of the phosphosites. Also shown in the expanded spectrum (relative intensity zoom = 25%) are the diagnostic triad consisting of y_{13}^{+3} (*m/z* = 499.4), the ion from the neutral loss of trimethylamine, $y_{13} - 59^{+3}$ (*m/z* = 479.1), and the ion from neutral loss of the thiocholine thiolate, $y_{13} - 119^{+3}$ (*m/z* = 459.3), as well as the peak corresponding to the loss of the thiocholine thiolate from the molecular ion $M - 119^{+3}$ (*m/z* = 488.9).

B. Identification of PKA mediated phosphorylation of $iPLA_2\beta$ at Ser582/Ser583 without thiocholine modification. p(SS)GAAPTYFRPN^{d}GR was identified in PKA phosphorylated $iPLA_2\beta$ without thiocholine modification by ESI-LTQ-Orbitrap. The product-ion spectrum of the doubly charged molecular ion (dominant charge state) at *m/z* 781.336 shows a strong ion peak at *m/z* 732.1 which corresponds to the neutral loss of H_3PO_4 from the parent ion. The fragment ions from Ser-Ser peptide bond cleavage are missing due to the cyclo-elimination of H_3PO_4. The specific site of phosphorylation could not be assigned from this approach. "p(SS)" indicates either serine residue may be phosphorylated, "S*" indicates the thiocholine-modified site and "N^{d}" indicates the deamidation of the asparagine residue.

Figure 2.11 Fragmentation of the thiocholine-modified peptide EIS*VADYTSHER identified in PKA phosphorylated $iPLA_2\beta$ at both the MS^2 and MS^3 levels.

A. The product-ion spectrum of the triply charged molecular ion at *m/z* 536.933

(EIS*VADYTSHER) was obtained with an ESI-LTQ-Orbitrap as described in the Materials and Methods section. The fragment ion resulting from the neutral loss of trimethylamine from the parent ion was not detected. Shown in the expanded spectrum are examples of the diagnostic triad consisting of the y_{10}^{+2} and b_6^{+} fragmentation ions resulting from peptide bond cleavage (*m/z* = 633.6 and 716.3) and further neutral loss of trimethylamine (-59 Da, *m/z* = 603.3 and 657.2) or the thiocholine thiolate (-119 Da, *m/z* = 574.1 and 597.2). "S*" indicates the thiocholine-modified site.

B. MS^3 spectrum of the y_{10}^{+2} ion at *m/z* 633.6 resulting from the fragmentation of the triply charged molecular ion at *m/z* 536.933 (EIS*VADYTSHER) obtained with an ESI-LTQ-Orbitrap as described in the Materials and Methods section. The ion peak at *m/z* 604.0 corresponds to the doubly charged fragment ion generated from the neutral loss of trimethylamine from the parent ion y_{10}^{+2}.

Figure 2.12 C**omparative quantification of phosphoproteins evaluated using β-casein as a model protein.**

Equal amounts of trypsinized β-Casein were modified with either "light" ($^{12}C,^{1}H$) or "heavy" ($^{13}C,d_3$) thiocholine and mixed at a 1:1 ratio (v/v). The mixture was separated on a reverse-phase C_{18} column and analyzed by an ESI-LTQ-Orbitrap as described in the Materials and Methods section. The full mass spectrum of the modified peptides is shown at the time of their co-elution. A doublet pattern of the peptides modified by "light" and "heavy" thiocholine is evident. The ion intensity ratio of "light" *vs.* "heavy" thiocholine-modified peptides obtained from full-mass spectra was 0.96±0.02 (average

adjusted ratio of five replicates with an expected ion intensity ratio of 1). "S*" indicates the $^{12}C,^{1}H$-thiocholine-modified site; "S**" indicates the $^{13}C,d_3$ thiocholine-modified site.

Figure 2.13 Comparison of the retention time of the thiocholine(*) and thiocholine-13C,d3(**)-modified peptides FQS*EEQQQTEDELQDK and FQSEEQQQTEDELQDK from the model protein β-casein.**

Two equal aliquots (1 and 2) of trypsinized β-casein were modified with thiocholine and thiocholine-13C,d3 respectively as described in the Materials and Methods section. Modified peptides of β-casein in aliquots 1 and 2 were then mixed at 1:1 (v:v; aliquot 1: aliquot 2, or light: heavy). The mixture was analyzed with a reverse phase HPLC-ESI-Orbitrap system as described in the Materials and Methods section. Shown are the extracted ion chromatograms of the thiocholine and thiocholine-13C,d3-modified peptides: FQS*EEQQQTEDELQDK (*m/z* 694.983; dashed line "---") and FQS**EEQQQTEDELQDK (*m/z* 696.323; solid line "—"). No chromatographic shift was observed between light and heavy thiocholine-modified peptides. The light versus heavy ratios (from data points A, B and C) are consistent at 0.96±0.02 with an expected ratio of 1 during the elution of the peak.

Figure 2.1

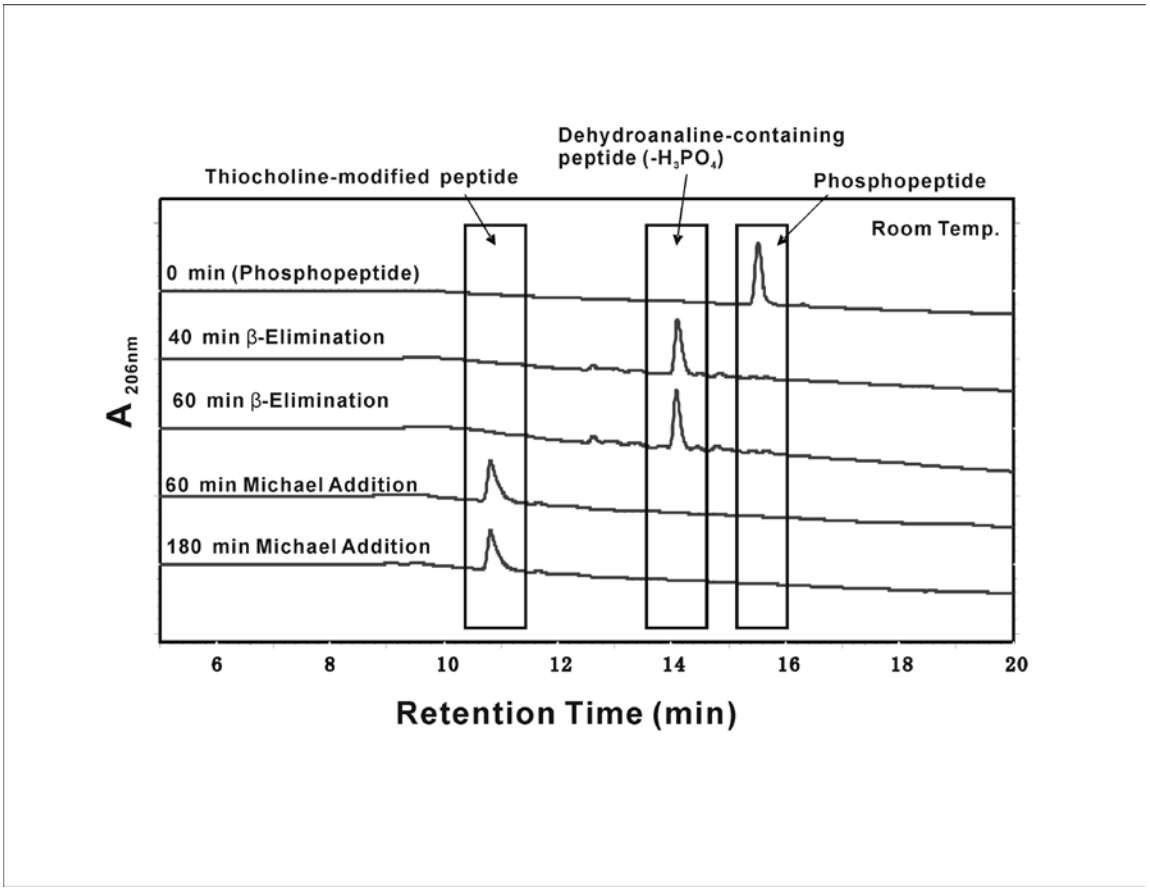
Dehydroanaline-containing peptide (-H3PO4)
Thiocholine-modified peptide
Phosphopeptide
Room Temp.
0 min (Phosphopeptide)
40 min β-Elimination
60 min β-Elimination
60 min Michael Addition
180 min Michael Addition
A206nm
6
8
10
12
14
16
18
20
Retention Time (min)

Figure 2.2

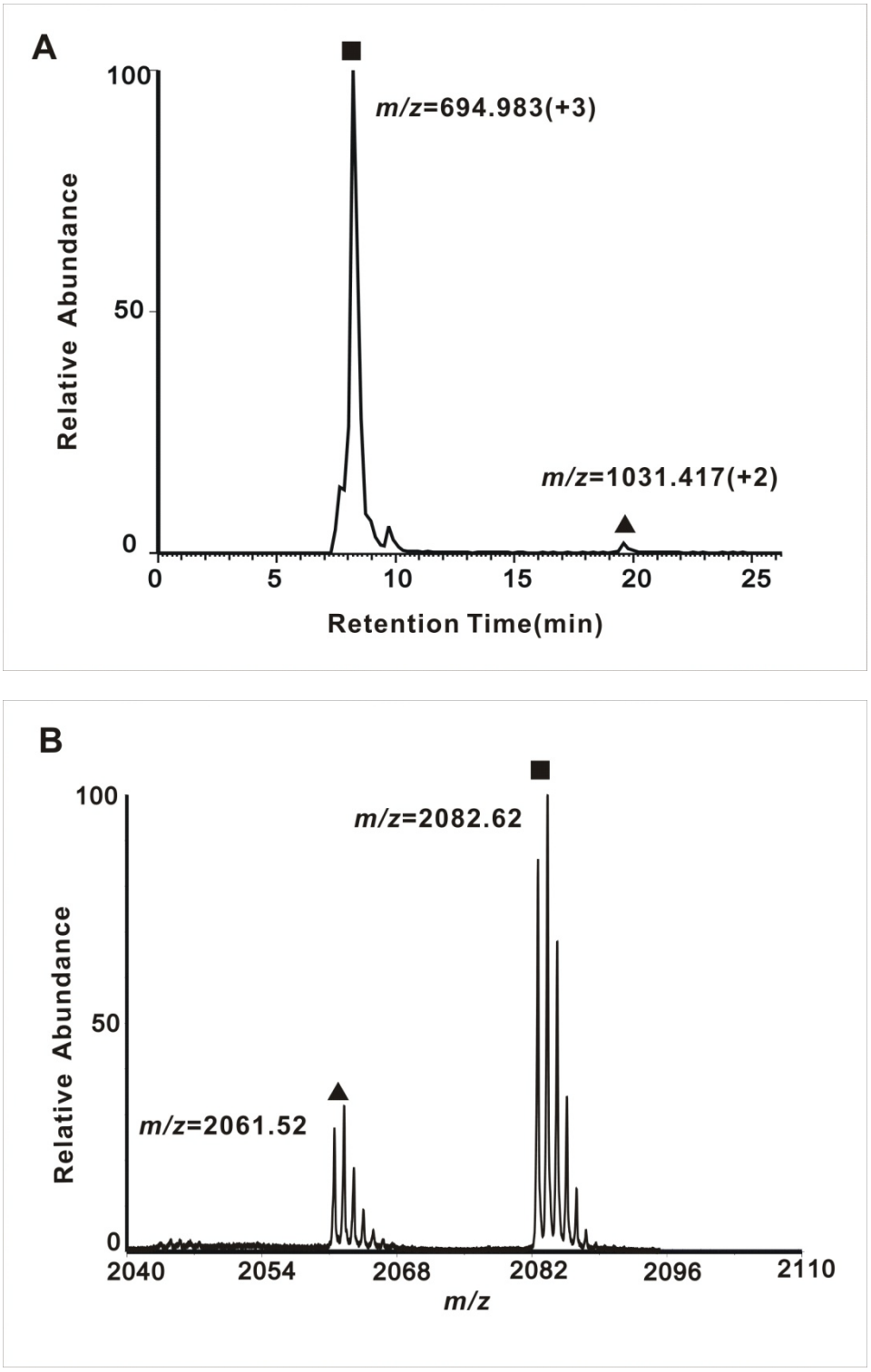
A
100
50
0
Relative Abundance
m/z=694.983(+3)
m/z=1031.417(+2)
0
5
10
15
20
25
Retention Time(min)
B
100
50
0
Relative Abundance
m/z=2082.62
m/z=2061.52
2040
2054
2068
2082
2096
2110
m/z

Figure 2.3

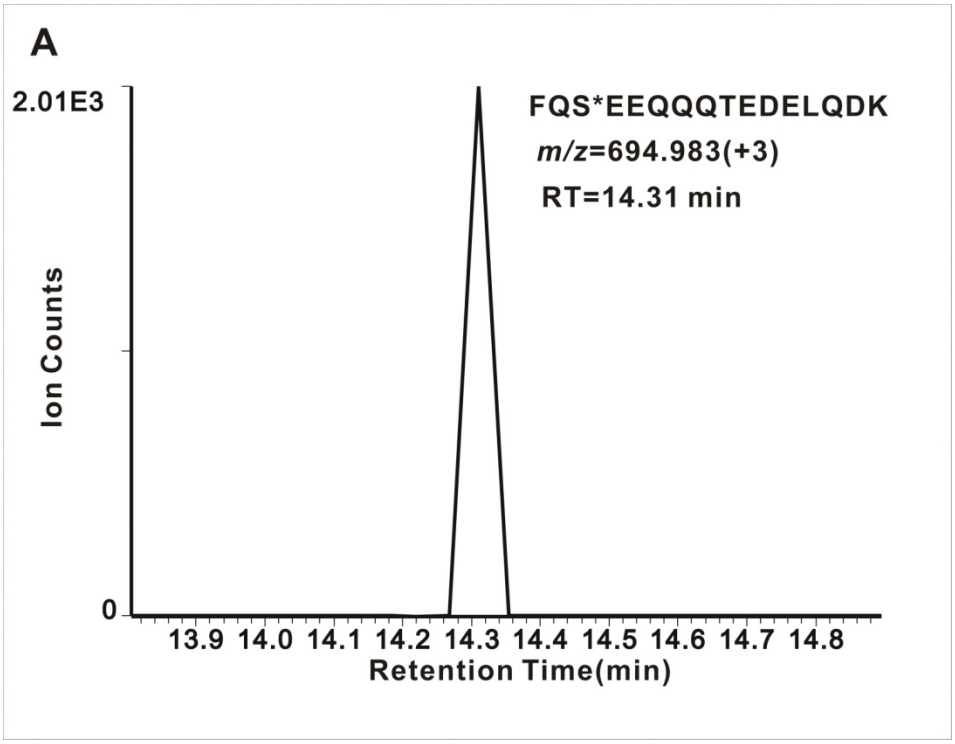
A
2.01E3
FQS*EEQQQTEDELQDK
m/z=694.983(+3)
RT=14.31 min
Ion Counts
0
13.9 14.0 14.1 14.2 14.3 14.4 14.5 14.6 14.7 14.8
Retention Time(min)

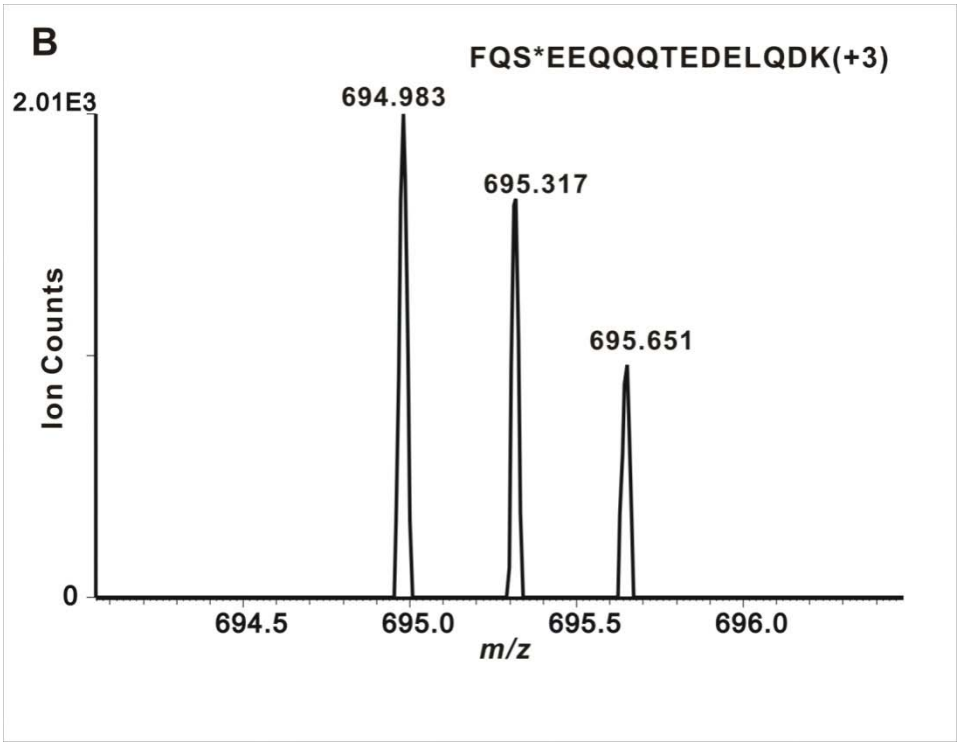
B
FQS*EEQQQTEDELQDK(+3)
2.01E3
694.983
695.317
695.651
Ion Counts
0
694.5
695.0
695.5
696.0
m/z

Figure 2.4

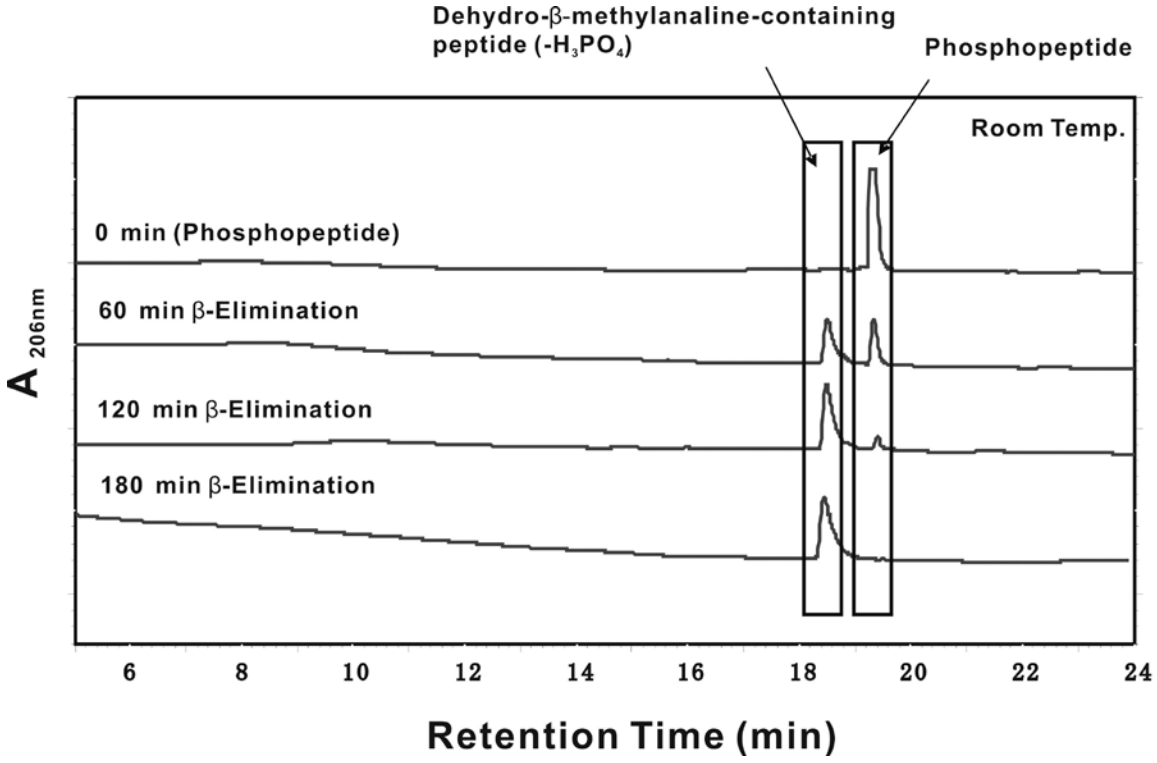
Dehydro-β-methylanaline-containing peptide (-H3PO4)
Phosphopeptide
Room Temp.
0 min (Phosphopeptide)
60 min β-Elimination
120 min β-Elimination
180 min β-Elimination
A 206nm
6
8
10
12
14
16
18
20
22
24
Retention Time (min)

Figure 2.5

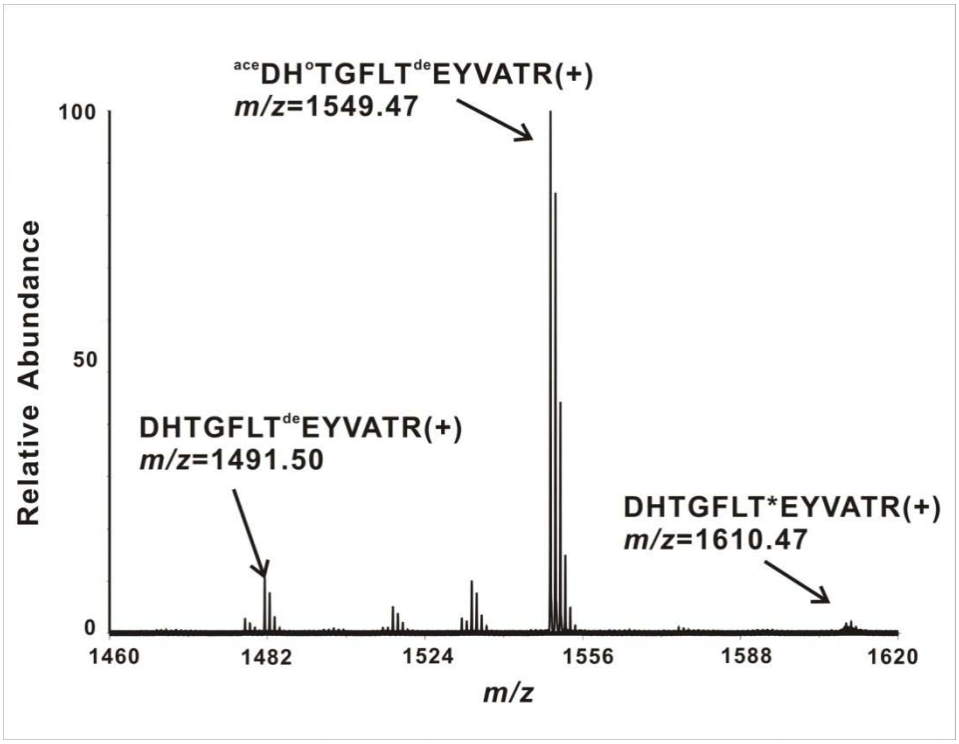
aceDHoTGFLTdeEYVATR(+)
m/z=1549.47
DHTGFLTdeEYVATR(+)
m/z=1491.50
DHTGFLT*EYVATR(+)
m/z=1610.47
Relative Abundance
100
50
0
1460
1482
1524
1556
1588
1620
m/z

Figure 2.6

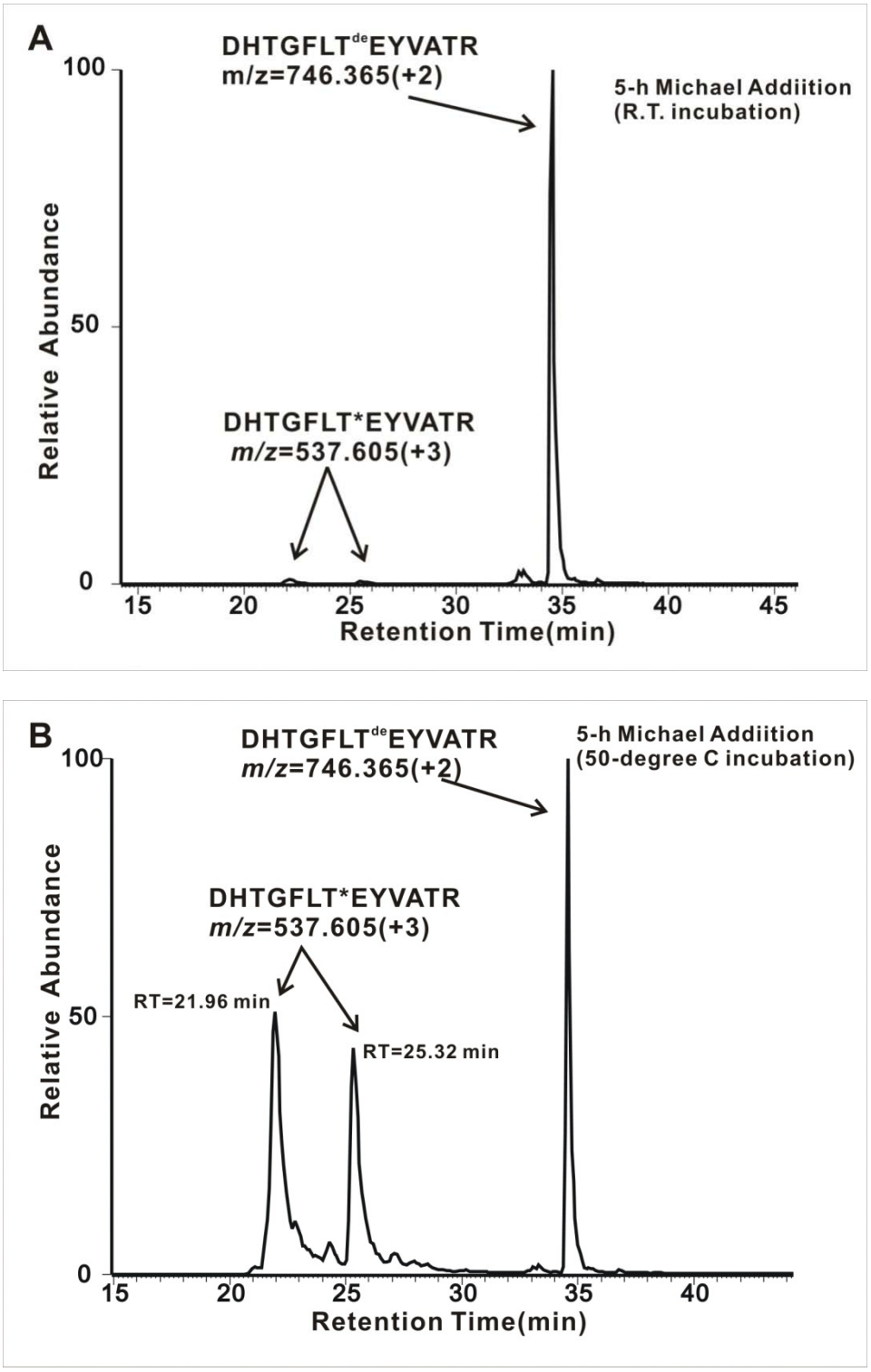
A
DHTGFLT^deEYVATR
m/z=746.365(+2)
5-h Michael Addiition
(R.T. incubation)
DHTGFLT*EYVATR
m/z=537.605(+3)
Relative Abundance
100
50
0
15
20
25
30
35
40
45
Retention Time(min)
B
DHTGFLT^deEYVATR
m/z=746.365(+2)
5-h Michael Addiition
(50-degree C incubation)
DHTGFLT*EYVATR
m/z=537.605(+3)
RT=21.96 min
RT=25.32 min
Relative Abundance
100
50
0
15
20
25
30
35
40
Retention Time(min)

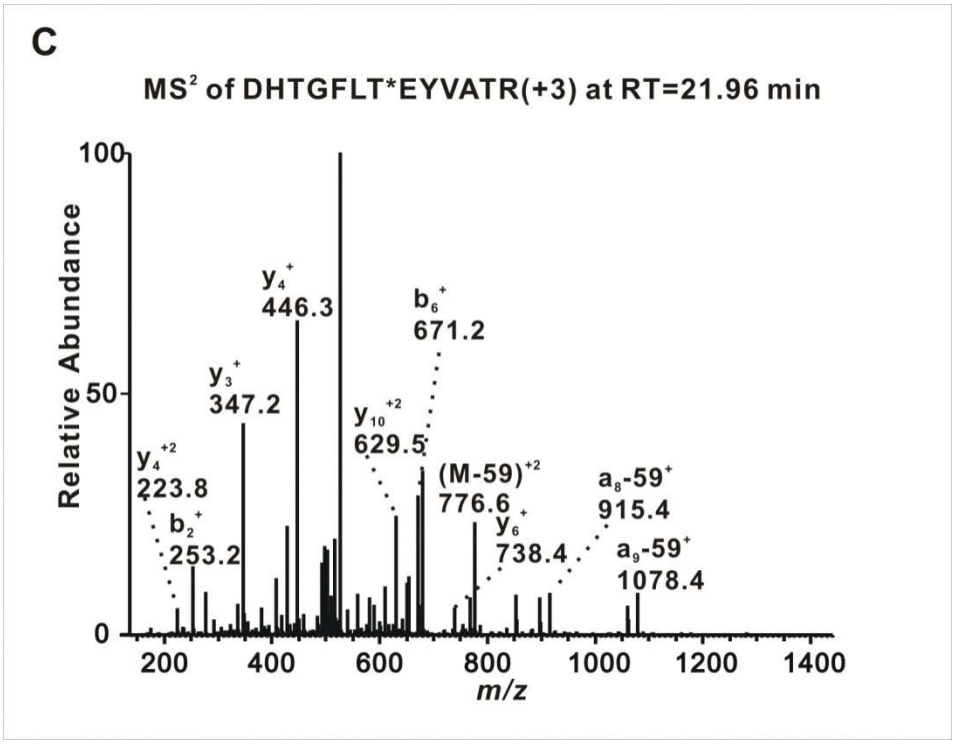
C
MS² of DHTGFLT*EYVATR(+3) at RT=21.96 min
Relative Abundance
m/z
y4+ 446.3
b6+ 671.2
y3+ 347.2
y10+2 629.5
y4+2 223.8
(M-59)+2 776.6
a8-59+ 915.4
b2+ 253.2
y6+ 738.4
a9-59+ 1078.4

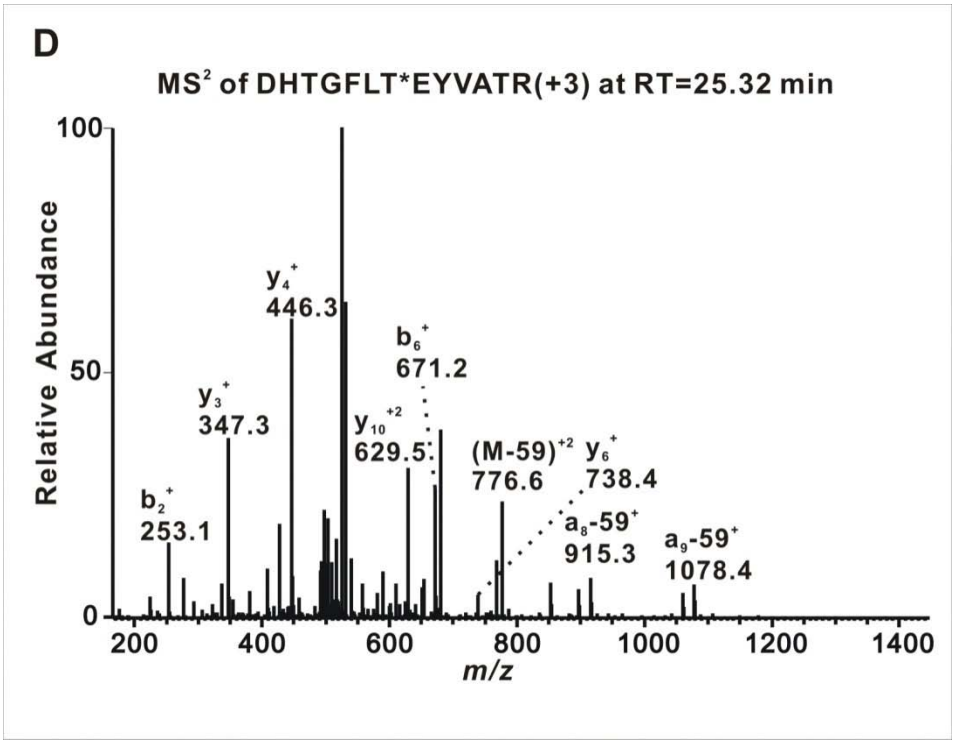
D
MS² of DHTGFLT*EYVATR(+3) at RT=25.32 min
Relative Abundance
m/z
y4+ 446.3
b6+ 671.2
y3+ 347.3
y10+2 629.5
(M-59)+2 776.6
y6+ 738.4
b2+ 253.1
a8-59+ 915.3
a9-59+ 1078.4

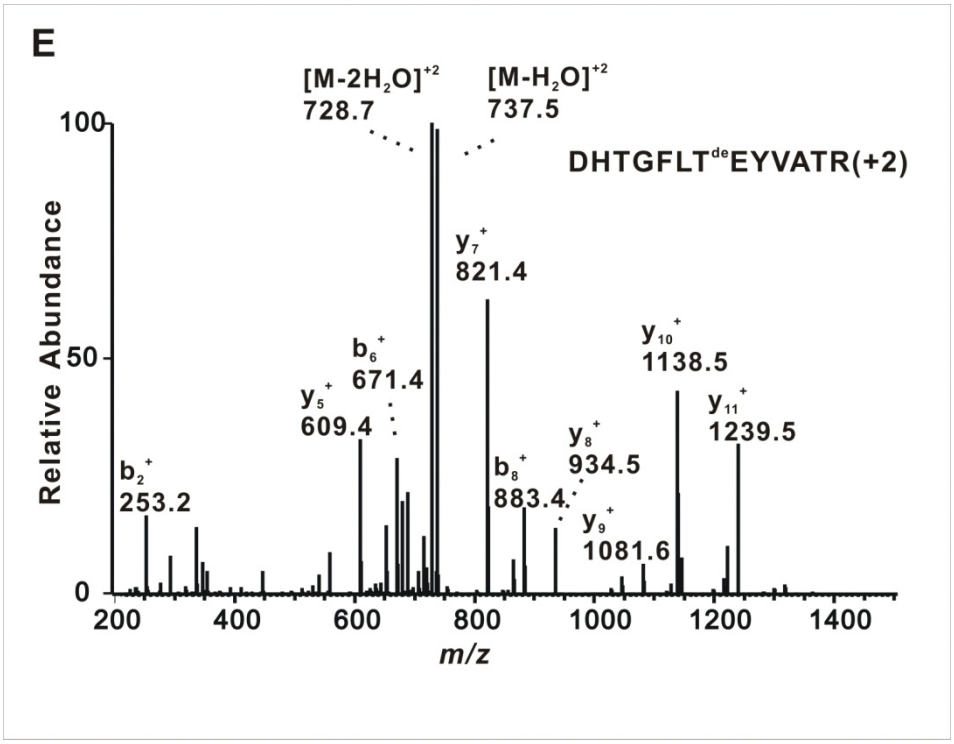
E
[M-2H2O]+2
728.7
[M-H2O]+2
737.5
DHTGFLTdeEYVATR(+2)
y7+
821.4
b6+
671.4
y5+
609.4
y10+
1138.5
y11+
1239.5
y8+
934.5
b8+
883.4
y9+
1081.6
b2+
253.2
Relative Abundance
100
50
0
200
400
600
800
1000
1200
1400
m/z

Figure 2.7

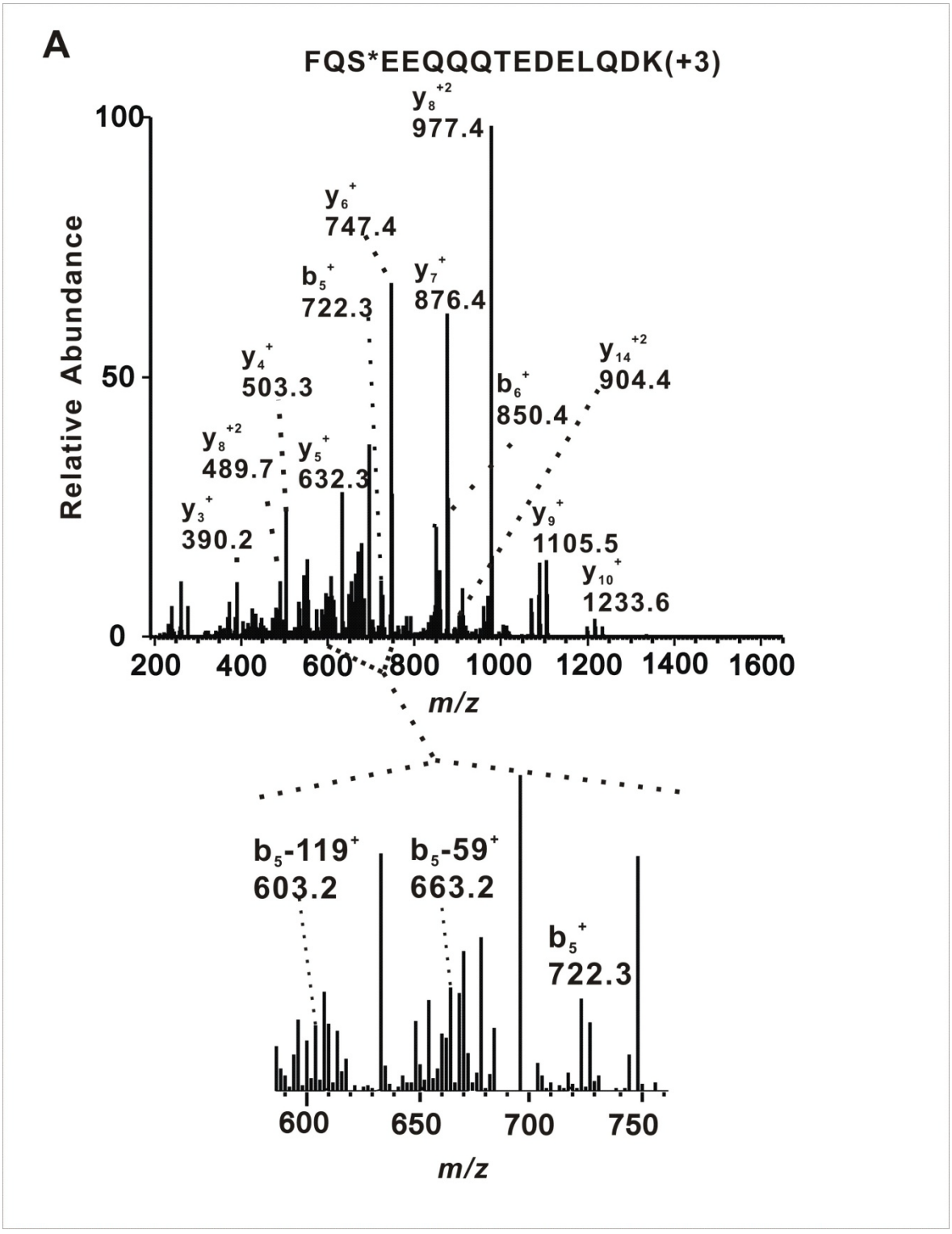
A
FQS*EEQQQTEDELQDK(+3)
Relative Abundance
100
50
0
200
400
600
800
1000
1200
1400
1600
m/z
y8+2 977.4
y6+ 747.4
b5+ 722.3
y7+ 876.4
y4+ 503.3
y14+2 904.4
b6+ 850.4
y8+2 489.7
y5+ 632.3
y3+ 390.2
y9+ 1105.5
y10+ 1233.6
b5-119+ 603.2
b5-59+ 663.2
b5+ 722.3
600
650
700
750
m/z

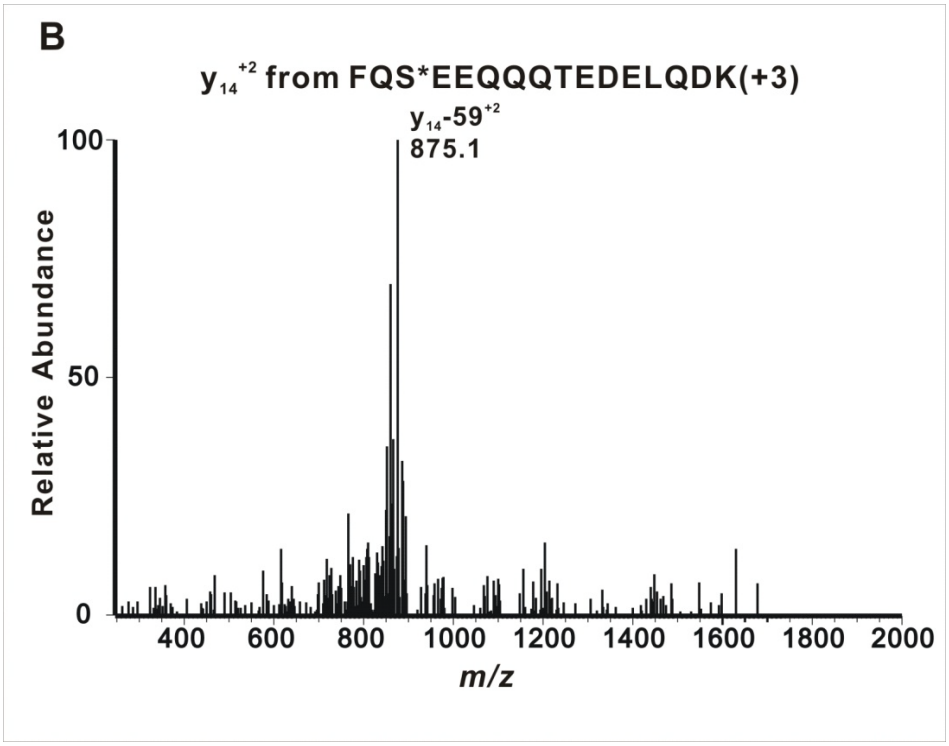
B
y_{14}^{+2} from FQS*EEQQQTEDELQDK(+3)
y_{14}-59^{+2}
875.1
100
50
0
Relative Abundance
400
600
800
1000
1200
1400
1600
1800
2000
m/z

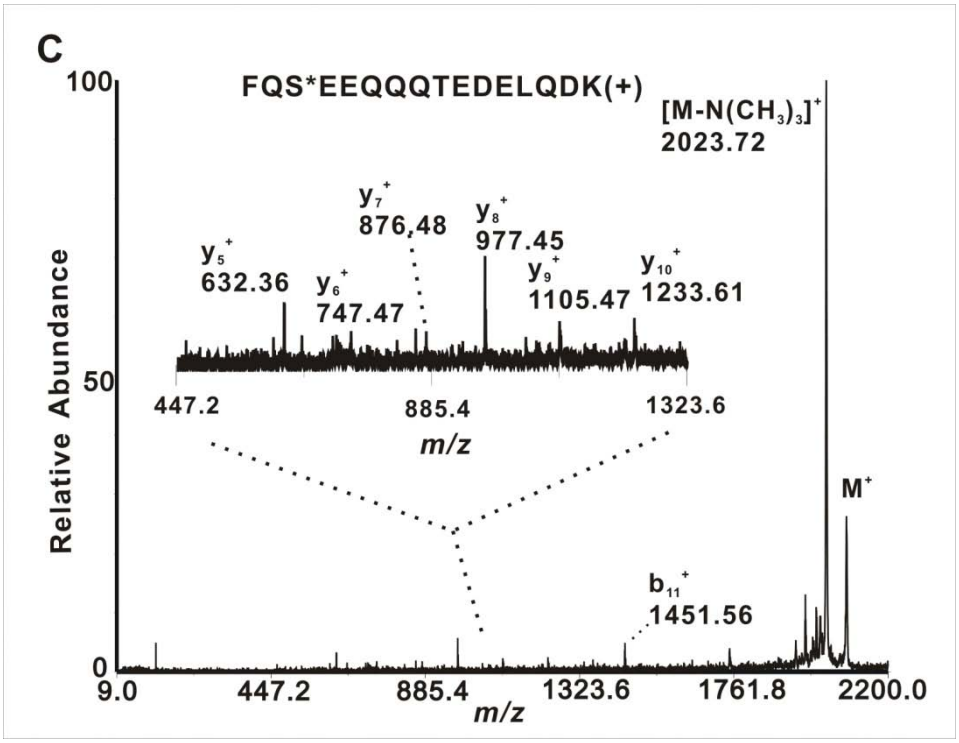
C
FQS*EEQQQTEDELQDK(+)
$[M-N(CH_3)_3]^+$
2023.72
y_7^+
876.48
y_8^+
977.45
y_5^+
632.36
y_6^+
747.47
y_9^+
1105.47
y_{10}^+
1233.61
447.2
885.4
1323.6
m/z
M^+
b_{11}^+
1451.56
100
50
0
Relative Abundance
9.0
447.2
885.4
1323.6
1761.8
2200.0
m/z

Figure 2.8

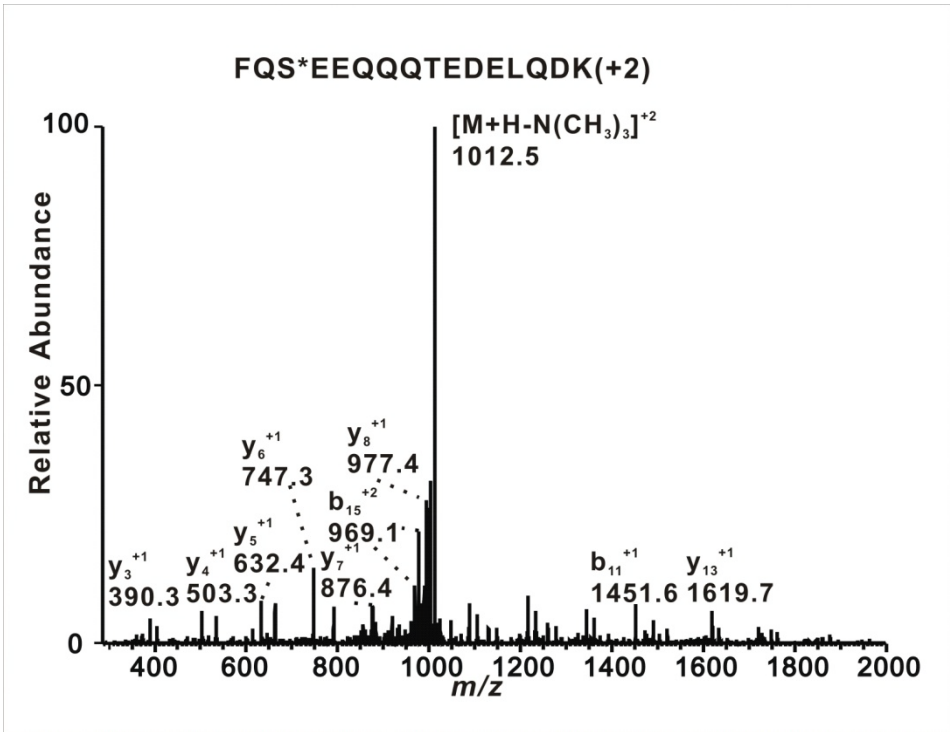
FQS*EEQQQTEDELQDK(+2)
100
50
0
Relative Abundance
[M+H-N(CH3)3]+2
1012.5
y6+1
747.3
y8+1
977.4
b15+2
969.1
y5+1
632.4
y7+1
876.4
y3+1
390.3
y4+1
503.3
b11+1
1451.6
y13+1
1619.7
400
600
800
1000
1200
1400
1600
1800
2000
m/z

Figure 2.9

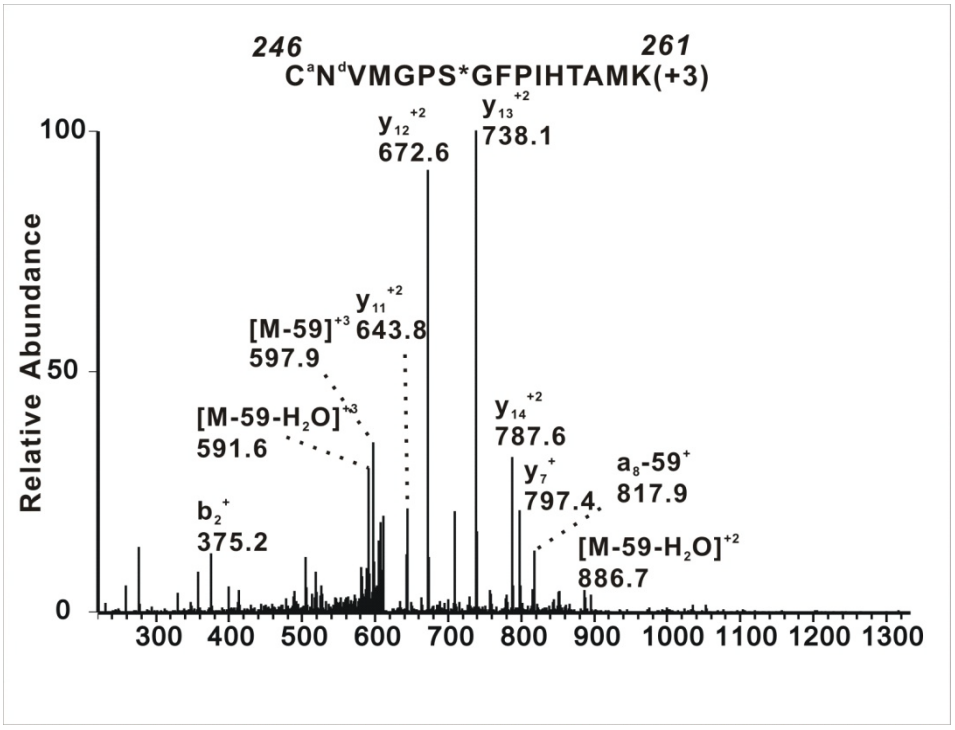
246
261
C[a]N[d]VMGPS*GFPIHTAMK(+3)
y12 +2 672.6
y13 +2 738.1
y11 +2 643.8
[M-59]+3 597.9
[M-59-H2O]+3 591.6
y14 +2 787.6
y7 + 797.4
a8-59+ 817.9
b2 + 375.2
[M-59-H2O]+2 886.7
Relative Abundance
100
50
0
300 400 500 600 700 800 900 1000 1100 1200 1300

Figure 2.10

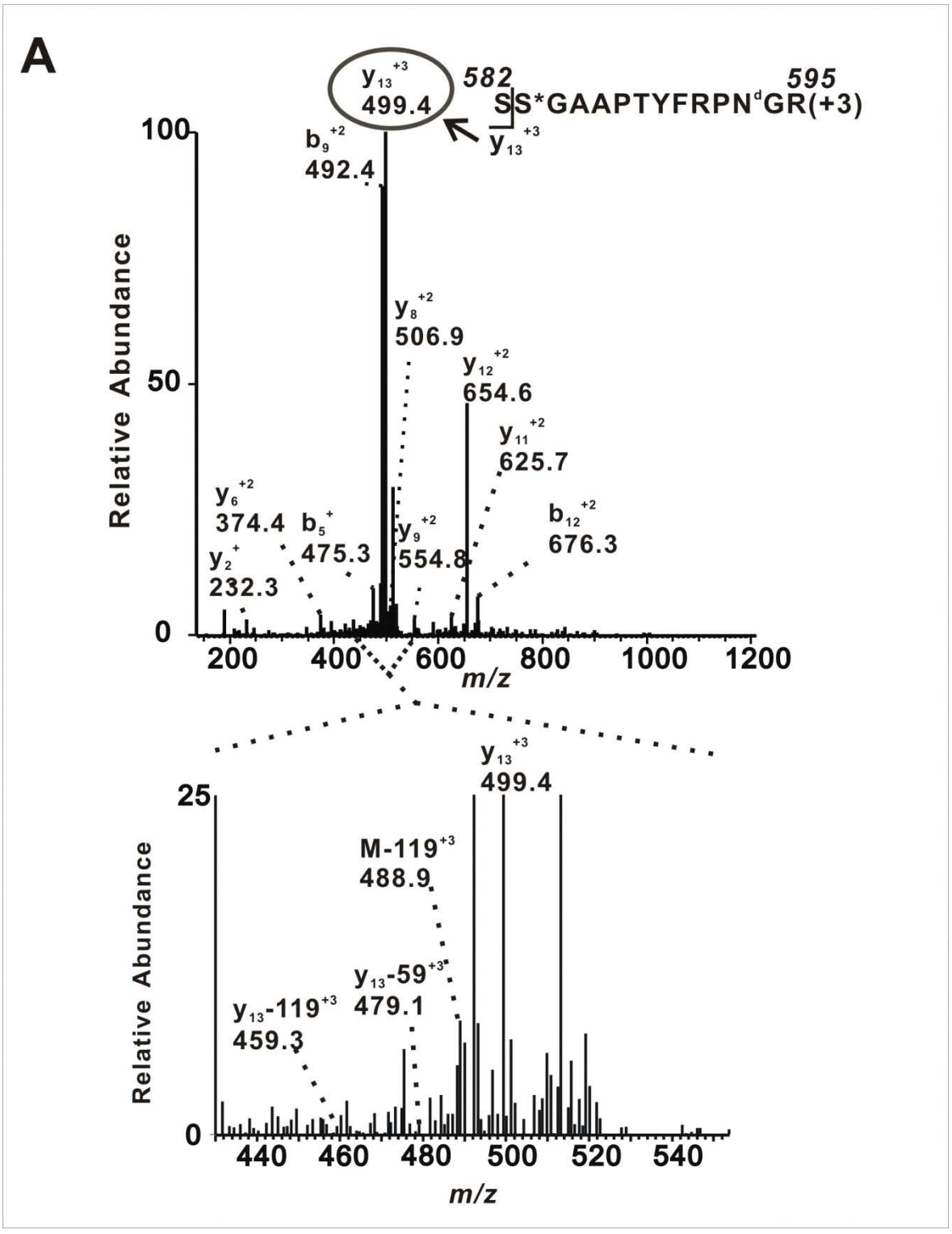
A
582
595
SS*GAAPTYFRPNdGR(+3)
y13 +3 499.4
y13 +3
b9 +2 492.4
y8 +2 506.9
y12 +2 654.6
y11 +2 625.7
b12 +2 676.3
y6 +2 374.4
b5 + 475.3
y9 +2 554.8
y2 + 232.3
Relative Abundance
m/z
M-119 +3 488.9
y13-59 +3 479.1
y13-119 +3 459.3

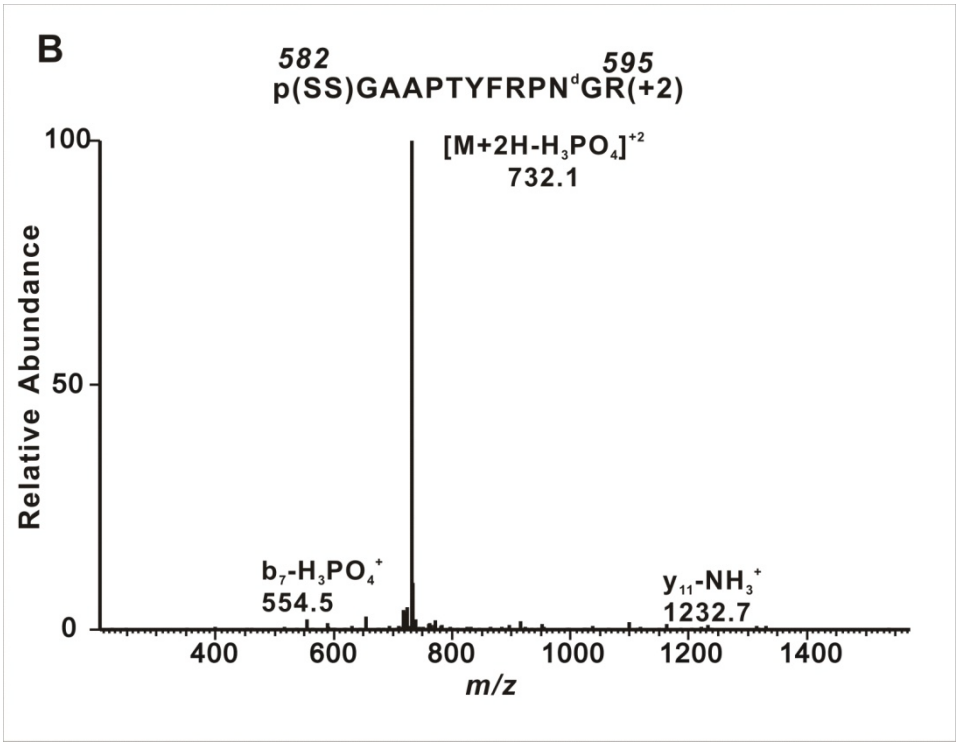
B
582
595
p(SS)GAAPTYFRPN^dGR(+2)
100
50
0
Relative Abundance
[M+2H-H3PO4]+2
732.1
b7-H3PO4+
554.5
y11-NH3+
1232.7
400
600
800
1000
1200
1400
m/z

Figure 2.11

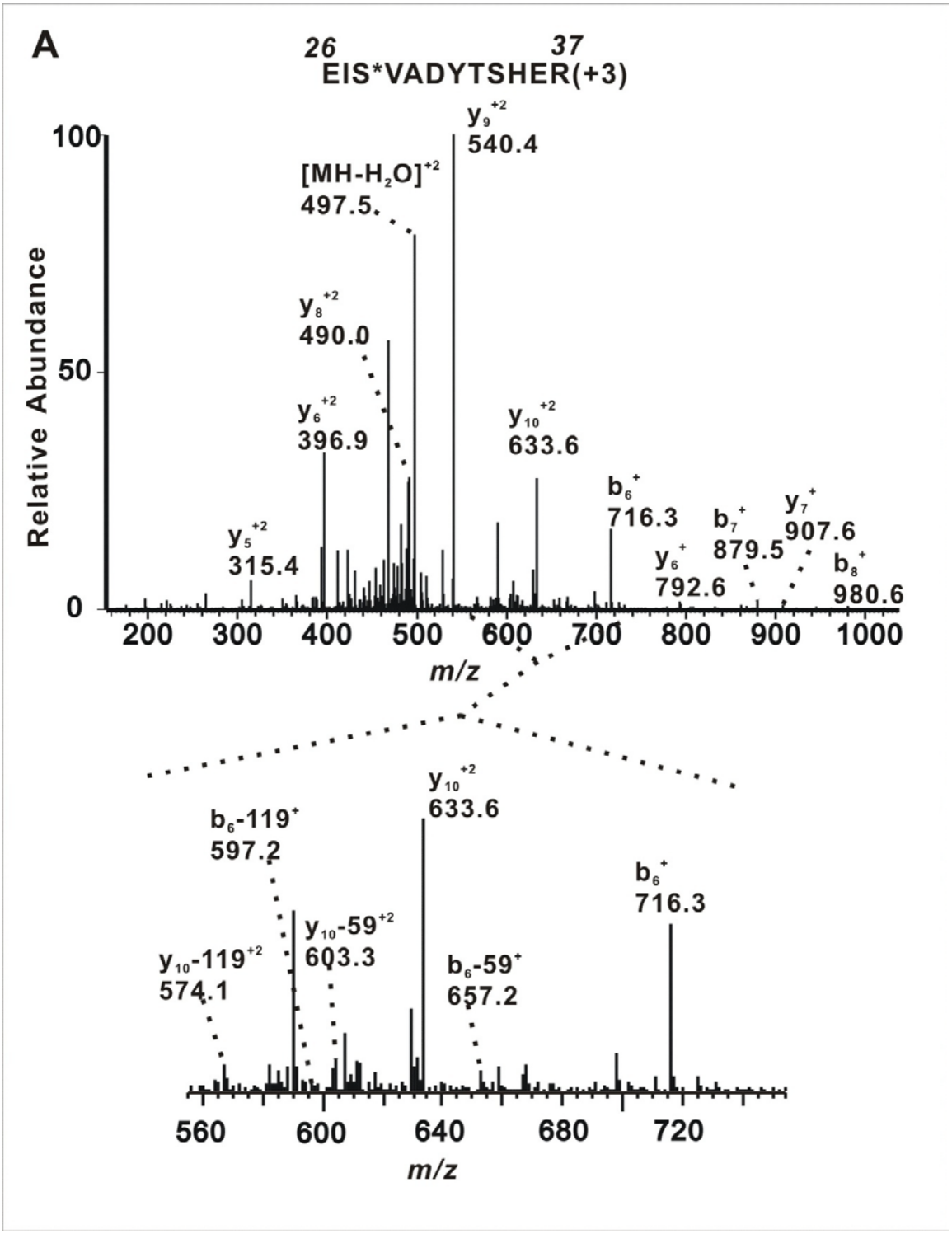
A
26
37
EIS*VADYTSHER(+3)
Relative Abundance
100
50
0
y9+2
540.4
[MH-H2O]+2
497.5
y8+2
490.0
y6+2
396.9
y10+2
633.6
b6+
716.3
b7+
879.5
y7+
907.6
y5+2
315.4
y6+
792.6
b8+
980.6
200
300
400
500
600
700
800
900
1000
m/z
y10+2
633.6
b6-119+
597.2
b6+
716.3
y10-59+2
603.3
y10-119+2
574.1
b6-59+
657.2
560
600
640
680
720
m/z

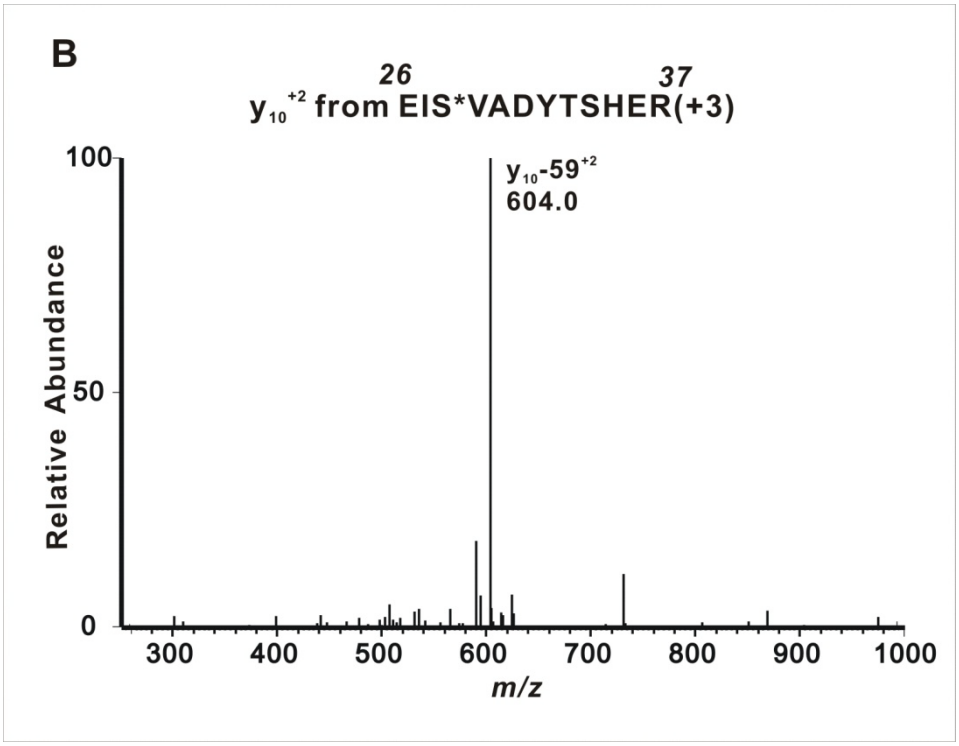
B
26
37
y10+2 from EIS*VADYTSHER(+3)
100
50
0
Relative Abundance
y10-59+2
604.0
300
400
500
600
700
800
900
1000
m/z

Figure 2.12

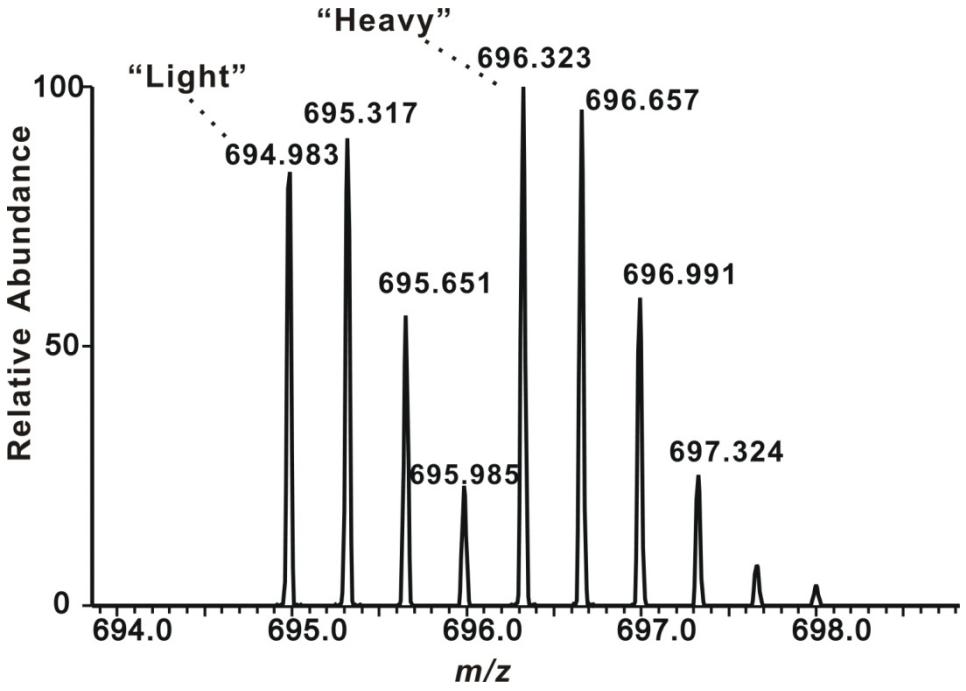

Figure 2.13

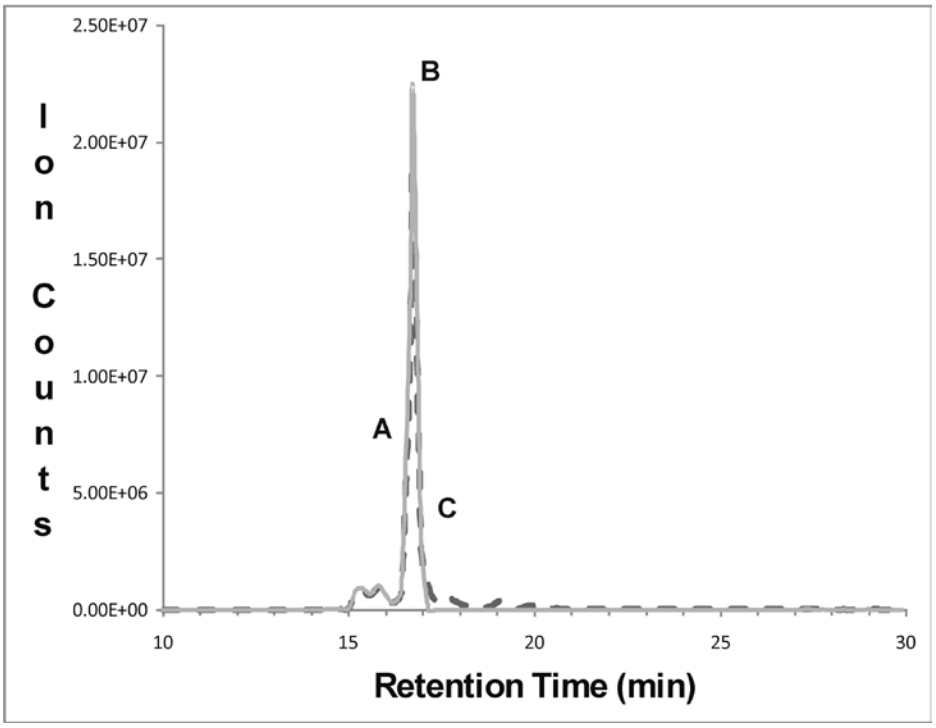

CHAPTER 3

Identification of Endogenous Phosphorylation Sites of iPLA$_2$β from Sf-9 Cells with and Without Thiocholine Modification

3.1 Abstract

In the previous chapter, the chemical replacement of the phosphate on phosphoserine and phosphothreonine residues via β-elimination and Michael addition with thiocholine was identified as an effective strategy for the characterization of phosphosites on model phosphoproteins. The increased ionization efficiency, improved sensitivity and the generation of characteristic diagnostic triads of fragmentation ions from signature neutral losses in tandem mass spectrometric analysis of thiocholine derivatives markedly improved peptide identification. To demonstrate further the utility of these procedures in living cells, BEMA with thiocholine was applied to identify the endogenous phosphorylation sites of calcium-independent phospholipase A$_2$β (iPLA$_2$β) heterologously expressed in *Spodoptera frugiperda* (Sf-9) cells. In parallel, traditional direct analysis of phosphopeptides with data-dependent acquisition MS^2 and neutral loss

of phosphoric acid triggered MS^3 was also performed to analyze $iPLA_2\beta$ phosphorylation. The two methods were compared and evaluated to show that a total of 12 unique phosphopeptides and 19 phosphorylation sites were identified using the thiocholine BEMA strategy, whereas only five peptides and six phosphorylation sites on $iPLA_2\beta$ were found with the traditional direct analysis. The larger number of phosphopeptides identified with the BEMA method with thiocholine resulted in improved sequence coverage compared to the traditional method. Finally, molecular modeling of $iPLA_2\beta$ was performed with the I-TASSER server to reveal the close spatial proximity of the phosphorylated residues to the catalytic site of the enzyme, suggesting the presence of phosphorylation mediated regulation of $iPLA_2\beta$.

3.2 Introduction

Reversible phosphorylation on serine and threonine residues is regarded as one of the most important molecular switches for the regulation of cellular signal transduction pathways [1-3]. However, the intrinsic chemical properties of phosphorylated serine and threonine-containing peptides hinder the detection and identification of phosphopeptides as well as the exact localization of phosphorylated residues in mass spectrometric analyses owing to poor ionization efficiency and subsequent low detection threshold. Furthermore, the facile neutral loss of phosphoric acid through cyclo-elimination during low-energy, collision-induced dissociation (CID) also contributes to the loss of phosphoprotein sequence coverage [4-6].

As reported in Chapter 2, a novel strategy was developed to overcome these hurdles for the sensitive detection and improved identification of pS/pT containing peptides [7]. Briefly, thiocholine is introduced into the peptide at the phosphorylation site via high-yield Ba^{2+} catalyzed β-elimination of phosphate and subsequent Michael addition (Scheme 1.1). Sample complexity is reduced through reductive alkylation of cysteines and development of optimized BEMA conditions for either pS or pT individually. This charge-switch strategy results in much improved ionization efficiencies during ESI with detection limits in the sub 500 amol/μL range. The sequence coverage of the modified peptides is also increased owing to the higher charge states of thiocholine-labeled tryptic peptides enabled by the endogenous positive charge on the

quaternary amine. Phosphopeptide identification has been substantially improved by exploiting the facile neutral loss of trimethylamine (m = 59 Da) and the thiocholine thiolate (m = 119 Da) from the thiocholine adduct (Scheme 1.2) during MS^2 and MS^3 analyses.

To demonstrate further the utility of these procedures in the detection of proteins phosphorylated in vivo, BEMA with thiocholine was applied to identify the endogenous phosphorylation sites of the calcium-independent phospholipase $A_2\beta$ ($iPLA_2\beta$) heterologously expressed in Sf-9 cells. In parallel, traditional direct analysis of phosphopeptides with data-dependent product-ion scan and neutral loss of phosphoric acid triggered MS^3 was also used for comparison with the current method. A total of 12 unique phosphopeptides and 19 phosphorylation sites were identified with the BEMA strategy compared to five peptides and six phosphorylation sites with the traditional method. The phosphopeptides identified with BEMA also showed better sequence coverage and higher ion scores than the traditional method.

A 3-dimensional (3-D) model of $iPLA_2\beta$ was also derived with the I-TASSER server [8-10]. All the phosphorylation sites identified either with BEMA with thiocholine or the traditional direct analysis were placed in the 3-D model to reveal the potential influence of these phosphorylated residues on the catalytic activity of the enzyme.

3.3 Materials and Methods

Materials

POROS 20 R2 resin was purchased from ABI (Foster City, CA); Slide-A-Lyzer MINI Dialysis Units, 7K MWCO were purchased from Pierce (Rockford, IL); Rapigest was purchased from Waters (Milford, MA); trypsin was purchased from Promega (Madison, WI); Solvents for mass spectrometric analyses were obtained from Honeywell Burdick&Jackson (Muskegon, MI). Other chemicals were obtained from Sigma-Aldrich (St. Louis, MO).

Synthesis of Thiocholine Chloride

Thiocholine chloride was prepared and the free thiol concentration of thiocholine chloride was determined as previously described in Chapter 2.

Purification of Calcium-independent Phospholipase $A_2\beta$ from Sf-9 Cells

Hexahistidine tagged calcium-independent phospholipase $A_2\beta$ ($iPLA_2\beta$) was expressed in Sf9 cells and purified as previously described by Jenkins *et al*. [11]. Sf9 cells grown to a density of 1 x 10^6 cells/mL were infected with a baculovirus encoding recombinant $iPLA_2\beta$ with a C-terminal 6x His tag at an MOI of ~2 viral particles/cell. The cells were incubated with constant agitation at 27 ^oC for 48 h. Next, cells suspended in the presence of Trypan blue were inspected for evidence of infection (cell swelling, limited cell death).

Infected cells were then centrifuged at 900 RPM for 10 min. The media was discarded and the cells were resuspended in an equal volume Graces's Insect Media without serum. Cells were centrifuged again 900 RPM for 10 min and resuspended in 10% of the original media volume of 25 mM potassium phosphate (pH 7.8) with 2 mM 2-mercaptoethanol, and 20% glycerol with 5 μg/mL each of aprotinin and leupeptin. Cells were sonicated at 30% max power for 30 x 1 s bursts and centrifuged at 100,000 g for 1 h. The supernatant was then applied to Co^{2+} metal affinity resin at 1mL resin per 200 mL original culture volume pre-equilibrated with 25 mM potassium phosphate (pH 7.8) with 2 mM 2-mercaptoethanol, and 20% glycerol. The column was washed with 25 mM potassium phosphate (pH 7.8) containing 2 mM 2-mercaptoethanol, 20% glycerol, and 5000 mM NaCl. A continuous gradient of 0-200 mM imidazole over 20 column volumes was employed to elute the bound $iPLA_2\beta(His)_6$. The fractions collected were tested for phospholipase activity. Active fractions were pooled and applied to a 1 mL ATP agarose pre-equilibrated with 20 mM imidazole (pH 7.6), 2mM 2-mercaptoethanol and 20% glycerol. The column was next washed with 20 mM imidazole (pH 7.6) 2 mM 2-mercaptoethanol, and 20% glycerol with 150mM NaCl and 1 mM AMP. Bound $iPLA_2\beta(His)_6$ was eluted with 20 mM imidazole (pH 7.6), 2 mM 2-mercaptoethanol and 20% glycerol with 150 mM NaCl, 5 mM ATP, in 1 mL fractions. All fractions were tested for the phospholipase activity and the most active fractions were pooled together. The protein concentration was determined using a Bradford assay [13].

Tryptic Proteolysis of Calcium-independent Phospholipase $A_2\beta$ Prepared from Sf-9 Cells

The calcium-independent phospholipase $A_2\beta$ ($iPLA_2\beta$) prepared from Sf-9 cells was dialyzed against deionized water for 8 h using a Slide-A-Lyzer MINI Dialysis Unit, dried in a SpeedVac apparatus (Savant, Holbrook, NY), and dissolved in 50 μL of 0.2% Rapigest in 50 mM NH_4HCO_3. Next, 2.5 μL of 100 mM dithiothreitol (DTT) was added to a final concentration of 5 mM. The sample was incubated at 60 °C for 30 min before 6 μL of 150 mM iodoacetamide was added to quench the reduction reaction and initiate alkylation. The sample was incubated for an additional 30 min in the dark at room temperature. Trypsin was added to the solution at a protease to protein ratio of 1:30 (w/w). The total volume of the sample solution was adjusted to 100 μL with 50 mM NH_4HCO_3. A total of 500 fmol/μL protein sample was incubated at 37 °C for 2 h and then acidified with 10 μL of 10% TFA to lower the pH to < 2. The sample was again incubated at 37 °C for 30 min and centrifuged at 13000 rpm to pellet the hydrolyzed Rapigest. Half of the resultant supernatant was used for thiocholine modification while the rest of the sample was subjected to MS analyses without modification.

BEMA of Trypsinized Calcium-independent Phospholipase $A_2\beta$ with Thiocholine

Half of the trypsinized $iPLA_2\beta$ sample was dried in a SpeedVac apparatus and reconstituted in 50 μL deionized water followed by the addition of 38 μL DMSO and 12 μL of absolute ethanol. The trypsinized protein solution was then divided into 2 equal

aliquots of 50 μL. The first aliquot was modified with a protocol optimized for pS containing peptides and the second aliquot was modified with a protocol optimized for pT containing peptides as follows: Aliquot 1 was mixed with 25 μL of freshly prepared saturated $Ba(OH)_2$. The reaction was incubated at room temperature under nitrogen for 1 h with gentle vortexing every 20 min. The final pH was 12~13. Next, 50 μL of 1 M thiocholine solution freshly prepared in water was directly added to the reaction. The reaction mixture was incubated at room temperature under nitrogen for 3 h at pH 8~9 and then terminated by the addition of 5 μL of 10% TFA and the resultant solution was desalted with a POROS 20 R2 microcolumn and dried. Aliquot 2 was mixed with 25 μL of freshly prepared saturated $Ba(OH)_2$. The reaction was incubated at room temperature under nitrogen for 3 h with gentle vortexing every 20 min. The final pH was 12~13. Next, the β-elimination reaction was terminated by addition of 10 μL of 10% TFA and the resultant solution was desalted with a POROS 20 R2 micro column [12]. Briefly, a POROS 20 R2 micro column was assembled by stamping out a small plug of C8 material from a 3 M Empore C8 extraction disk using a HPLC syringe needle and placing this plug in the constricted end of a GELoader tip. Next, POROS R2 beads that were suspended 50% acetonitrile at 5mg/200 μL were packed in the GELoader tip by pressing air through the micro column using an Eppendorf syringe. The length of the packed POROS R2 resin was about 3~6 mm. Then the column was washed with 30 μL 50% acetonitrile and equilibrated with 30 μL 0.1% trifluoroacetic acid. The sample solution was then loaded onto the POROS R2 micro column. The sample was slowly passed

through the micro column by pressing air through using a Eppendorf syringe. The column was washed twice with 30 μL 0.1% trifluoroacetic acid and the bounded peptides were eluted first using 30 μL 70% acetonitrile with 0.05 % trifluoroacetic acid, then 5 μL 30% acetonitrile with 0.05% trifluoroacetic acid. The purified peptide solution was dried and reconstituted in 50 μL of 0.5 M thiocholine solution freshly prepared in 0.1 M NaOH. The mixture was incubated at 50 °C under nitrogen for 5 h at pH 8~9. The reaction was terminated by the addition of 5 μL 10% TFA and the resultant solution was again desalted with a POROS 20 R2 microcolumn and dried.

HPLC-ESI-MS^2/MS^3 Mass Spectrometric Analyses

The desalted and dried peptide samples were reconstituted in 0.1% formic acid before injection and separation using a Surveyor HPLC system (Autosampler and pump, ThermoFisher, San Jose, CA) equipped with a reverse-phase C18 PepMap100 Nano-LC column (75 μm I.D. × 15 cm, 3μm, 100 Å; Dionex, Sunnyvale, CA). The flow rate was maintained at 220–280 nL/min. Samples elut ing from the column were directed to the nanospray apparatus (i.e., NanoMate HD with LC coupler, Advion Bioscience Ltd., Ithaca, NY) and sprayed directly into a linear ion trap in tandem with an Orbitrap (LTQ-Orbitrap) mass spectrometer (ThermoFisher, San Jose, CA) at a spray voltage of 1.7 kV in the positive ion mode. iPLA$_2$β samples, modified by the two optimized protocols, were analyzed first in survey runs, which consisted of a 90 min gradient from 100% A to 50% A, 50% B (Buffer A: 90% water, 10% acetonitrile, 0.1% formic acid;

Buffer B: 10% water, 90% acetonitrile, 0.1% formic acid, v:v)) and data-dependent MS^2 analyses: full mass scans in the Orbitrap (300–1600 *m/z*, mass resolution = 30000) were followed by product-ion scans in the LTQ for the five most abundant ions. The ions of interest from the survey runs were then included in the parent mass list of the target runs. The target runs consisted of a 180 min gradient from 100% A to 75% A, 25% B (120 min), then to 50% A, 50% B (60 min) and data-dependent MS^2/MS^3 analyses: full mass scans in the Orbitrap (300–1600 *m/z*, mass resolution = 30000) were followed by product-ion scans in the LTQ of the three most abundant ions from the parent mass list and the MS^3 scans in the LTQ of the 10 most intense fragment ions following each of the three product-ion scans. A control unmodified trypsinized $iPLA_2\beta$ sample was analyzed using the same survey run method as the thiocholine-modified samples. The target run for the unmodified sample consisted of an inclusion list generated from the survey run, a 180 min gradient (100% A to 75% A, 25% B (120 min), then to 50% A, 50% B (60 min)), and data-dependent MS^2/MS^3 analyses which consisted of an initial full mass scans in the Orbitrap (300–1600 *m/z*, mass resolution = 30000) followed by product-ion scans of the five most abundant ions from the parent mass list with neutral loss of H_3PO_4 triggered MS^3 scans in the LTQ. The normalized collision energy for CID was set at 25 for all data-dependent scans.

Data Processing

The local MASCOT server was used to conduct all database searches. A single-protein

(iPLA$_2$β) database was created by *in silico* trypsinolysis. Thiocholine with neutral losses of trimethylamine and thiolate were integrated into MASCOT for customized processing of the designed covalent modifications for serine and threonine residues. Carbamidomethylation of cysteine(C) residues was set as a fixed modification for the trypsinized iPLA$_2$β samples. Common variable modifications included N-terminal and lysine acetylation (N-terminus, K), asparagine and glutamine deamidation (N,Q) and methionine oxidation (M). A maximum of two missed cleavages were allowed. Full mass and product-ion mass accuracy were set at 5 ppm and 1 Da, respectively. All identifications by MASCOT were manually verified. All MS^3 scans were analyzed manually. The 3-D model of iPLA$_2$β was generated by a web based program on the I-TASSER server developed by Y. Zhang at the University of Michigan [8-10]. The results are presented in the format of a PDB file visualized using ViewerLite freeware and the distances between the amino acid residues were measured using the "Monitor--Distance" feature included in the software.

3.4 Results and Discussion

Calcium-independent phospholipase $A_2\beta$ ($iPLA_2\beta$) belongs to the superfamily of phospholipases A_2 [14]. Phospholipases A_2 catalyze the hydrolysis of phospholipids at the *sn*-2 position to release fatty acids [15-16], such as arachidonic acids and lysophospholipids, which are the precursors of multiple bioactive messengers [17-18]. According to their different properties, such as sequence homology, substrate selectivity, subcellular location and dependence on calcium ion, phospholipases A_2 can be grouped into three categories: secretory phospholipases A_2 ($sPLA_2$s), cytosolic phospholipases A_2 ($cPLA_2$s) and calcium-independent phospholipases A_2 ($iPLA_2$s) [19-20]. Cytosolic phospholipases A_2 are important intracellular phospholipases whose members contain (with the exception of $cPLA_2\gamma$) a calcium-binding domain (C2), which upon binding Ca^{2+} results in their translocation from cytosol to intercellular membrane compartments to hydrolyze their phospholipid substrates at the *sn*-2 position and release fatty acids [21].

The phosphorylation and Ca^{2+} mediated regulation of $cPLA_2\alpha$ was extensively studied [22-24]. The endogenous phosphorylation sites of $cPLA_2\alpha$ heterologously expressed in Sf-9 cells were previously identified as ser-437, ser-454, ser-505 and ser-727 by mass spectrometry and automated Edman sequencing [25]. Treatment of $cPLA_2\alpha$ with the phosphatase inhibitor okadaic acid resulted in a 4.5 fold increase in the phosphorylation at serine 727 and an increased release of arachidonic acid. These results, in conjunction with previous studies demonstrated that

phosphorylation/dephosphorylation of cPLA$_2$α is an important molecular mechanism underlying the regulation of arachidonic acid release [25]. Similarly, iPLA$_2$β is likely regulated by phosphorylation/dephosphorylation mechanism, although current methods have failed to identify specific residues whose phosphorylation correlate with alterations in catalytic activity. Thus, it is of particular importance to gain insight into the phosphorylation state of iPLA$_2$β *in vivo* to provide a molecular foundation for further investigation of the role of phosphorylation/dephosphorylation of iPLA$_2$β in diverse processes of substantial biologic significance such as cardiac function, arachidonic acid release, cell proliferation and apoptosis [26-29]. A primary purpose of this study is to compare the utility of the developed BEMA strategy with a traditional direct analysis method in a system where the protein phosphorylation level is not artificially elevated.

Hexahistidine-tagged calcium-independent phospholipase A$_2$β (iPLA$_2$β) was expressed in Sf9 cells and purified as previously described by Jenkins *et al*. [11]. Purified iPLA$_2$β was modified with thiocholine by using two separate protocols optimized for either pS or pT-containing phosphopeptides. Modified and unmodified peptides were analyzed with HPLC-ESI-MS^2/MS^3 as described in the Materials and Methods section.

As shown in Table 3.1, six different endogenous phosphorylated sites, originating from five unique phosphopeptides, were identified in iPLA$_2$β without thiocholine modification using the traditional MS analysis strategy as described in the Materials and Methods. No neutral loss of phosphoric acid triggered MS^3 were obtained for any of the identified peptides.

Conversely, as shown in Table 3.2, with the β-elimination and Michael addition strategy, a total of 19 different phosphorylated residues were identified. These phosphorylation sites originated from 14 phosphopeptides. Identified peptides with missed tryptic cleavages are listed together with the completely trypsinized peptides indicated by bold-bordered boxes. The peptides contained within the bold-bordered boxes are considered as one unique sequence. Thus, there are 12 unique phosphopeptides found by the BEMA method. The phosphorylation sites listed in the table separated with a "/" indicate that the monophosphopeptide has more than one non-concurrent phosphorylation site. The product-ion spectra of all the peptides identified were verified manually, all of which contained signature peaks generated by the neutral loss of trimethylamine and/or thiocholine thiolate. As indicated in bold font in Table 3.1, 11 phosphopeptides from nine unique sequences showed at least one dominant peak resulting from the neutral loss of trimethylamine (-59 Da) at the level of MS^3 analyses out of 14 phosphopeptides and 12 unique sequences.

The sequence coverage of the identified peptides was calculated using all b and y ions present in the product-ion spectra over the number of all possible b and y ions. The phosphopeptides identified with the BEMA strategy showed better sequence coverage than those identified with the traditional method. Eleven out of 14 phosphopeptides modified with thiocholine had sequence coverage greater than 50%; whereas three out of five phosphopeptides without any modification identified with traditional mass spectrometric methods showed sequence coverage above 50%.

Figure 3.1-A shows the product-ion spectrum of the triply charged thiocholine-modified peptide VKEIS*VADYTSHER (24–37). This spectrum consists of b and y ions with diagnostic triads of all thiocholine containing peptidic fragment ions. Shown in the expanded spectrum are the representative diagnostic triads from y_{12}^{+2} fragment ions resulting from peptide bond cleavage (*m*/*z* = 754.7) and further neutral loss of trimethylamine (-59 Da, *m*/*z* = 725.1) and the thiocholine thiolate (-119 Da, *m*/*z* = 695.2). Of the ions generated at MS^2 level, the ten most abundant ions were chosen to be further fragmented at the MS^3 level. Examination of the y_{10}^{+2} ion at *m*/*z* 633.5 (among the top ten ions selected) demonstrated that it also possessed an intact thiocholine side chain, which led to a signature neutral loss pattern in its MS^3 spectrum (Figure 3.1-B). The ion at *m*/*z* 603.9 is formed by the neutral loss of trimethylamine from the precursor y_{10}^{+2} at *m*/*z* 633.5.

The product-ion spectrum shown in Figure 3.2 is the triply charged peptide VKEIpSVADYTSHERVR (24-39) identified with the traditional method, corresponding to the phosphopeptide VKEIS*VADYTSHER (Figure 3.1-A) with one additional missed cleavage. The spectrum provides minimal sequence informative ions in comparison to that of the thiocholine-modified peptide with lower sequence coverage and a lower ion score.

Examination of the fragmentation pattern of VKEIS*VADYTSHER demonstrated that the thiocholine side chain enabled a unique tandem fragmentation pattern ideal for proteomic analyses, since sequencing of the peptide at the MS^2 level is not compromised

by subsequent neutral losses but rather strengthened by the presence of diagnostic triads of fragment ions in conjunction with the signature neutral loss at the MS^3 level. As previously discussed, one of the promising prospects of this approach is the use of these unique and predictable diagnostic triads of fragmentation ions from thiocholine-modified peptides in a weighted scoring system, where the intrinsic chemical properties of the modified peptide could enhance identification of phosphorylated peptides and phosphosites. Even though such a scoring system is not currently available, combining the current MASCOT score with high mass accuracy (< 5ppm) and the diagnostic triad of fragment ions in both MS^2 and MS^3 levels will ensure the identification of the modified peptides are made with high confidence.

To gain insight into the potential mechanistic significance of the identified iPLA$_2$β phosphosites, a three-dimensional model of iPLA$_2$β was generated using the I-TASSER server, an internet service that predicts protein structures and generates protein 3-D models [8-10]. The I-TASSER program was developed by Yang *et al*. at the University of Michigan. 3D models are predicted based on multiple-threading alignments generated by Local Meta-Threading-Server (LOMETS) that generates protein 3-D models by collecting target-to-template alignments with high scores as well as iterative TASSER simulations. The I-TASSER server was ranked as the No. 1 server with the best global distance test total score (GDT-TS), which is a measure of the similarity between two different protein structures with the same primary structure, but different tertiary structures, in the server section of both the 7th and 8th CASPs (Critical Assessment of

Techniques for Protein Structure Prediction). As shown in Figure 3.3-A, the catalytic serine located within the lipase consensus sequence GXSXG resides within the central catalytic core adjacent to the nucleotide binding motif (GXGXXG) (S465) [30]. All the phosphorylation sites identified either with BEMA with thiocholine or through the traditional direct analysis were located in the 3-D model. The distance (in Å) between these phosphorylated serine/threonine residues and the active site of serine 465 measured by using atom-to-atom distances between the hydroxyl oxygen of phosphorylated serines/threonines residues and the hydroxyl oxygen of serine 465 are listed in Table 3.3. The closest of the identified phosphorylated residues, threonine 521 is predicted to be at a distance of 8.67 Å from the catalytic site in this model, which is also labeled in Figure 3.3-A. At this distance, the phosphorylation/dephosphorylation of threonine 521 could significantly influence the catalytic activity of the enzyme.

Other phosphorylated serines/threonines within the catalytic core, labeled in Figure 3.3-B, undergo phosphorylation/dephosphorylation that could also affect the activity of iPLA$_2$β. As shown in Figure 3.3-C, many of the observed phosphosites in iPLA$_2$β are located within the ankyrin repeat domain; these residues likely facilitate specific binding to protein partners in a phosphorylation-dependent fashion. The phosphorylation/dephosphorylation cycling of these residues could impact the regulation of protein-protein interactions during the binding of iPLA$_2$β to cellular membranes that contain ankyrin-binding proteins.

3.5 Conclusion and Perspective

We demonstrated the utility of the β-elimination and Michael addition strategy in the identification of endogenous phosphorylation sites of iPLA$_2$β heterologously expressed in Sf-9 cells. In comparison to the traditional direct mass spectrometric analyses of phosphopeptides, the BEMA strategy identified more phosphopeptides with more phosphorylation sites, and demonstrated improved sequence coverage and ion scores. A diagnostic triad of fragment ions also facilitated improved phosphosite determination at higher confidence levels of the peptides identified by MASCOT. The 3-D model of iPLA$_2$β showed that threonine 521 was spatially the closest identified phosphosite to serine 465 in the catalytic domain. The phosphorylation/dephosphorylation of these sites likely affects the catalytic activity, membrane binding and trafficking of iPLA$_2$β.

3.6 References

(1) Hunter, T. *Cell* **2000**, *100*, 113-127.

(2) Cohen, P. *Nat. Cell Biol.* **2002**, *4*, E127-130.

(3) Bender, E.; Kadenbach, B. *FEBS Lett.* **2000**, *466*, 130-134.

(4) Yates, J. R.; Ruse, C. I.; Nakorchevsky, A. *Annu. Rev. Biomed. Eng.* **2009**, *11*, 49-79.

(5) Syka, J. E.; Coon, J. J.; Schroeder, M. J.; Shabanowitz, J.; Hunt, D. F. *Proc. Natl. Acad. Sci. U. S. A.* **2004**, *101*, 9528-9533.

(6) Mann, M.; Ong, S. E.; Gronborg, M.; Steen, H.; Jensen, O. N.; Pandey, A. *Trends Biotechnol.* **2002**, *20*, 261-268.

(7) Chen, M.; Su, X.; Yang, J.; Jenkins, C. M.; Cedars, A. M.; Gross, R. W. *Anal. Chem.* **2010**, *82*, 163-171.

(8) Zhang, Y. *BMC Bioinf.* **2008**, *9*, 40.

(9) Zhang, Y. *Proteins* **2009**, *77 Suppl 9*, 100-113.

(10) Roy, A.; Kucukural, A.; Zhang, Y. *Nat. Protoc.* **2010**, *5*, 725-738.

(11) Jenkins, C. M.; Yan, W.; Mancuso, D. J.; Gross, R. W. *J. Biol. Chem.* **2006**, *281*, 15615-15624.

(12) Thingholm, T. E.; Jorgensen, T. J.; Jensen, O. N.; Larsen, M. R. *Nat. Protoc.* **2006**, *1*, 1929-1935.

(13) Bradford, M. M. *Anal Biochem* **1976**, *72*, 248-254.

(14) Ackermann, E. J.; Dennis, E. A. *Biochim. Biophys. Acta* **1995**, *1259*, 125-136.

(15) Gross, R. W. *J. Lipid Mediators Cell Signalling* **1995**, *12*, 131-137.

(16) Ma, Z.; Turk, J. .*Prog. Nucleic Acid Res. Mol. Biol.* **2001**, *67*, 1-33.

(17) Yedgar, S.; Lichtenberg, D.; Schnitzer, E. *Biochim. Biophys. Acta* **2000**, *1488*, 182-187.

(18) Snyder, F. *Biochem. J* **1995**, *305 (Pt 3)*, 689-705.

(19) Six, D. A.; Dennis, E. A. *Biochim Biophys Acta* **2000**, *1488*, 1-19.

(20) Murakami, M.; Kudo, I. *J Biochem* **2002**, *131*, 285-292.

(21) Loeb, L. A.; Gross, R. W. *J Biol Chem* **1986**, *261*, 10467-10470.

(22) Borsch-Haubold, A. G.; Bartoli, F.; Asselin, J.; Dudler, T.; Kramer, R. M.; Apitz-Castro, R.; Watson, S. P.; Gelb, M. H. *J Biol Chem* **1998**, *273*, 4449-4458.

(23) Borsch-Haubold, A. G.; Ghomashchi, F.; Pasquet, S.; Goedert, M.; Cohen, P.; Gelb, M. H.; Watson, S. P. *Eur J Biochem* **1999**, *265*, 195-203.

(24) Hefner, Y.; Borsch-Haubold, A. G.; Murakami, M.; Wilde, J. I.; Pasquet, S.; Schieltz, D.; Ghomashchi, F.; Yates, J. R., 3rd; Armstrong, C. G.; Paterson, A.; Cohen, P.; Fukunaga, R.; Hunter, T.; Kudo, I.; Watson, S. P.; Gelb, M. H. *J Biol Chem* **2000**, *275*, 37542-37551.

(25) de Carvalho, M. G.; McCormack, A. L.; Olson, E.; Ghomashchi, F.; Gelb, M. H.; Yates, J. R., 3rd; Leslie, C. C. *J Biol Chem* **1996**, *271*, 6987-6997.

(26) Larsson Forsell, P. K.; Kennedy, B. P.; Claesson, H. E. *Eur. J. Biochem.* **1999**, *262*, 575-585.

(27) Mancuso, D. J.; Abendschein, D. R.; Jenkins, C. M.; Han, X.; Saffitz, J. E.; Schuessler, R. B.; Gross, R. W. *J. Biol. Chem.* **2003**, *278*, 22231-22236.

(28) Atsumi, G.; Murakami, M.; Kojima, K.; Hadano, A.; Tajima, M.; Kudo, I. *J. Biol. Chem.* **2000**, *275*, 18248-18258.

(29) Ramanadham, S.; Hsu, F. F.; Bohrer, A.; Ma, Z.; Turk, J. *J. Biol. Chem.* **1999**, *274*, 13915-13927.

(30) Derewenda, Z. S.; Sharp, A. M. *Trends Biochem. Sci* **1993**, *18*, 20-25.

(31) Whitesides, G. M.; Lilburn, J. E.; Szajewski, R. P. *J. Org. Chem.* **1977**, *42*, 332-338.

3.7 Table Legends

Table 3.1

Identification of endogenous phosphorylation sites in iPLA$_2$β heterologously expressed in Sf-9 cells without thiocholine modification.

Tryptic iPLA$_2$β peptides were desalted, separated using reverse-phase nanobore HPLC, and analyzed with an LTQ-Orbitrap system. Candidate peptides were identified using MASCOT with the designated thiocholine modification as well as common amino acid modifications as described in the Materials and Methods. A total of five unique phosphopeptides and six different phosphorylated residues were identified. “p” denotes identified phosphorylation sites; “(p)” denotes that more than one phosphorylation site was identified in the same peptide. Those that were not concurrent are indicated by “/”. The superscripts “ace”, “d”, and “o” denote the following modifications: acetylation (N-terminus), deamidation (NQ), and oxidation (M), respectively. All cysteine residues were carbamidomethylated.

Table 3.2

Identification of endogenous phosphorylation sites in iPLA$_2$β heterologously expressed in Sf-9 cells with thiocholine modification.

Tryptic iPLA$_2$β peptides were modified with thiocholine using two different protocols optimized for either phosphoserine or phosphothreonine as described in the Materials and

Methods. The thiocholine-modified peptides were desalted, separated using reverse-phase nanobore HPLC, and analyzed with an LTQ-Orbitrap system. Candidate peptides were identified using MASCOT with the designated thiocholine modification as well as common amino acid modifications as described in Materials and Methods. A total of 12 unique phosphopeptides and 19 different phosphorylated residues were identified. "*" denotes identified phosphorylation sites; "(*)" denotes that more than one phosphorylation site was identified in the same peptide. Those that were not concurrent are indicated by "/". The superscripts "d", and "o" denote the following modifications: deamidation (NQ) and oxidation (M), respectively. All cysteine residues were carbamidomethylated. Identified peptides with missed cleavages are listed together with the completely trypsinized peptides outlined by bold-bordered boxes. Peptides which yielded a signature neutral loss pattern in MS^3 are highlighted in bold.

Table 3.3

Calculated distances between the catalytic site serine 465 of iPLA$_2$β and the identified phosphorylation sites of iPLA$_2$β heterologously expressed in Sf-9 cells utilizing the BEMA strategy or traditional direct analysis in the 3-D model of iPLA$_2$β molecule generated by I-TASSER.

A 3-D model of iPLA$_2$β was generated using the I-TASSER server. All the phosphorylation sites identified either with β-elimination and Michael with thiocholine addition (denoted as "BEMA" in the table) or the traditional direct mass spectrometric

method (denoted as “Direct” in the table) were located in the 3-D model. The distance between the identified phosphorylated residues and the catalytic site serine 465 are given in Å. The distance measured is the atom-to-atom distance between the hydroxyl oxygen of serine 465 and the hydroxyl oxygens of the phosphorylated serines/threonines. Threonine 521 is the most proximal residue (8.67 Å) to the catalytic site in this model.

Table 3.1

Sequence#	Sequence	Phosphorylation Site	Ion Score	Δm (ppm)	Coverage%
24-39	VKEIpSVADYTSHERVR	S28	5.7	-2.34	63%
208-218	^{ace}NApSAGLNQVNK	S210	16.3	-2.59	82%
266-282	^{ace}GCAEMIISM^{o}DSpSQIHSK	S277	6.34	1.23	35%
396-407	Q^{d}LQ^{d}DLMPIpSRAR	S404	8.15	-1.86	42%
633-643	LSIVV(p)SLGpTGR	S638/T641	22.87	-3.39	91%

Table 3.2

Sequence#	Sequence	Phosphorylation Site	Ion Score	Δm (ppm)	Coverage%
24-37	**VKEIS*VADYTS$^{(*)}$HER**	S28/S34	54.62	-2.02	86%
26-37	**EIS*VADYTS$^{(*)}$HER**	S28/S34	34.13	-2.52	92%
38-53	**VREEGQLILFQNAS*NR**	S51	58.41	-1.06	81%
246-261	**CN^{d}VMGPSGFPIHT*AMK**	S252/S258	7.47	-1.03	75%
307-327	GCDVDSTS*AAGNTALHVAVM^{o}R	S314	3.72	-0.98	38%
396-405	**Q^{d}LQDLMPIS*R**	S404	16.69	-3.99	70%
408-417	**KPAFILS*S$^{(*)}$MR**	S414/S415	14.77	-1.36	70%
408-420	**KPAFILS*S$^{(*)}$MRDEK**	S414/S415	19.21	-2.71	69%
479-489	S*MAYMRGVYFR	S479	9.31	-3.31	45%
497-511	GS*RPYES$^{(*)}$GPLEEFLK	S498/S503	33.45	-1.66	80%
513-524	**EFGEHTKM^{o}T*DVK**	T521	9.85	0.72	42%
528-537	**VMLT*GT$^{(*)}$LS$^{(*)}$DR**	T531/T533/S535	33.06	-1.68	90%
582-595	**SS*GAAPT$^{(*)}$YFRPN^{d}GR**	S583/T588	29.26	-1.14	71%
694-705	**AWS*EMVGIQYFR**	S696	34.15	-1.51	92%

Table 3.3

Residue number	Identification Method	Distance to Serine 465 (Å)
Serine 28	BEMA/Direct	35.88
Serine 34	BEMA	33.99
Serine 51	BEMA	45.80
Serine 210	Direct	49.78
Serine 252	BEMA	43.60
Serine 258	BEMA	39.18
Serine 277	Direct	48.68
Serine 314	BEMA	45.88
Serine 404	BEMA/Direct	56.62
Serine 414	BEMA	54.70
Serine 415	BEMA	50.77
Serine 479	BEMA	27.49
Serine 498	BEMA	27.53
Serine 503	BEMA	26.44
Threonine 521	BEMA	8.67
Threonine 531	BEMA	17.09
Threonine 533	BEMA	17.66
Serine 535	BEMA	22.70
Serine 583	BEMA	25.98
Threonine 588	BEMA	26.00
Serine 638	Direct	34.45
Threonine 641	Direct	27.08
Serine 696	BEMA	43.57

3.8 Figure Legends

Figure 3.1 Fragmentation of the thiocholine-modified peptide VKEIS*VADYTSHER identified in iPLA$_2$β at both the MS^2 and MS^3 levels.

A. The product-ion spectrum of the triply charged molecular ion at *m*/*z* 578.966 (VKEIS*VADYTSHER) was obtained with an ESI-LTQ-Orbitrap as described in the Materials and Methods. The fragment ion resulting from the neutral loss of trimethylamine from the parent ion was present at *m*/*z* 559.5. Shown in the expanded spectrum (relative intensity zoom = 24%) are examples of the diagnostic triad consisting of the y_{12}^{+2} fragmentation ions resulting from peptide bond cleavage (*m*/*z* = 754.7) and further neutral loss of trimethylamine (-59 Da, *m*/*z* = 725.1) or the thiocholine thiolate (-119 Da, *m*/*z* = 695.2). Also shown is the y_{11}^{+2} (*m*/*z* = 690.1) and its corresponding ion peak of the neutral loss of trimethylamine (-59 Da) at *m*/*z* = 660.5. "S*" indicates the thiocholine-modified site.

B. The MS^3 spectrum of the y_{10}^{+2} ion at *m*/*z* 633.5 resulting from the fragmentation of the triply charged molecular ion at *m*/*z*578.966 (VKEIS*VADYTSHER) obtained with an ESI-LTQ-Orbitrap as described in the Materials and Methods section. The ion peak at *m*/*z* 603.9 corresponds to the doubly charged fragment ion generated from the neutral loss of trimethylamine from the parent ion y_{10}^{+2}.

Figure 3.2 Fragmentation of the phosphopeptide VKEIpSVADYTSHERVR identified in iPLA$_2$β without thiocholine modification.

The product-ion spectrum of the triply charged molecular ion at *m*/*z* 656.988 (VKEIpSVADYTSHERVR) was obtained with an ESI-LTQ-Orbitrap as described in the Materials and Methods section. The fragment ion resulting from the neutral loss of H_3PO_4 from the parent ion was not observed. "pS" indicates the phosphorylated site.

Figure 3.3 3-D model of iPLA$_2$β generated by the I-TASSER server.

The primary amino acid sequence file of iPLA$_2$β was submitted to I-TASSER server located at http://zhanglab.ccmb.med.umich.edu/I-TASSER/. The 3-D model in PDB format was generated and displayed with ViewerLite freeware.

A. The catalytic site serine 465 and phosphorylated residue threonine 521 are labeled. The atom-to-atom distance between the hydroxyl oxygen of serine 465 and the hydroxyl oxygen of the threonine 521 is calculated to be 8.67 Å in this model.

B. Phosphorylated residues within the catalytic core are labeled as follows: serine 28, serine 34, serine 51, serine 210, serine 252, serine 258, serine 277, serine 314, serine 304, serine 414, and serine 415.

C. Phosphorylated residues within the ankyrin domain of iPLA$_2$β are labeled as follows: serine 479, serine 498, serine 503, threonine 521, threonine 531, threonine 533, serine 535, serine 583, threonine 588, serine 638, threonine 641, and serine 696.

Figure 3.1

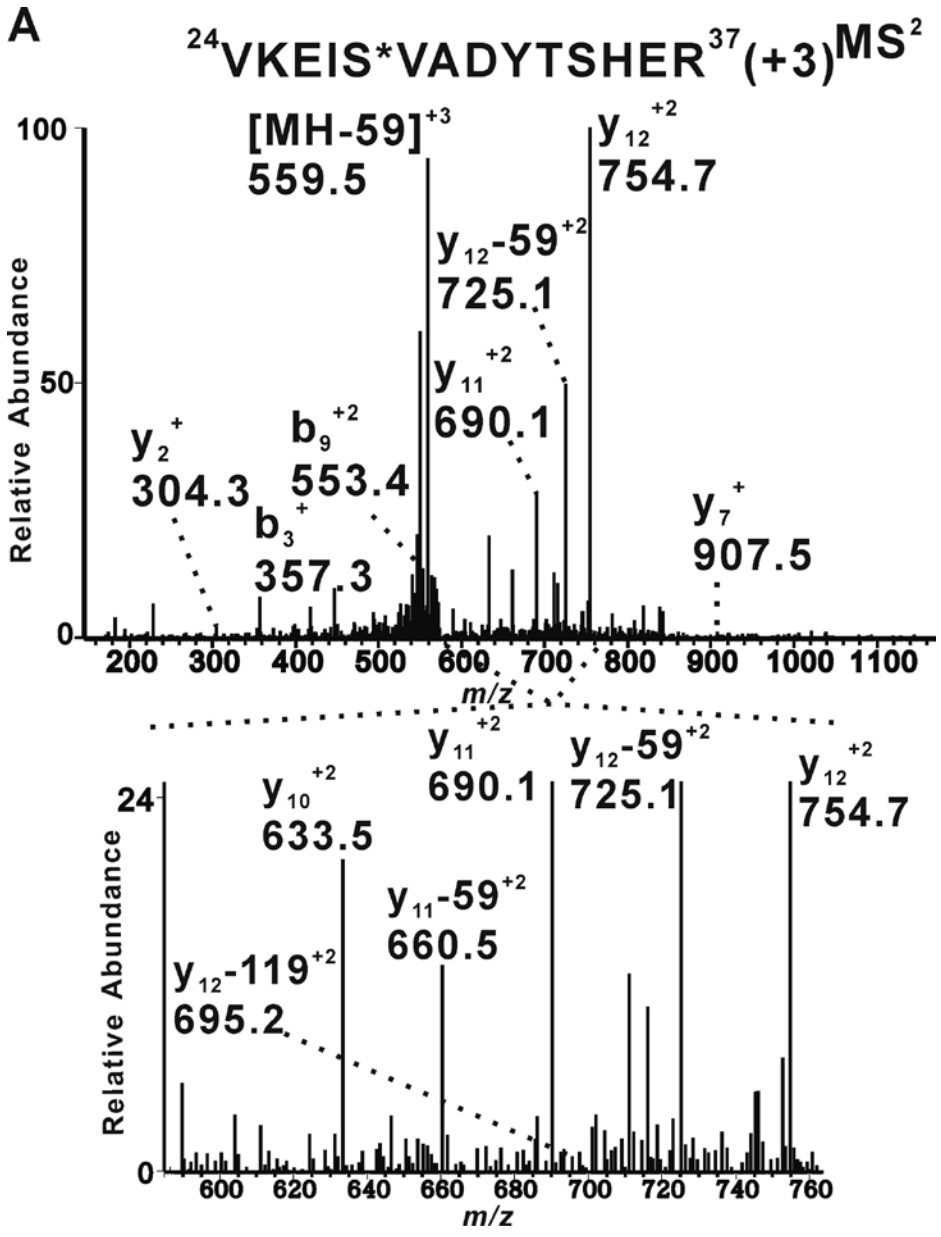
A
24VKEIS*VADYTSHER37(+3)MS2
[MH-59]+3
559.5
y12+2
754.7
y12-59+2
725.1
y11+2
690.1
y2+
304.3
b9+2
553.4
b3+
357.3
y7+
907.5
Relative Abundance
m/z
y11+2
690.1
y12-59+2
725.1
y12+2
754.7
y10+2
633.5
y11-59+2
660.5
y12-119+2
695.2
Relative Abundance
m/z

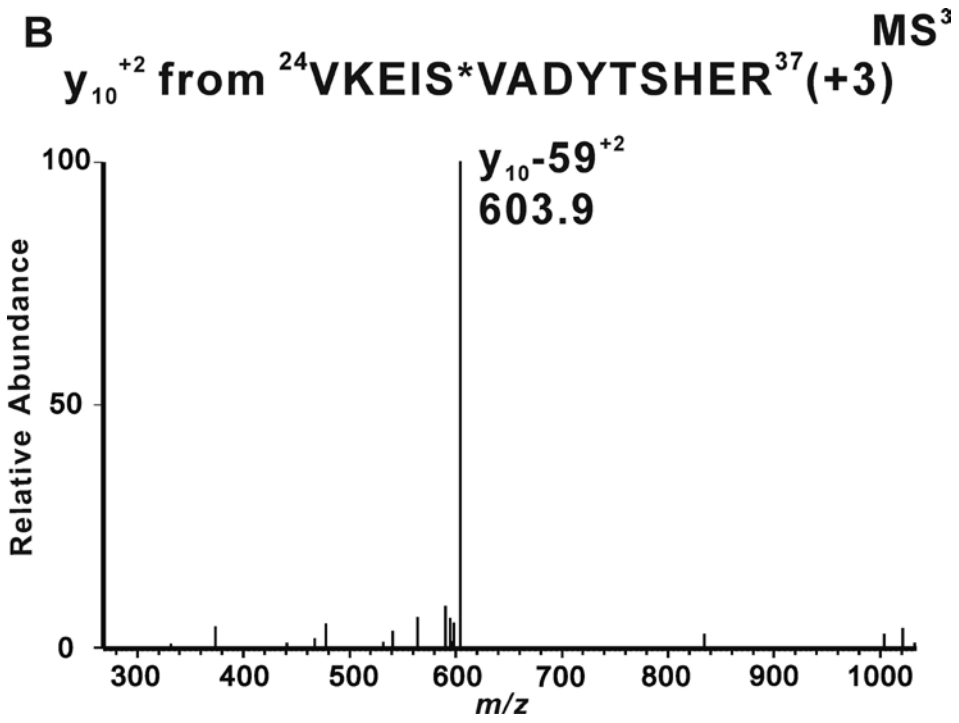
B
MS3
y10+2 from 24VKEIS*VADYTSHER37(+3)
y10-59+2
603.9
Relative Abundance
100
50
0
300
400
500
600
700
800
900
1000
m/z

Figure 3.2

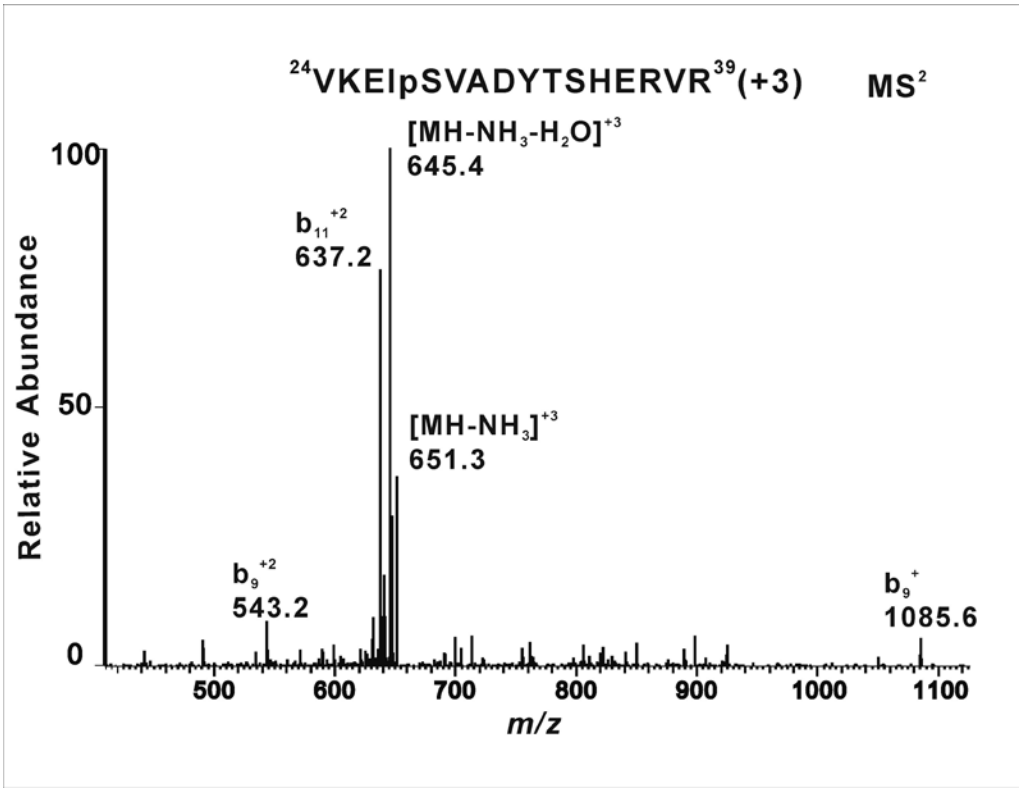
24VKEIpSVADYTSHERVR39(+3) MS2
[MH-NH3-H2O]+3
645.4
b11+2
637.2
[MH-NH3]+3
651.3
b9+2
543.2
b9+
1085.6
Relative Abundance
100
50
0
500
600
700
800
900
1000
1100
m/z

Figure 3.3

A.

B.

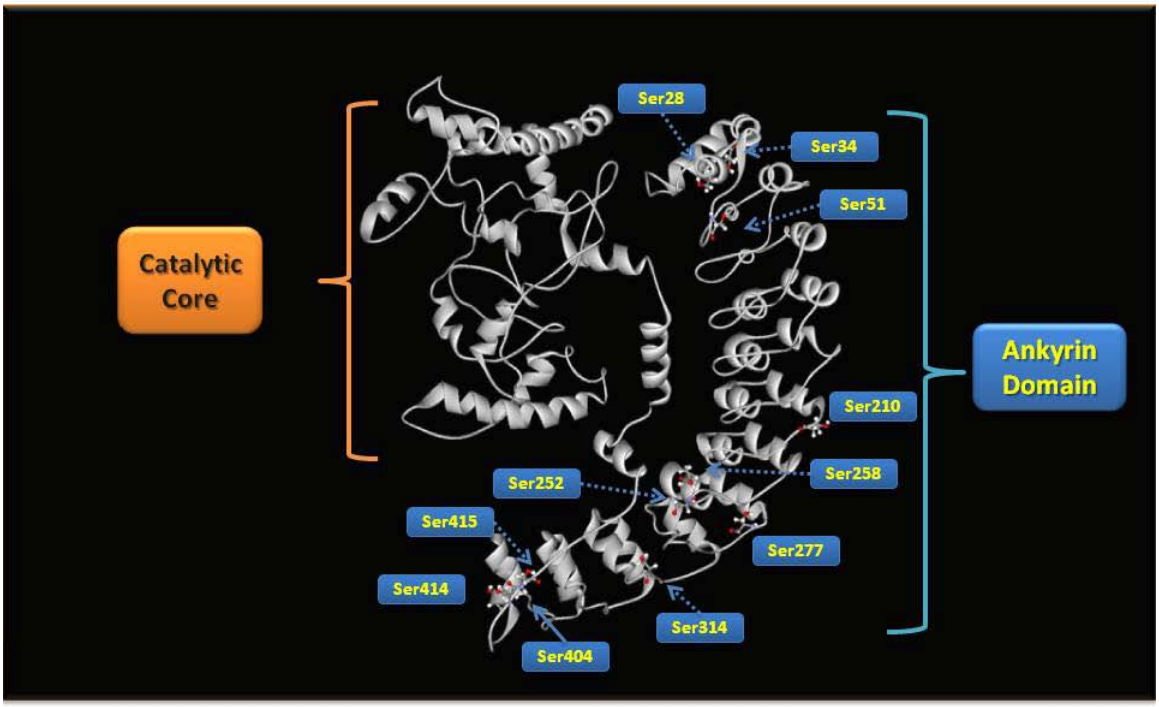
Catalytic Core
Ankyrin Domain
Ser28
Ser34
Ser51
Ser210
Ser258
Ser252
Ser415
Ser277
Ser414
Ser314
Ser404

C.

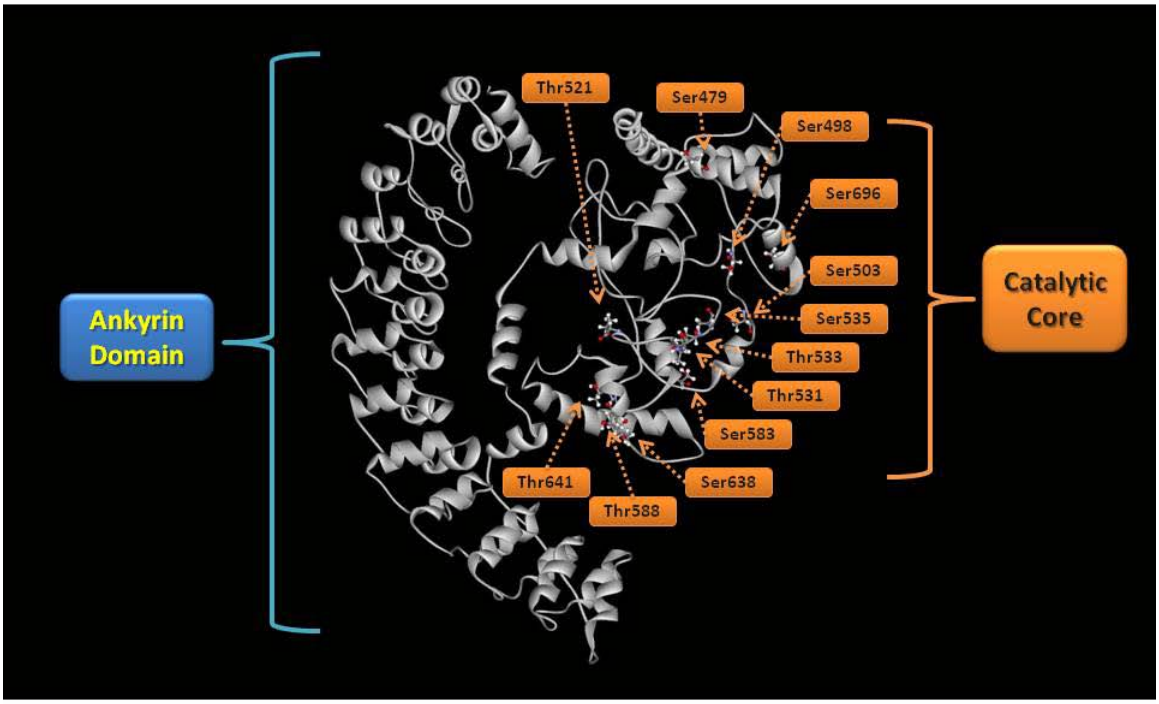
Ankyrin Domain
Thr521
Ser479
Ser498
Ser696
Ser503
Ser535
Thr533
Thr531
Ser583
Ser638
Thr588
Thr641
Catalytic Core

CHAPTER 4

Quantitative Analysis of Alterations in the Myocardial Mitochondrial Phosphoproteome Induced by Cardiac Ischemia Assessed using β-Elimination and Michael Addition with Light and Heavy Thiocholine

4.1 Abstract

Quantitative analysis of alterations in the murine myocardial mitochondrial phosphoproteome induced by global cardiac ischemia was performed using the developed mass spectrometric strategy of β-elimination of phosphate and subsequent Michael addition (BEMA) with natural abundance (light) thiocholine and stable-isotope labeled (heavy) thiocholine. The developed strategy exploited the increased ionization efficiency, sensitivity and diagnostic triads of fragmentation ions to identify 141 phosphopeptides from 133 distinct proteins that include the identification of 36 phosphopeptides from 35 mitochondrial proteins containing 37 previously unreported mitochondrial phosphosites. The identities of these novel phosphosites were first determined using the MASCOT search engine and were substantiated through rescoring using the Percolator algorithm. Quantitation of alterations in mitochondrial protein phosphorylation resulting from

cardiac ischemia were achieved by comparing phosphopeptides modified by heavy thiocholine obtained from mitochondria in ischemic hearts (i.e., global ischemia) to those modified by light thiocholine in control hearts (i.e., normal flow perfusion). Collectively, these results demonstrate that β-elimination of phosphate and subsequent Michael addition (BEMA) using light and heavy thiocholine represent an effective mass-spectrometry-based strategy for comparative quantitative phosphoproteomics in whole organ systems during pathophysiologic perturbations.

4.2 Introduction

The reversible protein phosphorylation and dephosphorylation of serine and threonine residues are the most ubiquitous posttranslational modifications that regulate critical signaling pathways in eukaryotic cells [1-3]. As in most biologic systems, protein phosphorylation plays multiple roles in regulating a diverse array of mitochondrial functions. Prior work demonstrated that numerous proteins are phosphorylated in the mitochondria of yeast [4], mouse liver [5], mouse brain [6], bovine heart [7], and in virtually every cell type and organ system studied [8-9]. In mitochondria, it is well established that the activities of enzymes, such as pyruvate dehydrogenase [10-14] and cytochrome oxidase [15-16] are regulated by reversible protein phosphorylation that contributes to cellular bioenergetics, substrate utilization and the deleterious sequelae of oxidative stress. However, a quantitative mass spectrometric approach for phosphoproteome analysis on a global scale identifying the number and magnitude of alterations in the phosphorylation at specific phosphosites of mitochondrial proteins after pathophysiologic perturbations has not been well defined.

Radiolabeling of biologic tissues with [γ-^{32}P]-ATP is a traditional quantitative approach that has been used to provide early insights into the mitochondrial phosphoproteome [8, 17]. Radiolabeling is a very sensitive technique for the detection of phosphoproteins and the characterization of overall changes in the level of protein phosphorylation. However, its utility is limited by its inability to localize readily the phosphosite without additional approaches such as site-directed mutagenesis, enrichment

processes, or Edman degradation. Although fluorescence labeling represents a sensitive nonradioactive alternative to ^{32}P radiolabeling [7] it suffers multiple limitations because fluorescence labeling alone cannot provide primary sequence information of the phosphorylated peptide or its phosphosite. Meanwhile, mass spectrometric approaches for phosphoproteome analysis are complicated by facile cyclo-elimination of phosphoric acid, resulting in ambiguities in phosphosite assignment and poor ionization efficiencies of phosphopeptides rendering their detection difficult. Thus, these techniques are not amenable to high-throughput quantitative analysis required for comprehensive phosphoproteome determination. [18].

Isobaric tags for relative and absolute quantitation (iTRAQ) is an effective mass-spectrometry-based labeling technique for multiplexed quantitative phosphoproteomics [19-21]. For this approach, tryptic peptides from proteins of different biological states are modified with different isobaric tags. The same phosphopeptides from different states are identical in the full-mass scan but can produce unique reporter ions during the tandem mass spectrometric analysis, thus providing information of comparative quantitation based on the relative abundances of the reporter ions. However, given that quantitation is achieved at the MS^2 level, the sensitivity of this strategy is limited and could lead to large run-to-run deviations and, thus, poor reproducibility.

Previously, we developed a sensitive method taking advantage of the unique chemistry of the quaternary amine to enhance ionization efficiency in conjunction with the strong nucleophilicity of the thiol present in thiocholine to effect the BEMA strategy with thiocholine as the Michael donor (as described in Chapter 2). This strategy results in

marked increase in ionization sensitivity during ESI accompanied by increased sequence coverage in model compounds as described in Chapters 2 and 3. More specifically, the definitive localization of phosphorylated residues is greatly facilitated by the thiocholine side chain through the generation of diagnostic triads of fragment ions resulting from peptide bond cleavage and further neutral loss of either trimethylamine (-59 Da/-63 Da) or thiocholine thiolate (-119 Da/-123 Da) during CID in MS^2 and MS^3experiments. Through utilization of titanium dioxide resin (TiO_2) for phosphopeptide enrichment, sample complexity is greatly reduced [23] leading to improved chromatographic coverage of the phosphopeptides of interest. To minimize false discovery rates, all database searches generated by MASCOT [24] were re-scored by Percolator [25-26], a semi-supervised machine learning algorithm further substantiating the identification of the observed phosphosites.

In this study, we successfully identified 141 phosphopeptides from 133 unique proteins with 228 phosphorylation sites from six independent biological replicates generated from 24 perfused mouse hearts (12 control-perfused, 12 global ischemic). Importantly, these data included 36 phosphopeptides from 35 mitochondrial proteins with 50 phosphosites, 37 of which are new mitochondrial phosphosites that have not been reported previously. Relative alterations in the magnitude of phosphorylation were evaluated for all phosphopeptides identified in three independent replicate samples using relative molecular ion peak intensity ratios. This study has demonstrated that β-elimination of phosphate and subsequent Michael addition (BEMA) using light and heavy thiocholine represents an effective mass-spectrometry based strategy for

comparative quantitative phosphoproteome analyses of intact organs subjected to pathologic perturbations.

4.3 Materials and Methods

Materials

Rapigest was purchased from Waters (Milford, MA); Protein concentrations or amounts were determined using a BCA protein assay kit was purchased from Pierce (Rockford, IL); trypsin was purchased from Promega (Madison, MI); Titansphere Titanium dioxide resin was purchased from GL Sciences (Torrance, CA); POROS 20 R2 resin was purchased from ABI (Foster City, CA). All solvents for mass spectrometric analyses were obtained from Honeywell Burdick&Jackson (Muskegon, MI); all other chemicals were obtained from Sigma-Aldrich (St. Louis, MO)

Synthesis of Thiocholine Chloride (Light) and Thiocholine-$^{13}C,d_3$ Chloride (Heavy)

Thiocholine chloride was prepared and the free thiol concentration of thiocholine chloride was determined as previously described in Chapter 2.

Perfusion of Isolated Langendorff Mouse Hearts

Animal protocols used were in strict accordance with the National Institutes of Health guidelines for humane treatment of animals and were reviewed and approved by the Animal Care Committee of Washington University. Mouse hearts were either perfused normally as controls or subjected to global ischemia, as previously described [28]. Briefly, mice were anesthetized with sodium pentobarbital and their hearts were excised and immersed in oxygenated Krebs-Henseleit buffer containing : 137 mM NaCl, 4.7 mM KCl,

1.2 mM $MgSO_4$, 1.2 mM KH_2PO_4, 15 mM $NaHCO_3$, 3mM $CaCl_2$, 0.5 mM NaEDTA and 11mM glucose equilibrated with O_2/CO_2 (95:5), plus insulin (70 mU/L) and BSA (2.8%), at 37 °C. Mouse hearts were then perfused by retrograde aortic flow with oxygenated buffer at 37 °C. Perfusion pressures were maintained constant at 45 to 50 mm Hg. All hearts were initially perfused with oxygenated buffer for a 15-minute equilibration period. 12 mouse hearts were perfused with oxygenated buffer for an additional 30 mins and served as controls. Another 12 mouse hearts were subjected to global ischemia for an additional 30 min.

Preparation of Mouse Mitochondria

Mitochondria were prepared as previously described with minor modifications [29-30]. Each perfused heart prepared as described above was immediately placed at 10% (w/v) in ice-cold pH 7.4 HEPES buffer containing 1 mM EDTA, 250 mM sucrose, phosphatase inhibitor cocktail (1 (Sigma) at a 100-fold dilution) and a customized phosphatase inhibitor cocktail (10 mM sodium fluoride, 4 mM sodium tartrate, 2 mM β-glycerophosphate, 2 mM sodium pyrophosphate). Hearts tissues were homogenized with a glass dounce homogenizer, centrifuged at 700 g for 10 min and the supernatant was collected. Next, the supernatant was centrifuged at 10,000 g for 15 min to pellet mitochondria. Mitochondria from two control hearts were pooled together to give six individual control samples while the same was done for the ischemic samples. All control and ischemic samples were processed using the same protocol except that light thiocholine was used for control hearts and heavy thiocholine was utilized for ischemic

hearts for the Michael addition reaction.

Tryptic Proteolysis of Mitochondrial Proteins

Mitochondria were re-suspended in 750 µL of 80% aqueous methanol solution in a 1.5-mL micro centrifuge tube and mitochondrial proteins were precipitated as previously described [31]. Briefly, 150 µL of $CHCl_3$ was added to the above mitochondrial suspension and vortexed, followed by the addition of 450 µL of H_2O. The mixture was vortexed again before centrifugation at 14,000 g for 15 min, separated into two layers, and the protein located at the interface appeared as a white layer. The upper layer (methanol and H_2O) was removed and another 450 µL of methanol was added. The sample was vortexed and centrifuged at 14,000 g for 10 min. The protein pelleted at the bottom of the tube was air-dried and re-suspended in 1000 µL of 0.2% Rapigest in 50 mM NH_4HCO_3 and incubated at 100 °C for 5 min. Protein content was determined using the micro-BCA protein assay kit (Pierce). 1 mg of total protein from each sample was used for subsequent preparations. The volume of each sample was adjusted to 1 mL using 50 mM NH_4HCO_3. Next, 52 µL of 100 mM dithiothreitol (DTT) was added to a final concentration of 5 mM. The sample was incubated at 60 °C for 30 min before 120 µL of 150 mM iodoacetamide was added to quench the reduction reaction and initiate alkylation. The sample was incubated for an additional 30 min in the dark. Trypsin was added to the solution at a protease to protein ratio of 1:30 (w/w). The solution was incubated at 37 °C overnight. The pH of the solution was lowered to < 2 to terminate the digestion and the incubated at 37 °C for 30 min. Hydrolyzed Rapigest was pelleted by

centrifugation at 13,000 rpm.

Highly Selective Enrichment of Phosphorylated Peptides by Titanium Dioxide (TiO_2) Micro Column Chromatography

Trypsinized protein samples were dried in a SpeedVac apparatus (Savant, Holbrook, NY), and reconstituted in 280 mg/mL 2,5-Dihydroxybenzoic acid (2,5-DHB) in 60% acetonitrile (ACN), 1.5% Trifluoroacetic acid (TFA). Phosphorylated peptides in the trypsinized samples were enriched using TiO_2 micro columns as previously described with minor modifications [32]. Bound phosphorylated peptides were eluted twice with 40 µL 25% ammonium hydroxide (pH > 10.5) and once with 30 µL 30% ACN. The fractions containing the eluted phosphopeptides were acidified by the addition of 15 µL 90% formic acid. 30 µL of water was added to reduce the organic solvent concentration to < 5%.

BEMA of Phosphorylated Peptides Enriched by TiO_2 Micro Column Chromatography with Light and Heavy Thiocholine

Phosphorylated peptides eluted from the TiO_2 micro columns were desalted using POROS 20 R2 micro columns as previously described [33]. Briefly, a POROS 20 R2 micro column was assembled by stamping out a small plug of C8 material from a 3M Empore C8 extraction disk using a HPLC syringe needle and placing this plug in the constricted end of a GELoader tip. Next, POROS R2 beads that were suspended in 50% acetonitrile at 5 mg/200 µL were packed into the GELoader tip by pressing air through

the micro column using an Eppendorf syringe. The length of the packed POROS R2 resin was about 3-6 mm. The column was then washed with 30 µL 50% acetonitrile and equilibrated with 30 µL 0.1% trifluoroacetic acid. Samples containing the phosphopeptides were then loaded onto the POROS R2 micro column. The sample was slowly passed through the micro column with compressed air from the Eppendorf syringe. The column was washed twice with 30 µL of 0.1% trifluoroacetic acid and the bound peptides were eluted first using 30 µL of 70% acetonitrile containing 0.05 % trifluoroacetic acid, then 5 µL of 30% acetonitrile containing 0.05% trifluoroacetic acid. The desalted phosphorylated peptides were dried in a SpeedVac apparatus and reconstituted in 50 µL deionized water followed by the addition of 38 µL DMSO and 12 µL of absolute ethanol. 25 µL of freshly prepared saturated $Ba(OH)_2$ was then added to the peptide solution to start the β-elimination reaction. After incubation at room temperature under nitrogen for 3 h with gentle vortexing every 20 min. The final pH was 12~13. 50 µL of 1 M thiocholine chloride was added to each of the six the control samples and 50 µL of 1 M thiocholine-$^{13}C,d_3$ chloride was added to each of the six the ischemic samples. The reaction mixture was incubated at room temperature under nitrogen for 5 h at pH 8~9 and then terminated by the addition of 5 µL of 10% TFA.

HPLC-ESI-MS^2/MS^3 Mass Spectrometric Analyses

Six control and six ischemic samples modified by light and heavy thiocholine respectively were randomly pooled in pairs to give six mixed samples for six individual replicates. The mixed samples were then desalted with POROS 20 R2 micro columns,

dried and reconstituted in 0.1% formic acid before injection and separation using a Surveyor HPLC system (Autosampler and pump, ThermoFisher, San Jose, CA) equipped with a reverse-phase C18 PepMap100 Nano-LC column (75 μm I.D. × 15 cm, 3 μm, 100 Å; Dionex, Sunnyvale, CA). The flow rate was maintained at 220280 nL/min. Samples eluting from the column were directed to the nanospray apparatus (i.e., NanoMate HD with LC coupler, Advion Bioscience Ltd., Ithaca, NY) and sprayed directly into a linear ion trap in tandem with an Orbitrap (LTQ-Orbitrap) mass spectrometer (ThermoFisher, San Jose, CA) at a spray voltage of 1.7 kV in the positive ion mode. Each of the six replicates was analyzed first in a survey run, which consisted of a 180 min gradient from 100% A to 75% A, 25% B (Buffer A: 90% water, 10% acetonitrile, 0.1% formic acid; Buffer B: 10% water, 90% acetonitrile, 0.1% formic acid, v:v) for 120 min, then to 50% A, 50% B (60 min). For data-dependent MS^2 analyses, full mass scans in the Orbitrap (300−1600 *m*/*z*, mass resolution = 30 000) were followed by product-ion scans in the LTQ of the five most abundant ions. These ions of interest generated from the survey run were then included in the parent mass list of a target run. The target run was conducted essentially the same as the survey run except that during the MS^2 data-dependent analyses, the five most abundant ions from the parent mass list were fragmented. A third run was conducted for MS^3 analyses. It consisted of a 180 min gradient from 100% A to 75% A, 25% B (120 min), then to 50% A, 50% B (60 min) for data-dependent MS^2/MS^3 analyses in which full mass scans in the Orbitrap (300−1600 *m*/*z*, mass resolution = 30 000) were followed by product-ion scans in the LTQ of the three most abundant ions from the parent mass list and the MS^3 scans in the LTQ of the ten most abundant

fragment ions following each of the three product-ion scans.

MASCOT Database Search

The local MASCOT server (version 2.1.1) with an up-to-date IPI mouse database was used to conduct all database searches [24]. The “auto decoy” option was chosen. Light and heavy thiocholine with neutral losses of trimethylamine and thiolate were integrated into MASCOT for customized processing of the designed covalent modifications for serine and threonine residues. Carbamidomethylation (C) was set as the fixed modification. Common variable modifications included acetylation (N-terminus, K), deamidation (NQ) and oxidation (M). A maximum of two missed cleavages were allowed. Full mass and product-ion mass accuracy were set at 5 ppm and 1 Da respectively. Database searches were conducted using an automatic decoy database provided by the local MASCOT server.

Post-MASCOT Processing using Percolator

All MASCOT search results were re-scored and re-ranked by a stand-alone version of the MASCOT Percolator [25-26]. All the programs utilized were downloaded using links from http://www.sanger.ac.uk/resources/software/mascotpercolator. Since the MASCOT searches were conducted using the option of “auto decoy”, the target and decoy MASCOT result files (.DAT) required by the Percolator program were the same. The “rankdelta N” value was set at default = “1”, indicating all peptide hit ranks that have a delta score of < 1 relative to the top hit match were processed. The false discovery rate

(FDR) was set at 1%. Peptide hits with a posterior error probability (PEP) value < 0.05 (score > 13) were considered automatic positive identifications. Peptides originating from mitochondrial proteins with a PEP > 0.05 but < 0.2 (7 < score < 13) were verified manually for false identifications. All MS^3 scans were analyzed manually for the signature neural loss of trimethylamine (-59 Da/-63 Da).

Comparative Quantitation of Light and Heavy Thiocholine-Modified Peptides

Relative changes in phosphorylation state were evaluated for all phosphopeptides identified in three or more independent replicate samples using relative peak intensity ratios of the molecular ions of light and heavy thiocholine-modified peptides at the time of their co-elution. The relative ratio was calculated by dividing the light peak intensity by the heavy peak intensity. Dixon's Q [34] test was used to eliminate outlier(s) with 95% confidence prior to calculations of sample average and standard deviation. The subcellular locations of the phosphoproteins identified were determined using the protein database UniProt [35-36] and LOCATE database [37-38].

4.4 Results and Discussion

In this study, the phosphoproteome of mitochondria isolated from Langendorff-perfused mouse hearts subjected to global ischemia was investigated. During prolonged ischemia, flux through the mitochondrial electron transport chain (ETC) is attenuated owing to the accumulation of reducing equivalents in the mitochondrial matrix in the absence of oxygen. This results in the dramatic reduction of ATP production because during ischemia, the redox reactions involving oxygen become the rate limiting steps for the production of ATP. This ultimately leads to profound decreases in cellular ATP, resulting in hemodynamic dysfunction [39-42]. The chain of signaling events in response to the depletion of oxygen is regulated, at least in part, by changes in protein phosphorylation [43-46]. However, the role of alterations in mitochondrial protein phosphorylation in this process is at its early stages of understanding. Specifically, the identity of the mitochondrial phosphoproteins and their specific phosphosites during ischemia are largely unknown. Accordingly, we sought to determine specifically changes in protein phosphorylation following myocardial ischemia using quantitative phosphoproteomics to gain insight into the signaling pathways and molecular mechanisms that are activated during myocardial ischemia and result in alterations in mitochondrial bioenergetics and signaling.

Comparative Quantitative Phosphoproteomics using β-Elimination and Michael Addition with Light and Heavy Thiocholine

As reported in Chapters 2 and 3, β-elimination of phosphate and subsequent Michael addition (BEMA) with light and heavy thiocholine as the Michael donors is a sensitive and effective strategy for the detection, identification, and quantitation of phosphoserine and phosphothreonine residues. The overall workflow based on BEMA with light and heavy thiocholine for the comparative quantitative phosphoproteomics of mitochondria from mouse hearts upon induction of cardiac ischemia is detailed in Figure 4.1. Mitochondria were isolated from both normally perfused and globally ischemic mouse hearts by differential centrifugation. Mitochondrial proteins were then isolated by methanol/chloroform precipitation, reconstituted in 0.2% Rapigest, and total protein content was determined using a BCA protein assay. Next, 1 mg of protein from each sample was subjected to trypsinolysis. The resultant tryptic peptides were affinity purified using a TiO_2 micro column for the selective enrichment of phosphopeptides. The affinity purified phosphopeptides were desalted and modified with either light thiocholine (control samples) or heavy thiocholine (ischemic samples). After the reactions were terminated, control and ischemic samples were mixed together, desalted and analyzed by using LC-MS/MS. The mass spectrometric data was searched by using MASCOT and re-scored by Percolator to identify phosphopeptides. Quantitative information was obtained from the relative peak intensity of the molecular ions of the phosphopeptides modified by light and heavy thiocholine, respectively. The subcellular localization of the identified proteins was determined using UniProt [35-36] and LOCATE [37-38] databases. Our

strategy emphasized the rapid purification of mitochondrial to prevent intrapreparative artifacts, recognizing that all mitochondrial preparations contain mitochondria-associated proteins.

Mass spectrometric analysis of BEMA thiocholine-modified samples of mitochondria from control and ischemic murine myocardium showed multiple ions which were identified by sequential MASCOT and Percolator. The total ion chromatography (TIC) obtained from a representative sample is shown in Figure 4.2-A. The extracted ion chromatography (XIC) of the full-mass scans is presented in Figure 4.2-B.

A representative example of the diagnostic triad present in thiocholine-modified peptides is shown in Figure 4.3-A. The product-ion spectrum of the quadruply charged molecular ion at *m/z* 425.200 of the heavy thiocholine-modified peptide YHGHS*MSDPGVSYR was identified as originating from the pyruvate dehydrogenase E1 component subunit α. The spectrum shows the peptide bond cleavage fragment ions B_8^{+2} at *m/z* 510.9, B_{10}^{+2} at *m/z* 588.2, B_{11}^{+2} at *m/z* 637.5, B_{12}^{+3} at *m/z* 454.6 and A_{11}^{+3} at *m/z* 416.2 (all fragment ions resulting from heavy thiocholine-modified peptides are presented in capital letters, such as B, A). Also shown in the spectrum are representative diagnostic triads consisting of the B_{10}^{+2} fragmentation ions resulting from peptide bond cleavage (to give an ion at *m/z* = 510.9) and further neutral loss of $^{13}C,d_3$-trimethylamine (-63 Da, *m/z* = 556.8) or the $^{13}C,d_3$-thiocholine thiolate (-123 Da, *m/z* = 526.7). Figure 4.3-B displays the expanded product-ion spectrum of the quadruply charged molecular ion modified by heavy thiocholine at *m/z* 425.200 (YHGHS*MSDPGVSYR) ranging from *m/z* 380 to *m/z* 640. The spectrum shows that the heavy thiocholine-containing B

ions are accompanied by the corresponding light thiocholine-containing b ions (all fragment ions resulting from light thiocholine-modified peptides are presented in lower-case letters) resulting from the fragmentation of the light thiocholine-modified molecular ion at *m/z* 424.195 (YHGHS*MSDPGVSYR): B_8^{+2} at *m/z* 510.9 with b_8^{+2} at *m/z* 509.0, B_{10}^{+2} at *m/z* 588.2 with b_{10}^{+2} at *m/z* 586.2, B_{11}^{+2} at *m/z* 637.5 with b_{11}^{+2} at *m/z* 635.7, B_{12}^{+3} at *m/z* 454.6 with b_{12}^{+3} at *m/z* 453.3 and B_{10}^{+3} at *m/z* 392.6 with b_{10}^{+3} at *m/z* 390.5. This indicates that during the data-dependent analysis both the light and heavy thiocholine-modified peptides were included for collision induced dissociation (CID). Given that the structures of the peptides are identical, they produced the same corresponding B/b ions in the Product-ion spectrum as indicated by the presence of multiple doublets. This is due to the low-resolution capability of the linear ion trap when selecting the ion of interest for fragmentation. With molecular mass 4 Da apart, both light and heavy thiocholine-modified peptides were included in the mass selection window at +4. The doublets of peptide bond cleavage fragment ions resulting from light and heavy thiocholine-modified peptides further confirm the identification of the peptide, the localization of the modified residue(s), and the phosphorylation site(s). The relative peak intensities of the doublets also serve as a redundant confirmation for the comparative quantitation conducted at the molecular level. Figure 4.3-C, D, E and F illustrate the signature neutral loss fragmentation pattern (loss of $^{13}C,d_3$-trimethylamine, -63 Da) at the MS^3 level of the heavy thiocholine containing fragment ions resulting from the peptide bond cleavages of the quadruply charged molecular ion modified by heavy thiocholine at *m/z* 425.200 (YHGHS*MSDPGVSYR). In Figure 4.3-C, B_{11} - 63^{+2} at *m/z* 606.1 is the dominant

neutral loss ion; in Figure 4.3-D, B_{10} - 63^{+2} at *m/z* 566.6 is the dominant neutral loss ion; in Figure 4.3-E, B_8 - 63^{+2} at *m/z* 479.5 is the dominant neutral loss ion; in Figure 4.3-F, B_{12} - 63^{+3} at *m/z* 433.6 is the dominant neutral loss ion.

Collectively, the BEMA with light and heavy thiocholine strategy provides a rich repertoire of information at the MS^2 and MS^3 levels that not only reveals the identification of the modified phosphopeptide, and the localization of thiocholine modification (phosphorylation), but also provides redundant comparative quantitative information at MS^2 level.

Improved MASCOT Results using the Post-Processing algorithm Percolator

MASCOT is one of the most widely used database search engines for the identification of proteins and peptides based on tandem mass spectrometric data [24]. MASCOT employs an algorithm that ranks the correlation between the experimental product-ion spectra and calculated peptide spectra based on the peptide sequences included in the protein database. The correlation between an experimental and a calculated spectrum is expressed by a score called peptide spectrum match (PSM). However, the ranking based on PSMs does not constitute formal proof of the peptide of interest in all cases. To substantiate results from MASCOT, the strategy of using decoy protein databases that randomize and reverse the protein sequences in the original databases [47-48] enabled the evaluation of peptide identifications using PSMs resulting from both original and decoy databases, thereby allowing the subsequent detection of false positives to determine the false discovery rate (FDR) [49]. MASCOT identifies

peptides based on the comparison between the PSM of each mass spectrum and a probability-based peptide identity score. If a PSM exceeds the threshold, the peptide identification is a true identification with a certain confidence interval (e.g., a value of 95% confidence is typically used). In addition, a second measurement of experimental vs. calculated spectra is the peptide homology threshold. If the PSM is lower than the homology threshold, it is considered an outlier [50]. As shown in Table 4.1, use of the decoy database in combination with identity and homology thresholds, the performance of MASCOT is not ideal, generating a FDR of over 11% FDR in each of the six individual samples, and an overall FDR of 12.49%. Therefore, the Percolator algorithm was employed to decrease the FDR obtained from MASCOT analysis alone. Percolator utilizes a semi-supervised machine-learning based algorithm called support vector machine (SVM) to compare the identifications resulting from the target and decoy databases using MASCOT [25-26]. The detailed workflow of the algorithm of Percolator is illustrated in Figure 4.4 (reproduced with permission from Figure 1 of the original publication (Journal of Proteome Research, *2009, 8*, 3176-3181 by M, Brosch, L. Yu, T. Hubbard, and J. Choudhary)). All MASCOT search results were re-scored and re-ranked by a stand-alone version of the Percolator downloaded from the website http://www.sanger.ac.uk/resources/software/mascotpercolator. The “rank delta N” value was set at default = “1”, which means all peptide hit ranks that have a delta score of < 1 to the top hit match were processed. The false discovery rate (FDR) was set at 1%. Table 4.1 shows that Percolator not only increased the total peptide hits by 15%, but also significantly decreased the FDR to 0.64% from the original 12.49%.

Collectively, Percolator provided a standard post-MASCOT approach for the significant improvement in increasing authentic phosphopeptide identification, and reducing false positives resulting in a decreased FDR.

Statistical Analysis of the Quantitation and Identification of Light and Heavy Thiocholine-Modified Phosphopeptides.

In our previous study, we employed BEMA with light and heavy thiocholine using the tryptic phosphopeptide FQpSEEQQQTEDELQDK from β-casein to show that five independent replicates at a theoretical ratio of 1:1 (light:heavy) produced an experimental average of 0.96 ± 0.02; three independent replicates at theoretical ratios of 1:2, 1:3, 1:4, 4:1, 3:1, 2:1 together with five independent replicates at a theoretical ratio of 1:1 (light:heavy) yielded an experimental correlation coefficient of $R^2 = 0.99$ (as described in Chapter 2). These results show that the BEMA strategy with light and heavy thiocholine is a reliable, reproducible and precise approach towards quantitative phosphoproteomics. However, when dealing with complex tissue based systems, such as subject of the current study, large deviations in the comparative quantitation analysis can be introduced through multi-step sample preparation, run-to-run fluctuations in instrumentation parameters, or simply by the intrinsic differences between individual biological replicates. Although useful information could still be obtained by a limited number of replicates [21], relative changes in phosphorylation were exclusively evaluated for all phosphopeptides identified in three or more independent replicate samples (six samples overall) using relative peak intensity ratios of the molecular ions of light and heavy thiocholine-modified peptides at

the time of their co-elution. The relative ratio was calculated by dividing the light peak intensity by the heavy peak intensity. Dixon's Q [34] test was used to eliminate the outlier(s) with 95% confidence prior to the calculations of sample average and standard deviation. A representative “M + 4” doublet pattern of the quadruply charged molecular ions of light and heavy thiocholine-modified YHGHS*MSDPGVSYR at *m/z* 424.195 and 425.200, respectively is evident in Figure 4.5. The greater peak intensity of the heavy thiocholine-modified YHGHS*MSDPGVSYR indicates that the phosphorylation level was increased for this peptide following the induction of cardiac ischemia.

Peptide hits with a Percolator-processed posterior error probability (PEP) value < 0.05 (score > 13) indicating a confidence level of 95%, were considered automatic positive identifications. Non-mitochondrial peptides with a score < 13 were considered false positives. Peptides originating from mitochondrial proteins with a PEP > 0.05 but < 0.2 (7 < score < 13), indicating a confidence level between 80% and 95%) were verified manually. Four mitochondrial peptides with a score between 7 and 13 were verified as positive identifications. The mass spectra of these peptides are shown in Figure 4.6. Phosphopeptides identified were categorized into six groups according to the number of hits from the six individual biological replicates. Table 4.2-A contains thiocholine-modified peptides identified in all six individual biological replicates. There are 21 unique peptides identified containing 36 phosphorylation sites, 16 of which were not reported in the literature. Ten out of the 21 peptides yielded a signature neutral loss in MS^3 which are highlighted in bold. The ratios in italic font indicate that the ratios are calculated using heavy peak intensity over light peak intensity. Table 4.2-B contains

thiocholine-modified peptides identified in five out of six individual biological replicates. There are eight unique peptides identified containing 13 phosphorylation sites, five of which were not reported before. Four out of the eight peptides yielded a signature neutral loss in MS^3. Table 4.2-C contains thiocholine-modified peptides identified in four out of six individual biological replicates. There are nine unique peptides identified containing 17 phosphorylation sites, 15 of which were not reported before. Five out of the nine peptides yielded a signature neutral loss in MS^3. Table 4.2-D contains thiocholine-modified peptides identified in three out six of individual biological replicates. There are eight unique peptides identified containing 16 phosphorylation sites, 14 of which were not reported before. One out of the eight peptides yielded a signature neutral loss in MS^3. Table 4.2-E shows the thiocholine-modified peptides identified in two out of six individual biological replicates. There are 11 unique peptides identified containing 20 phosphorylation sites, all of which were not reported before. Four out of the 11 peptides yielded a signature neutral loss in MS^3. Table 4.2-F shows thiocholine-modified peptides identified in one out of six individual biological replicates. There are 84 unique peptides identified containing 126 phosphorylation sites, 119 of which are novel. Three out of the 84 peptides yielded a signature neutral loss in MS^3. No evaluation of quantitation was assessed for peptides in the 1-hit and 2-hit groups out of six. Overall, 141 phosphopeptides were identified from 133 unique proteins with 228 phosphorylated sites from six independent biological replicates, with 189 novel sites. Twenty-seven out 141 thiocholine-modified peptides yielded a signature neutral loss in MS^3, with 24 out 57 if 1-hit peptides are not included. Mitochondrial proteins were determined using the protein

database UniProt [35-36] and the LOCATE database [37-38]. Proteins identified with either the UniProt or LOCATE databases as mitochondrial proteins were considered to be mitochondrial in origin. There are 36 phosphopeptides identified from 35 mitochondrial proteins with 50 phosphorylated sites, of which 37 were not reported before. As shown in Table 4.3, relative changes in phosphorylation were evaluated for mitochondrial phosphopeptides identified in three or more independent replicate samples

To validate the above strategy, the well-characterized phosphorylation of cardiac phospholamban at serine 16 induced during global cardiac ischemia in mouse hearts was used as a test case for the methodology developed in this study. As previously reported, phosphorylation at serine 16 of cardiac phospholamban was increased by 20-40 fold upon 20-min of ischemia in Langendorff-perfused rat hearts [17]. In our study, we identified the light and heavy thiocholine-modified peptide RAS*TIEMPQQAR with a light over heavy ratio of 0.05 ± 0.00 calculated from six replicates indicating an approximately 20-fold increase in phosphorylation of the peptide, which is consistent the previous results obtained using a traditional ^{32}P-radiolabeling method from a similar system thereby validating the quantitative approach employed in the current study.

Among all the mitochondrial peptides indentified, the peptide IVS*AQSLAEDDVE showed the most significant and consistent change throughout all six samples. The heavy thiocholine-modified peptide IVS*AQSLAEDDVE was identified, with extremely high confidence and high mass accuracy (Table 4.3), in each and every sample. The absence of the ion peak corresponding to the light thiocholine-modified IVS*AQSLAEDDVE indicates that the net phosphorylation level was increased dramatically during the

induced cardiac ischemia. The peptide IVS*AQSLAEDDVE (133-145) is a tryptic peptide from the protein called mitochondrial import receptor subunit TOM20 located in the outer membranes of mitochondria, which is an important receptor protein for precursors of mitochondrial proteins that are synthesized in cytoplasm [51]. The phosphorylation site of serine residue 135 is located within a domain that was characterized in previous study [52] as a critical region responsible for the recognition of protein possessing internal signaling sequence, rendering the phosphorylation of serine 135 a potential mechanism for the adaptive reactions of mitochondria during oxygen deficiency.

4.5 Conclusion

We demonstrated that β-elimination of phosphate and subsequent Michael addition (BEMA) with light and heavy thiocholine together with TiO_2 phosphopeptide enrichment and the Percolator machine learning algorithm based MASCOT re-scoring program provides a highly effective strategy for *in vivo* quantitative phosphoproteomics of tissue-based systems. The application of this strategy for the quantitative analysis of alterations in the murine myocardial mitochondrial phosphoproteome subjected to global cardiac ischemia resulted in the identification of 141 phosphopeptides from 133 unique proteins with 228 phosphorylated sites, 189 of which were not reported before. Among all the peptides identified, 36 were phosphopeptides from 35 mitochondrial proteins containing 50 phosphosites, 37 of which were not reported before. The strategy was validated by the well-characterized phosphorylation of phospholamban at serine 16 during induced global cardiac ischemia in mouse myocardium.

4.6 References

(1) Krebs, E. G. *Philos. Trans. R. Soc. Lond. B. Biol. Sci.* **1983**, *302*, 3-11.

(2) Zolnierowicz, S.; Bollen, M. *EMBO J.* **2000**, *19*, 483-488.

(3) Mann, M.; Ong, S. E.; Gronborg, M.; Steen, H.; Jensen, O. N.; Pandey, A. *Trends Biotechnol.* **2002**, *20*, 261-268.

(4) Reinders, J.; Wagner, K.; Zahedi, R. P.; Stojanovski, D.; Eyrich, B.; van der Laan, M.; Rehling, P.; Sickmann, A.; Pfanner, N.; Meisinger, C. *Mol Cell Proteomics* **2007**, *6*, 1896-1906.

(5) Villen, J.; Beausoleil, S. A.; Gerber, S. A.; Gygi, S. P. *Proc Natl Acad Sci U S A* **2007**, *104*, 1488-1493.

(6) Ballif, B. A.; Villen, J.; Beausoleil, S. A.; Schwartz, D.; Gygi, S. P. *Mol Cell Proteomics* **2004**, *3*, 1093-1101.

(7) Schulenberg, B.; Aggeler, R.; Beechem, J. M.; Capaldi, R. A.; Patton, W. F. *J Biol Chem* **2003**, *278*, 27251-27255.

(8) Aponte, A. M.; Phillips, D.; Hopper, R. K.; Johnson, D. T.; Harris, R. A.; Blinova, K.; Boja, E. S.; French, S.; Balaban, R. S. *J Proteome Res* **2009**, *8*, 2679-2695.

(9) Lee, J.; Xu, Y.; Chen, Y.; Sprung, R.; Kim, S. C.; Xie, S.; Zhao, Y. *Mol Cell Proteomics* **2007**, *6*, 669-676.

(10) Linn, T. C.; Pettit, F. H.; Reed, L. J. *Proc Natl Acad Sci U S A* **1969**, *62*, 234-241.

(11) Roche, T. E.; Reed, L. J. *Biochem Biophys Res Commun* **1974**, *59*, 1341-1348.

(12) Sugden, P. H.; Hutson, N. J.; Kerbey, A. L.; Randle, P. J. *Biochem J* **1978**, *169*,

433-435.

(13) Sugden, P. H.; Randle, P. J. *Biochem J* **1978**, *173*, 659-668.

(14) Harris, R. A.; Popov, K. M.; Zhao, Y.; Kedishvili, N. Y.; Shimomura, Y.; Crabb, D. W. *Adv Enzyme Regul* **1995**, *35*, 147-162.

(15) Bender, E.; Kadenbach, B. *FEBS Lett* **2000**, *466*, 130-134.

(16) Ludwig, B.; Bender, E.; Arnold, S.; Huttemann, M.; Lee, I.; Kadenbach, B. *Chembiochem* **2001**, *2*, 392-403.

(17) Vittone, L.; Mundina-Weilenmann, C.; Said, M.; Ferrero, P.; Mattiazzi, A. *J Mol Cell Cardiol* **2002**, *34*, 39-50.

(18) Yan, J. X.; Packer, N. H.; Gooley, A. A.; Williams, K. L. *J Chromatogr A* **1998**, *808*, 23-41.

(19) Ross, P. L.; Huang, Y. N.; Marchese, J. N.; Williamson, B.; Parker, K.; Hattan, S.; Khainovski, N.; Pillai, S.; Dey, S.; Daniels, S.; Purkayastha, S.; Juhasz, P.; Martin, S.; Bartlet-Jones, M.; He, F.; Jacobson, A.; Pappin, D. J. *Mol Cell Proteomics* **2004**, *3*, 1154-1169.

(20) Reinl, T.; Nimtz, M.; Hundertmark, C.; Johl, T.; Keri, G.; Wehland, J.; Daub, H.; Jansch, L. *Mol Cell Proteomics* **2009**, *8*, 2778-2795.

(21) Boja, E. S.; Phillips, D.; French, S. A.; Harris, R. A.; Balaban, R. S. *J Proteome Res* **2009**, *8*, 4665-4675.

(22) Chen, M.; Su, X.; Yang, J.; Jenkins, C. M.; Cedars, A. M.; Gross, R. W. *Anal Chem* **2010**, *82*, 163-171.

(23) Larsen, M. R.; Thingholm, T. E.; Jensen, O. N.; Roepstorff, P.; Jorgensen, T. J.

Mol. Cell. Proteomics **2005**, *4*, 873-886.

(24) Perkins, D. N.; Pappin, D. J. C.; Creasy, D. M.; Cottrell, J. S. *Electrophoresis* **1999**, *20*, 3551-3567.

(25) Kall, L.; Canterbury, J. D.; Weston, J.; Noble, W. S.; MacCoss, M. J. *Nat Methods* **2007**, *4*, 923-925.

(26) Brosch, M.; Yu, L.; Hubbard, T.; Choudhary, J. *J Proteome Res* **2009**, *8*, 3176-3181.

(27) Whitesides, G. M.; Lilburn, J. E.; Szajewski, R. P. *J. Org. Chem.* **1977**, *42*, 332-338.

(28) Lerner, D. L.; Yamada, K. A.; Schuessler, R. B.; Saffitz, J. E. *Circulation* **2000**, *101*, 547-552.

(29) Ricci, J. E.; Gottlieb, R. A.; Green, D. R. *J Cell Biol* **2003**, *160*, 65-75.

(30) Mancuso, D. J.; Sims, H. F.; Han, X.; Jenkins, C. M.; Guan, S. P.; Yang, K.; Moon, S. H.; Pietka, T.; Abumrad, N. A.; Schlesinger, P. H.; Gross, R. W. *J Biol Chem* **2007**, *282*, 34611-34622.

(31) Wessel, D.; Flugge, U. I. *Anal Biochem* **1984**, *138*, 141-143.

(32) Mazanek, M.; Mituloviae, G.; Herzog, F.; Stingl, C.; Hutchins, J. R.; Peters, J. M.; Mechtler, K. *Nat. Protoc.* **2007**, *2*, 1059-1069.

(33) Thingholm, T. E.; Jorgensen, T. J.; Jensen, O. N.; Larsen, M. R. *Nat. Protoc.* **2006**, *1*, 1929-1935.

(34) Rorabacher, D. B. *Analytical Chemistry* **1991**, *63*, 139-146.

(35) Boeckmann, B.; Bairoch, A.; Apweiler, R.; Blatter, M. C.; Estreicher, A.;

Gasteiger, E.; Martin, M. J.; Michoud, K.; O'Donovan, C.; Phan, I.; Pilbout, S.; Schneider, M. *Nucleic Acids Res* **2003**, *31*, 365-370.

(36) Bairoch, A.; Bougueleret, L.; Altairac, S. *Nucleic Acids Research* **2007**, *35*, D193-D197.

(37) Fink, J. L.; Aturaliya, R. N.; Davis, M. J.; Zhang, F.; Hanson, K.; Teasdale, M. S.; Kai, C.; Kawai, J.; Carninci, P.; Hayashizaki, Y.; Teasdale, R. D. *Nucleic Acids Res* **2006**, *34*, D213-217.

(38) Sprenger, J.; Lynn Fink, J.; Karunaratne, S.; Hanson, K.; Hamilton, N. A.; Teasdale, R. D. *Nucleic Acids Res* **2008**, *36*, D230-233.

(39) Murfitt, R. R.; Stiles, J. W.; Powell, W. J., Jr.; Sanadi, D. R. *J Mol Cell Cardiol* **1978**, *10*, 109-123.

(40) Rouslin, W. *Am J Physiol* **1983**, *244*, H743-748.

(41) Arduini, A.; Mezzetti, A.; Porreca, E.; Lapenna, D.; DeJulia, J.; Marzio, L.; Polidoro, G.; Cuccurullo, F. *Biochim Biophys Acta* **1988**, *970*, 113-121.

(42) Baker, J. E.; Kalyanaraman, B. *FEBS Lett* **1989**, *244*, 311-314.

(43) Zivin, J. A.; Kochhar, A.; Saitoh, T. *Stroke* **1990**, *21*, III117-121.

(44) Albert, C. J.; Ford, D. A. *Am J Physiol* **1999**, *276*, H642-650.

(45) Mundina-Weilenmann, C.; Said, M.; Vittone, L.; Ferrero, P.; Mattiazzi, A. *Mol Cell Biochem* **2003**, *252*, 239-246.

(46) Williams, S. D.; Ford, D. A. *Am J Physiol Heart Circ Physiol* **2001**, *281*, H168-176.

(47) Moore, R. E.; Young, M. K.; Lee, T. D. *J Am Soc Mass Spectrom* **2002**, *13*, 378-

386.

(48) Colinge, J.; Masselot, A.; Giron, M.; Dessingy, T.; Magnin, J. *Proteomics* **2003**, *3*, 1454-1463.

(49) Benjamini, Y.; Hochberg, Y. *Journal of the Royal Statistical Society Series B-Methodological* **1995**, *57*, 289-300.

(50) Brosch, M.; Swamy, S.; Hubbard, T.; Choudhary, J. *Mol Cell Proteomics* **2008**, *7*, 962-970.

(51) Schleiff, E.; Shore, G. C.; Goping, I. S. *FEBS Lett* **1997**, *404*, 314-318.

(52) Schleiff, E.; Turnbull, J. L. *Biochemistry* **1998**, *37*, 13043-13051.

4.7 Table Legends

Table 4.1

Improvement of peptide identification in MASCOT search results using Percolator.

A local MASCOT server with an up-to-date IPI mouse database was used to conduct all searches as described in Materials and Methods. Database searches were conducted using an automatic decoy database provided by the local MASCOT server. All MASCOT search results were re-scored and re-ranked by a stand-alone version of the MASCOT Percolator as described in Materials and Methods. The false discovery rate (FDR) was set at 1%. All peptide hits with ion score greater than the "identification score" or the "homology score" in the direct output results generated by MASCOT were counted. For the Percolator processed results, all peptide hits with a posterior error probability (PEP) value < 0.05 (score > 13) were counted. The "decoy hits" were those product-ion spectra that matched peptide sequences in the decoy database. The False Identification Rate (FDR%) was calculated by dividing the overall hits using the decoy hits. The Percolator program not only increased the total hit number in each of the six samples, but also significantly lowered the FDR%. Percolator increased the total number of peptide hits by roughly 15% and lowered the overall FDR% from 12.29% to 0.64%.

Table 4.2

Identification of phosphorylation sites in proteins from mitochondria isolated from control and ischemic mouse hearts using BEMA with light and heavy thiocholine.

Tryptic peptides from proteins associated with mitochondria isolated from control and ischemic mouse hearts were TiO_2-enriched, and modified by light and heavy thiocholine, respectively. The resultant light and heavy thiocholine samples were mixed, desalted, separated using reverse-phase nanobore HPLC, and analyzed with an LTQ-Orbitrap system as described in Materials and Methods. Mass spectrometry data were searched utilizing MASCOT with the designated thiocholine modification as well as common amino acid modifications as described in the Materials and Methods. Peptides were identified using Percolator-processed MASCOT results as described in the Materials and Methods. Relative change in phosphorylation due to ischemia was evaluated for all phosphopeptides identified in three or more independent replicates as described in the Materials and Methods. The ratios in italic font indicate that they were calculated using heavy peak intensity over light peak intensity. "*" denotes phosphorylation sites; "(*)" denotes that more than one phosphorylation site was identified in the same peptide and that they were not concurrent. The superscripts "ace", "ac", "d", and "o" denote the following modifications: acetylation (N-terminus), acetylation (K), deamidation (NQ) and oxidation (M), respectively. All cysteine residues were carbamidomethylated. Peptides which yielded a signature neutral loss pattern in MS^3 are highlighted in bold.

A. Thiocholine-modified peptides identified in all six individual biological replicates. There are 21 unique peptides identified containing 36 phosphorylation sites, 16 of which were not reported before. Ten out of the 21 peptides yielded a signature neutral loss in MS^3.

B. Thiocholine-modified peptides identified in five out of six individual biological replicates. There are eight unique peptides identified containing 13 phosphorylation sites, five of which were not reported before. Four out of the eight peptides yielded a signature neutral loss in MS^3.

C. Thiocholine-modified peptides identified in four out of six individual biological replicates. There are nine unique peptides identified containing 17 phosphorylation sites, 15 of which were not reported before. Five out of the nine peptides yielded a signature neutral loss in MS^3.

D. Thiocholine-modified peptides identified in three out six of individual biological replicates. There are eight unique peptides identified containing 16 phosphorylation sites, 14 of which were not reported before. One out of the eight peptides yielded a signature neutral loss in MS^3.

E. Thiocholine-modified peptides identified in two out of six individual biological replicates. There are 11 unique peptides identified containing 20 phosphorylation sites, all of which were not reported before. Four out of the 11 peptides yielded a signature neutral loss in MS^3.

F. Thiocholine-modified peptides identified in one out of six individual biological replicates. There are 84 unique peptides identified with 126 phosphorylation sites, 119 of which were not reported before. Three out of the 84 peptides yielded a signature neutral loss in MS^3.

Table 4.3

Identification of phosphorylation sites from mitochondrial proteins isolated from control and ischemic mouse hearts using BEMA with light and heavy thiocholine.

Tryptic peptides from proteins associated with mitochondria isolated from control and ischemic mouse hearts were TiO_2-enriched, and modified by light and heavy thiocholine, respectively. The modified peptides were mixed, desalted, and separated using reverse-phase nanobore HPLC, before analysis with an LTQ-Orbitrap system as described in Materials and Methods. Mass spectrometry data were searched utilizing MASCOT with the designated thiocholine modification as well as common amino acid modifications as described in the Materials and Methods. Peptides were identified using Percolator-processed MASCOT results as described in the Materials and Methods. Mitochondrial proteins were identified using both UniProt and LOCATE. No attempts have been made to reassign the subcellular locations predicted by UniProt and LOCATE. Relative changes in phosphorylation were evaluated only for mitochondrial phosphopeptides identified in three or more independent replicates as described in the Materials and Methods. The ratios in italic font indicate that they were calculated using heavy peak intensity over light peak intensity. "*" denotes phosphorylation sites; "(*)" denotes that more than one phosphorylation site was identified in the same peptide that were not concurrent with other phosphorylation sites within the same peptide. The superscripts "ace", "ac", "d", and "o" denote the following modifications: acetylation (N-terminus), acetylation (K), deamidation (NQ) and oxidation (M), respectively. All cysteine residues were carbamidomethylated. Peptides which yielded a signature neutral loss pattern in MS^3 are

highlighted in bold. Collectively, there were 36 unique peptides identified with 50 phosphorylation sites, 37 (indicated with underscore) of which were not reported before. Eight out of the 36 peptides yielded a signature neutral loss in MS^3.

"[a]": Proteins that are known to be other subcellular locations but are associated with mitochondria and are listed as mitochondrial proteins in UniProt and LOCATE.

Table 4.1

Sample	MASCOT Hits	MASCOT Decoy Hits	FDR%	Percolator Hits	Percolator Decoy Hits	FDR%
1	1509	194	12.86	1782	9	0.51
2	1815	210	11.57	2165	14	0.65
3	2156	274	12.71	2429	17	0.70
4	1867	241	12.91	2177	15	0.69
5	2013	259	12.87	2288	14	0.61
6	2177	263	12.08	2464	16	0.65
Total	11537	1441	12.49	13305	85	0.64

Table 4.2

A.

Protein	Peptide Sequence	Δm (ppm)	Percolator Score	Ratio
Isoform 1 of Tropomyosin alpha-1 chain	**AISEELDHALNDMT(*)S*I**	1.2	152.2	1.08±0.36
Alpha-crystallin B chain	**APS*WIDTGLSEMR**	1.4	94.6	0.00±0.00
Vinculin	DPNAS*PGDAGEQAIR	0.1	152.7	0.67±0.25
Prostaglandin E synthase 3	**DWEDDS*DEDMSNFDR**	-0.1	114.5	0.53±0.40
Uncharacterized protein C6orf203 homolog	EADEEDS*DEETS(*)YPER	1.0	127.2	1.15±0.23
Isoform SERCA2A of Sarcoplasmic/endoplasmic reticulum calcium ATPase 2	EFDELSPS*AQR	1.7	16.4	1.22±0.21
Isoform 2 of Spectrin beta chain, brain 1	**GDQVS*Q^{d}NGLPAEQGSPR**	2.2	106.4	*0.91±0.11*
Isoform Somatic of Angiotensin-converting enzyme	**GPQFGS*EVELR**	1.7	44.3	2.13±0.79
Mitochondrial import receptor subunit TOM20 homolog	IVS*AQSLAEDDVE	-0.6	152.7	0.00±0.00
AHNAK nucleoprotein isoform 1	LPSGS*GPAS(*)PTTGSAVDIR	2.0	88.3	0.52±0.19
Gap junction protein	QAS*EQNWANYSAEQNR	1.3	152.9	1.48±0.32
Isoform A of Heat shock protein beta-1	QLS*SGVSEIR	1.9	29.0	0.04±0.08
Cardiac phospholamban	RAS*T(*)IEMPQQAR	3.4	151.0	0.05±0.05
Tensin 1	S(*)QS*FPDVEPQLPQAPTR	2.0	63.6	0.65±0.33
Ras GTPase-activating protein-binding protein 1	**S(*)T(*)S*PAPADVAPAQEDLR**	2.2	69.2	0.79±0.28
Isoform 1 of Protein NDRG2	**TAS(*)LT*S(*)AASIDGSR**	1.0	152.4	0.34±0.28
Oxsr1 Serine/threonine-protein kinase OSR1	**TEDGGWEWS*DDEFDEESEEGR**	-3.1	152.7	0.80±0.40

Protein	Peptide Sequence	Δm (ppm)	Percolator Score	Ratio
Putative uncharacterized protein	T(*)LS(*)PT*PS(*)AEGYQDVR	1.4	152.9	0.87±0.18
Isoform 1 of Protein NDRG2	T(*)LS*QSS(*)ESGTLPSGPPGHTMEVSC	0.6	152.7	0.39±0.29
Pyruvate dehydrogenase E1 component subunit alpha	**YHGHS(*)MS*DPGVSYR**	0.8	39.5	0.57±0.43
Ubiquinone biosynthesis protein COQ9, mitochondrial	YTDQS*GEEEEDYESEEQLQHR	1.1	152.6	1.36±0.37

B.

Protein	Peptide Sequence	Δm (ppm)	Percolator Score	Ratio
EH domain-containing protein 2	**GPDEAIEDGEEGS*EDDAEWVVTK**	1.2	152.9	0.61±0.27
Ubiquitin-associated protein 2	GVS*VS(*)SGTGLPDM^{o}T*GSVYNK^{ac}	3.2	21.7	0.00±0.00
ATP synthase subunit alpha, mitochondrial	**ILGADT*S(*)VDLEETGR**	0.0	56.2	1.49±0.52
Gap junction protein	**MGQAGS*T(*)IS(*)NSHAQPFDFPDDSQNAK**	-0.5	128.6	1.00±0.08
Isoform 1 of Cyclin-Y	S*ASADNLILPR	1.0	35.5	0.81±0.21
Histone H1.4	^{ace}S*ET(*)APAAPAAPAPAEK	1.2	45.6	1.02±0.25
Catenin alpha-1	TPEELDDS*DFETEDFDVR	-1.7	47.1	0.83±0.13
Thioredoxin-related transmembrane protein 1	VEEEQEADEEDVS*EEEAEDR	0.8	152.9	1.28±0.43

C.

Protein	Peptide Sequence	Δm (ppm)	Percolator Score	Ratio
Isoform 3 of LIM domain-binding protein 3	**DPALDTN^{d}GSLATPS*PS(*)PEAR**	-0.3	48.5	0.37±0.17
Signal transducer and activator of transcription 5B	^{ace}EAN^{d}N^{d}GSSPAGSLADAMS*QK	0.8	31.3	1.72±0.61
Isoform 1 of Zinc finger protein 106	^{ace}EQ^{d}SRQDEPPSNSQ^{d}EVN^{d}S*DDR	0.1	33.6	*0.00±0.00*
Creatine kinase S-type, mitochondrial	**LGYILTCPS(*)NLGT*GLR**	0.5	24.8	1.32±0.32
Gap junction protein	**MGQAGS(*)T*IS*NS(*)HAQPFDFPDDSQNAK**	1.6	27.4	*0.00±0.00*
Electron transfer flavoprotein-ubiquinone oxidoreductase, mitochondrial	NLS*IYDGPEQR	1.1	20.0	0.88±0.51
Ryanodine receptor 2, cardiac	**RIS(*)QT*SQVSIDAAHGYSPR**	3.0	47.3	1.06±0.70
Isoform 1 of MAP7 domain-containing protein 1	RS*SQPSPT(*)T(*)VPASDSPPAK	1.6	26.2	0.14±0.28
LIM homeobox transcription factor 1-beta	S*EDEDGDM^{o}K^{a}PAK^{a}GQGSQSK^{a}GS(*)GDDGK^{ac}	-2.8	50.0	0.00±0.00

D.

Protein	Peptide Sequence	Δm (ppm)	Percolator Score	Ratio
Troponin I, cardiac muscle	^{ace}ADESS*DAAGEPQPAPAPVR	0.4	16.73	1.62±0.70
Isoform 1 of Protein FAM54B	AS(*)S*FADMMGILK	1.2	65.52	0.00±0.00
Putative uncharacterized protein	^{ace}DQPGHES(*)NT(*)SGNGSNM^{o}WPNFPS*Q^{d}DK	-0.1	17.19	0.00±0.00
Discs, large homolog 3	^{ace}ENM^{o}AQEN^{d}SIQ^{d}EQGVTSNT*SDSES(*)SS(*)K	-1.7	61.24	0.00±0.00
Isoform 1 of Trinucleotide repeat-containing gene 6B protein	GPSGTDT*VS(*)GQSNSGN^{d}NGNNGKDR	-3.1	31.50	0.00±0.00
Isoform 1 of Mitochondrial fission factor	NDS*IVTPSPPQAR	0.3	19.41	*0.32±0.30*
Similar to E1B 19K/Bcl-2-binding protein homolog	NST(*)LS*EEDYIER	4.2	19.87	1.05±0.12
ATP synthase subunit alpha, mitochondrial	**TGTAEMS(*)S*ILEER**	1.8	51.80	0.73±0.78

E.

Protein	Peptide Sequence	Δm (ppm)	Percolator Score
Metabotropic glutamate receptor 8	^{ace}AVN^{d}FNGS*AGTPVTFNEN^{d}GDAPGR	0.9	15.6
5'-AMP-activated protein kinase subunit beta-2	**DLS*SS(*)PPGPYGQEMYVFR**	-0.8	114.1
Similar to mKIAA1614 protein isoform 1	EN^{d}LQNGNLNDPS*SIESS(*)NGQ^{d}WPK^{ac}	0.2	14.0
Transcription factor Sp4	**EN^{d}NVS*Q^{d}PASS(*)SSSSSSSN^{d}N^{d}GSSSPTKTK**	3.6	16.7
Myosin regulatory light chain 2, ventricular/cardiac muscle isoform	IEGGS(*)SNVFS*MFEQTQIQEFK	0.6	60.0
Ryanodine receptor 2, cardiac	IS(*)QTS*QVSIDAAHGYSPR	1.0	67.0
Isoform 1 of Coiled-coil domain-containing transmembrane protein C7orf53 homolog	**LYVVDS*INDLNK**	0.5	24.2
CXXC-type zinc finger protein 5	^{ace}M^{o}S*SLGGGSQDAGGSSSSSN^{d}TN^{d}SSSGS*GQ^{d}K^{ac}	4.7	19.1
Solute carrier family 2 (facilitated glucose transporter), member 4	T(*)PS*LLEQEVKPSTELEYLGPDEND	0.3	34.5
Putative uncharacterized protein	**VAEPEES*EAEEPAAEGR**	0.0	20.9
Vasodilator-stimulated phosphoprotein	WLPAGTGPQAFSR	3.2	27.4

F.

Protein	Peptide Sequence	Δm (ppm)	Percolator Score
Poliovirus receptor	AGGDIRVLVPYNSTGVLGGSTTLHCSLT*S*N[d]EN[d]VT*ITQ[d]ITWMKK[ac]	-3.3	80.4
Coiled-coil domain-containing protein 93	YS*DRKK	2.2	56.0
Putative uncharacterized protein	DRSDSDDQMLVAN[d]GSPS*SNLSSSVR	0.1	50.0
Rap1 GTPase-activating protein	SENS*STQ[d]SSPEM[o]PTTKNR	4.0	47.9
Isoform 2 of Protein MRVI1	FNALN[d]LPGQ[d]APS*S*SPM[o]PSLPALSESSNGK[ac]SSISVS*PALPALLENGK	-4.1	43.0
Dnajc5 protein	SLS*TSGESLYHVLGLDK	1.0	40.0
Synaptotagmin-12	NVST*GVVELK	-0.5	38.0
Isoform 2 of YEATS domain-containing protein 2	T*IVVGN[d]VSK	2.1	31.7
Metallothionein	[ace]MDPN[d]CS*CAAGDSCTCAGSCK[ac]	0.0	31.5
Isoform 1 of PDZ domain-containing RING finger protein 3	[ace]VAEGSS*EGATANIEAYRPSPK	1.4	31.3
Proteasome activator complex subunit 1	EPALNEAN[d]LS*NLK	5.0	31.0
Isoform 1 of CAP-Gly domain-containing linker protein 4	TVAENDAAQ[d]PGSMSSSSSS*SSLDHK	0.0	30.7
Isoform 1 of LIM domain-binding protein 1	K[ac]MSGGSTM[o]S*S*GGGNTNN[d]SNSK[ac]K	1.8	29.7
Tyrosine 3-monooxygenase	[ace]AVSEQ[d]DT*KQAEAVT*SPR	-0.7	26.6
Aspartyl-tRNA synthetase, cytoplasmic	QSNS*YDMFM[o]RGEEILSGAQ[d]R	4.5	26.5
Olfactory receptor Olfr270	S*IS*FLGCALQMVIS*LGLGS*TECVLLAVMAYDRYAAICNPLR	0.1	26.3
Isoform 2 of SWI/SNF-related matrix-associated actin-dependent regulator of chromatin subfamily A containing DEAD/H box 1	GEESNESAEASS*N[d]WEK	3.5	26.1
FUN14 domain-	NPPPQDYES*DDESYEVLDLTEYAR	2.8	25.9

Protein	Peptide Sequence	Δm (ppm)	Percolator Score
containing protein 1			
Tensin 1	HLGGSGSVVPGS*PSLDR	2.0	25.4
Diphosphoinositol polyphosphate phosphohydrolase 3-alpha	[ace]LGGSPTN[d]GNS*AAPS*PPES*EP	3.8	22.5
Membrane-spanning 4-domains, subfamily A, member 4C	MQGQEQ[d]T*T*M[o]AVVPGGAPPSENSVM[o]K	0.1	22.3
60S acidic ribosomal protein P1	EES*EES*EDDMGFGLFD	-0.3	21.4
Ep300 protein	TDGKEEEEQPSTS*ATQSSPAPGQSK	2.8	21.2
Isoform 1 of GAS2-like protein 1	YSGDSDSSASSAQS*GPM[o]GARSDDSATGSR	2.8	20.9
Junctophilin-2	RSDSAPPSPVS*ATVPEEEPPAPR	2.4	20.6
Putative uncharacterized protein	EVQN[d]DLMLQ[d]S*N[d]GS*QYSPNEIRENSPSVS*PT*ANI AAPFGLKPR	4.1	20.4
Ring finger protein 112	[ace]SFM[o]GNSSN[d]SWS*HAS*FPK[ac]	1.1	20.0
Isoform 2 of CCR4-NOT transcription complex subunit 10	[ace]QEN[d]GSKSSSQLGGNTESSES*SETCSK[ac]	-3.6	19.7
IgE-binding protein	TDNGPAYT*SQ[d]K	1.4	19.7
[Protein ADP-ribosylarginine] hydrolase-like protein 1	**ENS*VLGSIQEELQK**	2.2	19.6
Secreted seminal-vesicle Ly-6 protein 1	LNS*SGICETAETSCEAT*N[d]N[d]R	1.4	19.5
Isoform 1 of Xin actin-binding repeat-containing protein 2	[ace]QEGIQNSSDASQSKLACET*SQ[d]SHK[a]	5.0	18.9
Similar to LOC635138 protein	M[o]AASAAAATAAGIAM[o]ATSVQSSTTVEQLS*S*S*VA EVIDQ[d]HSVLSAQLK	2.9	18.8
Cell surface glycoprotein CD200 receptor 2	[ace]NIT*WAS*TPDHIPDLQIS*AVALQHEGNYLCEITT*P EGNFHK	4.8	18.6
ADAM DEC1	N[d]N[d]VALVALMS*HELGHALGM[o]K	-2.4	18.5
Isoform 1 of Pleckstrin homology domain-containing family H member 2	S*QSGVK	4.4	18.4
Glycerol-3-phosphate acyltransferase 1, mitochondrial	**SDEEDEDS*DFGEEQR**	0.2	18.2

Protein	Peptide Sequence	Δm (ppm)	Percolator Score
COMM domain-containing protein 4	VDYT*LS*SSLLHSVEEPM^{o}VHLQLQ^{d}VVPAPGTQAQP VSM^{o}SLS*ADK^{ac}	0.9	18.1
Ankyrin repeat and SOCS box protein 7	^{ace}MLYNYGADT*NTR	-4.1	18.1
22 kDa protein	^{ace}AEKLS*EQ^{d}PQS*AAS*GSSAAGPSQSK^{ac}QGSLLN^{d}LL AEPSKPVGHASIFK	0.0	18.1
Vomeronasal 2, receptor 95	^{ace}CTPCAVNEIS*NETDVDQ^{d}CVK	0.6	17.4
Ras GTPase-activating protein-binding protein 1	**YQDEVFGGFVTEPQEES*EEEVEEPEER**	-0.8	17.2
Transformation/transcription domain-associated protein	VLQ^{d}HILNPAFLYSFEKGEGEQLLGPPNPEGDN^{d}PESIT* S*VFITK^{ac}	-0.9	17.0
Voltage-gated potassium channel subunit beta-1	N^{d}EGVSSVLLGS*S*T*PEQdLIENLGAIQ^{d}VLPK^{ac}M^{o}TSH VVN^{d}EIDN^{d}ILR	0.3	16.6
Protocadherin-21	^{ace}MASSM^{o}VAQQ^{d}TVPTVSGSLTPQ^{d}PSPQ^{d}LPTPKTLGG PVQS*SLVSELKQK	-2.2	16.3
Hypothetical protein isoform 2	GDTTS*S*AET*Q^{d}PASSSSAEGPAAK	-2.7	16.3
Hydrocephalus inducing protein	FS*VNdAVYS*K	-0.1	16.1
Isoform 1 of Voltage-dependent L-type calcium channel subunit beta-4	^{ace}HS*NHSTEN^{d}SPIER	-0.4	16.1
Isoform 1 of Transmembrane protein 154	^{ace}QEPSSQGSQS*ALQ^{d}THELGGETLK	-1.7	16.1
ADP/ATP translocase 1	DFLAGGIAAAVS*K	0.8	16.0
60 kDa SS-A/Ro ribonucleoprotein	ALGSVLN^{d}AS*TVAAAMCMVVTR	-2.0	15.7
B-cell CLL/lymphoma 9 protein	^{ace}GMAADVGMGGFS*Q^{d}GPGN^{d}PGN^{d}MMF	-3.3	15.5
THO complex subunit 1	^{ace}S*GLSDLAESLTNDTET*NS*	2.1	15.3
Isoform 1 of Fibroblast growth factor receptor 3	DDAT*DK^{ac}DLSDLVS*EM^{o}EMMK	3.8	15.2
Biorientation of chromosomes in cell division 1-like	^{ace}N^{d}EECDGLMAS*TASCDVSN^{d}KDSLAGSK	-1.6	15.2
Expressed sequence AA415398	HTEESAQMVET*PR	1.1	15.2
Isoform 1 of Perilipin-4	^{ace}DTVCAGVTS*AMNMAK	0.8	15.1

Protein	Peptide Sequence	Δm (ppm)	Percolator Score
Prickle-like 2 isoform a	[ace]M[o]EQNQ[d]S*Q[d]SPLQ[d]LLSQ[d]CNIR	-1.6	15.1
Signal recognition particle receptor subunit alpha	LIDGIVLTKFDTIDDK[ac]VGAAISM[o]T*YITSK[ac]PIVFVGT GQTYCDLR	-3.3	15.0
Putative uncharacterized protein	TTS*LQ[d]NGT*FHLK	0.4	14.9
Putative uncharacterized protein	CRAS*AWASISMAS*TVHGCMR	-1.3	14.8
Nucleolar protein 12	[ace]QEEGSTS*QEGGGTPR	-0.1	14.7
Coiled-coil domain-containing protein 87	Q[d]SCTFTGSSSQ[d]ALVAPGN[d]T*PTTH	-0.8	14.6
Protocadherin 15 isoform CD1-4	[ace]ETTSTT*QPPASN[d]PQ[d]WGAEPHR	2.0	14.5
Isoform 1 of DENN domain-containing protein 5B	[ace]K[ac]S*DSGVMLPTLR	-4.0	14.5
Isoform 1 of Calcium/calmodulin -dependent protein kinase kinase 2	[ace]MSLQ[d]EPSQGGPASSSNS*LDMNGR	2.2	14.4
Protein AF-10	TYTSTSNN[d]SISGSLNRLEDT*AAR	4.3	14.4
Zinc finger, FYVE domain containing 9	[ace]TDLGISNSFSHSS*GELLIK	1.2	14.3
Isoform 2 of Nipped-B-like protein	[ace]Q[d]N[d]ENRPCDT*KPN[d]DNK	-1.7	14.1
Isoform 1 of Integrin beta-2-like protein	CLKDNS*AIK	3.0	14.0
Isoform 1 of LIM domain-binding protein 2	K[ac]N[d]STSST*S*NSSAGNTTN[d]SAGSK	4.2	13.8
Glutamate [NMDA] receptor subunit epsilon-1	[ace]N[d]ISNM[o]S*NMN[d]SSR	1.1	13.8
Similar to hCG2038359	[ace]LLGVLATSS*SSLGFESDPETSCR	1.8	13.5
Mucin 5, subtype B, tracheobronchial	[ace]S*GFS*K[a]NGVTVSLSGATTM[o]SVNISTIGTIIT*FDGNI FQIWLPYR	-0.2	13.5
Clusterin-associated protein 1	SGS*NDDSDIDIQEDDES*DSELEDR	0.7	13.4
Fibrillin-1	[ace]CDEGYES*GFM[o]M[o]M[o]K[ac]N[d]CMDIDECQ[d]R	4.9	13.3
Sphingosine-1-phosphate receptor 1	DDGDN[d]PET*IMSSGN[d]VNSSS	-3.3	13.3
Mitochondrial import receptor	[ace]AAAVAAAGAGEPLS*PEELLPK	-0.2	13.3

Protein	Peptide Sequence	Δm (ppm)	Percolator Score
subunit TOM22 homolog			
Isoform 2 of Tumor protein 63	Q^{d}T*SMQ^{d}SQ^{d}SSYGN^{d}SSPPLNK^{ac}MN^{d}SM^{o}N^{d}K^{ac}	0.3	13.2
Similar to 1700001E04Rik protein isoform 5	TMLDM^{o}N^{d}EMTQSIIGS*MQYSK	3.6	13.1
Trifunctional enzyme subunit alpha, mitochondrial	AGLEQGSDAGYLAES*QK	2.1	9.5
Isoform 3 of A kinase anchor protein 1, mitochondrial	RLS*EEACPGVLSVAPTVTQPPGR	1.6	9.2
Cytochrome b-c1 complex subunit 2, mitochondrial	AVAQGNLSS*ADVQAAK	2.4	9.1
Branched chain keto acid dehydrogenase E1, alpha polypeptide	IGHHSTSDDS*SAYR	0.9	8.4

Table 4.3

Protein	Peptide Sequence	Hits	Ratio	Source	Percolator Score	Δm (ppm)
Alpha-crystallin B chain	**APS*WIDTGLSEMR**	6	0.00±0.00	Both	94.6	1.4
Uncharacterized protein C6orf203 homolog	EADEEDS*DEETS(*)YPER	6	1.15±0.23	Both	127.2	1.0
Mitochondrial import receptor subunit TOM20 homolog	IVS*AQSLAEDDVE	6	0.00±0.00	Both	152.7	-0.6
Isoform A of Heat shock protein beta-1	QLS*SGVSEIR	6	0.04±0.08	LOCATE	29.0	1.9
Cardiac phospholamban[a]	RAS*T(*)IEMPQQAR	6	0.05±0.05	Both	151.0	3.4
Pyruvate dehydrogenase E1 component subunit alpha, somatic form, mitochondrial	**YHGHS(*)MS*DPGVSYR**	6	0.57±0.43	Both	39.5	0.8
Ubiquinone biosynthesis protein COQ9, mitochondrial	YTDQS*GEEEEDYESEEQLQHR	6	1.36±0.37	Both	152.6	1.1
EH domain-containing protein 2	**GPDEAIEDGEEGS*EDDAEWVVTK**	5	0.61±0.27	LOCATE	152.9	1.2
ATP synthase subunit alpha, mitochondrial	**ILGADT*S(*)VDLEETGR**	5	1.49±0.52	Both	56.2	0.0
Creatine kinase S-type, mitochondrial	**LGYILTCPS(*)NLGT*GLR**	4	1.32±0.32	Both	24.8	0.5
Electron transfer flavoprotein-ubiquinone oxidoreductase, mitochondrial	NLS*IYDGPEQR	4	0.88±0.51	Both	20.0	1.1
Isoform 1 of Mitochondrial fission factor	NDS*IVTPSPPQAR	3	*0.32±0.30*	UniProt	19.4	0.3
ATP synthase subunit alpha, mitochondrial	**TGTAEMS(*)S*ILEER**	3	0.73±0.78	Both	51.8	1.8
Isoform 1 of CAP-Gly domain-containing linker protein 4	TVAENDAAQ[d]PGSMSSSSSS*SSLDHK	1	--	LOCATE	30.7	0.0
FUN14 domain-containing protein 1	NPPPQDYES*DDESYEVLDLTEYAR	1	--	LOCATE	25.9	2.8
60S acidic	EES*EES*EDDMGFGLFD	1	--	LOCATE	21.4	-0.3

Protein	Peptide Sequence	Hits	Ratio	Source	Percolator Score	Δm (ppm)
ribosomal protein P1						
Ring finger protein 112	[ace]SFM[o]GNSSN[d]SWS*HAS*FPK[ac]	1	--	LOCATE	20.0	1.1
IgE-binding protein	TDNGPAYT*SQ[d]K	1	--	LOCATE	19.7	1.4
[Protein ADP-ribosylarginine] hydrolase-like protein 1	**ENS*VLGSIQEELQK**	1	--	LOCATE	19.6	2.2
Glycerol-3-phosphate acyltransferase 1, mitochondrial	**SDEEDEDS*DFGEEQR**	1	--	Both	18.2	0.2
COMM domain-containing protein 4	VDYT*LS*SSLLHSVEEPM[o]VHLQLQ[d]VVPAPGTQAQPVSM[o]SLS*ADK[ac]	1	--	LOCATE	18.1	0.9
Voltage-gated potassium channel subunit beta-1	N[d]EGVSSVLLGS*S*T*PEQ[d]LIENLGAIQ[d]VLPK[ac]M[o]TSHVVN[d]EIDN[d]ILR	1	--	LOCATE	16.6	0.3
Protocadherin-21	[ace]MASSM[o]VAQQ[d]TVPTVSGSLTPQ[d]PSPQ[d]LPTPKTLGGPVQS*SLVSELKQK	1	--	LOCATE	16.3	-2.2
Hydrocephalus inducing protein	FS*VN[d]AVYS*K	1	--	LOCATE	16.1	-0.1
ADP/ATP translocase 1	DFLAGGIAAAVS*K	1	--	Both	16.0	0.8
Isoform 1 of Perilipin-4	[ace]DTVCAGVTS*AMNMAK	1	--	LOCATE	15.1	0.8
Signal recognition particle receptor subunit alpha	LIDGIVLTKFDTIDDK[ac]VGAAISM[o]T*YITSK[ac]PIVFVGTGQTYCDLR	1	--	LOCATE	15.0	-3.3
Putative uncharacterized protein	TTS*LQ[d]NGT*FHLK	1	--	LOCATE	14.9	0.4
Protocadherin 15 isoform CD1-4	[ace]ETTSTT*QPPASN[d]PQ[d]WGAEPHR	1	--	LOCATE	14.5	2.0
Isoform 1 of DENN domain-containing protein 5B	[ace]K[ac]S*DSGVMLPTLR	1	--	LOCATE	14.5	-4.0
Clusterin-associated protein 1	SGS*NDDSDIDIQEDDES*DSELEDR	1	--	LOCATE	13.4	0.7
Mitochondrial import receptor subunit TOM22 homolog	[ace]AAAVAAAGAGEPLS*PEELLPK	1	--	Both	13.3	-0.2
Trifunctional enzyme subunit alpha, mitochondrial	AGLEQGSDAGYLAES*QK	1	--	Both	9.5	2.1
Isoform 3 of A	RLS*EEACPGVLSVAPTVTQPPG	1	--	Both	9.2	1.6

Protein	Peptide Sequence	Hits	Ratio	Source	Percolator Score	Δm (ppm)
kinase anchor protein 1, mitochondrial	R					
Cytochrome b-c1 complex subunit 2, mitochondrial	AVAQGNLSS*ADVQAAK	1	--	Both	9.1	2.4
Branched chain keto acid dehydrogenase E1, alpha polypeptide	IGHHSTSDDS*SAYR	1	--	Both	8.4	0.9

4.8 Figure Legends

Figure 4.1 Workflow of comparative quantitative phosphoproteomics of mitochondria from control mouse hearts and hearts rendered ischemic.

Mitochondria were isolated from both normally perfused and global ischemic mouse hearts. Next mitochondrial proteins were extracted by methanol/chloroform precipitation. Precipitated proteins were solubilized in Rapigest detergent and the protein concentration was determined using a BCA kit. From each sample 1 mg of protein was trypsinized in the presence of Rapigest. The resultant tryptic peptides were passed through a titanium dioxide micro column for the selective enrichment of phosphopeptides. The phosphopeptides were then desalted and modified with light thiocholine (control) and heavy thiocholine (ischemic). Control and ischemic samples were mixed together, desalted and analyzed using LC-MS/MS. The mass spectrometry data were searched using MASCOT and re-scored by Percolator program to yield the identification of the peptide. Quantitative information was obtained from the relative peak intensity of the molecular ions of the phosphopeptides modified by light and heavy thiocholine respectively. Proteins of mitochondrial origin were confirmed using both the UniProt and LOCATE databases.

Figure 4.2 The total ion chromatography (TIC) (0-185 min) obtained from a representative sample using LTQ-Orbitrap as described in Materials and Methods (A). The extracted ion chromatography (XIC) (0-185 min) of the full-mass scans

from the TIC (B).

Figure 4.3 Fragmentation of the heavy thiocholine-modified peptide YHGHS*MSDPGVSYR identified in the subunit α of pyruvate dehydrogenase E1 at both the MS^2 and MS^3 levels. All fragment ions resulting from heavy thiocholine-modified peptides are presented in capital letters (e.g., A, B and Y). All fragment ions resulting from light thiocholine-modified peptides are presented in lower case letters (e.g., a, b and y).

A. The product-ion spectrum of the quadruply charged molecular ion modified by heavy thiocholine at *m*/*z* 425.200 (YHGHS*MSDPGVSYR) was obtained with an ESI-LTQ-Orbitrap instrument as described in the Materials and Methods. Shown in the spectrum are the series of B ions, B_8^{+2} at *m/z* 510.9, B_{10}^{+2} at *m/z* 588.2, B_{11}^{+2} at *m/z* 637.5, B_{12}^{+3} at *m/z* 454.6. Also shown in the spectrum is an example of the diagnostic triad consisting of the B_{10}^{+2} fragmentation ions resulting from peptide bond cleavage (*m*/*z* = 510.9) and further neutral loss of $^{13}C,d_3$-trimethylamine (-63 Da, *m*/*z* = 556.8) or the $^{13}C,d_3$-thiocholine thiolate (-123 Da, *m*/*z* = 526.7). "S*" indicates the thiocholine-modified site.

B. The expanded product-ion spectrum of the quadruply charged molecular ion modified by heavy thiocholine at *m*/*z* 425.200 (YHGHS*MSDPGVSYR) ranging from *m/z* 380 to *m/z* 640. As shown in the spectrum, the heavy thiocholine containing B ions are accompanied by the corresponding light thiocholine containing b ions resulting from the fragmentation of the light thiocholine-modified molecular ion at *m/z* 424.195 (YHGHS*MSDPGVSYR) that could not be excluded during the data-dependent

dissociation, thereby generating a series of B/b ion doublets at the MS^2 level with relative ratios that further confirmed the comparative quantitation at the molecular level.

C. The MS^3 spectrum of the B_{11}^{+2} ion at *m*/*z* 637.5 resulting from the fragmentation of the quadruply charged molecular ion modified by heavy thiocholine at *m*/*z* 425.200 (YHGHS*MSDPGVSYR) obtained with an ESI-LTQ-Orbitrap as described in the Materials and Methods. The ion peak at *m*/*z* 606.1 corresponds to the doubly charged fragment ion generated from the neutral loss of $^{13}C,d_3$-trimethylamine (-63 Da) from the parent ion B_{11}^{+2}.

D. The MS^3 spectrum of the B_{10}^{+2} ion at *m*/*z* 588.2 resulting from the fragmentation of the quadruply charged molecular ion modified by heavy thiocholine at *m*/*z* 425.200 (YHGHS*MSDPGVSYR) obtained with an ESI-LTQ-Orbitrap as described in the Materials and Methods. The ion peak at *m*/*z* 556.6 corresponds to the doubly charged fragment ion generated from the neutral loss of $^{13}C,d_3$-trimethylamine (-63 Da) from the parent ion B_{10}^{+2}.

E. The MS^3 spectrum of the B_8^{+2} ion at *m*/*z* 510.9 resulting from the fragmentation of the quadruply charged molecular ion modified by heavy thiocholine at *m*/*z* 425.200 (YHGHS*MSDPGVSYR) obtained with an ESI-LTQ-Orbitrap as described in the Materials and Methods. The ion peak at *m*/*z* 479.5 corresponds to the doubly charged fragment ion generated from the neutral loss of $^{13}C,d_3$-trimethylamine (-63 Da) from the parent ion B_8^{+2}.

F. The MS^3 spectrum of the B_{12}^{+3} ion at *m*/*z* 454.6 resulting from the fragmentation of the quadruply charged molecular ion modified by heavy thiocholine at *m*/*z* 425.200

(YHGHS*MSDPGVSYR) obtained with an ESI-LTQ-Orbitrap as described in the Materials and Methods. The ion peak at *m*/*z* 433.6 corresponds to the triply charged fragment ion generated from the neutral loss of $^{13}C,d_3$-trimethylamine (-63 Da) from the parent ion B_{12}^{+3}.

Figure 4.4 Workflow of MASCOT Percolator reproduced with permission from Journal of Proteome Research, *2009, 8,* 3176-3181 by M, Brosch, L. Yu, T. Hubbard, and J. Choudhary.

Figure 4.5 Comparative quantitation of light and heavy thiocholine-modified peptides.

Relative changes in phosphorylation were evaluated for all phosphopeptides identified in three or more independent replicate samples as described in the Materials and Methods. Evident in the spectrum is the "M + 4" doublet pattern of the quadruply charged molecular ions of light and heavy thiocholine-modified YHGHS*MSDPGVSYR at *m/z* 424.195 and 425.200 respectively. The greater peak intensity of the heavy thiocholine-modified YHGHS*MSDPGVSYR indicates that the phosphorylation level was increased for this peptide during induced cardiac ischemia. The relative ratio of the light and heavy molecular ion "S*" indicates that the phosphoserine residue was either modified by light or heavy thiocholine.

Figure 4.6 Tandem mass spectra of manually verified mitochondrial peptides with a score greater than 7 and less than 13. All fragment ions resulting from heavy thiocholine-modified peptides are presented in capital letters (e.g., A, B and Y). All fragment ions resulting from light thiocholine-modified peptides are presented in lower case letters (e.g., a, b and y).

A. The product-ion spectrum of the triply charged molecular ion of AGLEQGSDAGYLAES*QK originating from protein trifunctional enzyme subunit α, modified by heavy thiocholine at *m*/*z* 610.307 was obtained with an ESI-LTQ-Orbitrap instrument as described in the Materials and Methods. "S*" indicates the thiocholine-modified site.

B. The product-ion spectrum of the triply charged molecular ion of AVAQGNLSS*ADVQAAK originating from protein cytochrome b-c1 complex subunit 2, modified by light thiocholine at *m*/*z* 544.292 was obtained with an ESI-LTQ-Orbitrap instrument as described in the Materials and Methods. "S*" indicates the thiocholine-modified site.

C. The product-ion spectrum of the quadruply charged molecular ion of IGHHSTSDDS*SAYR originating from protein branched chain keto acid dehydrogenase E1-α polypeptide, modified by light thiocholine at *m*/*z* 409.191 was obtained with an ESI-LTQ-Orbitrap instrument as described in the Materials and Methods. "S*" indicates the thiocholine-modified site.

D. The product-ion spectrum of the triply charged molecular ion of

RLS*EEACPGVLSVAPTVTQPPGR originating from protein isoform 3 of A kinase anchor protein 1, modified by heavy thiocholine at *m*/*z* 842.788 was obtained with an ESI-LTQ-Orbitrap instrument as described in the Materials and Methods. “S*” indicates the thiocholine-modified site.

Figure 4.1

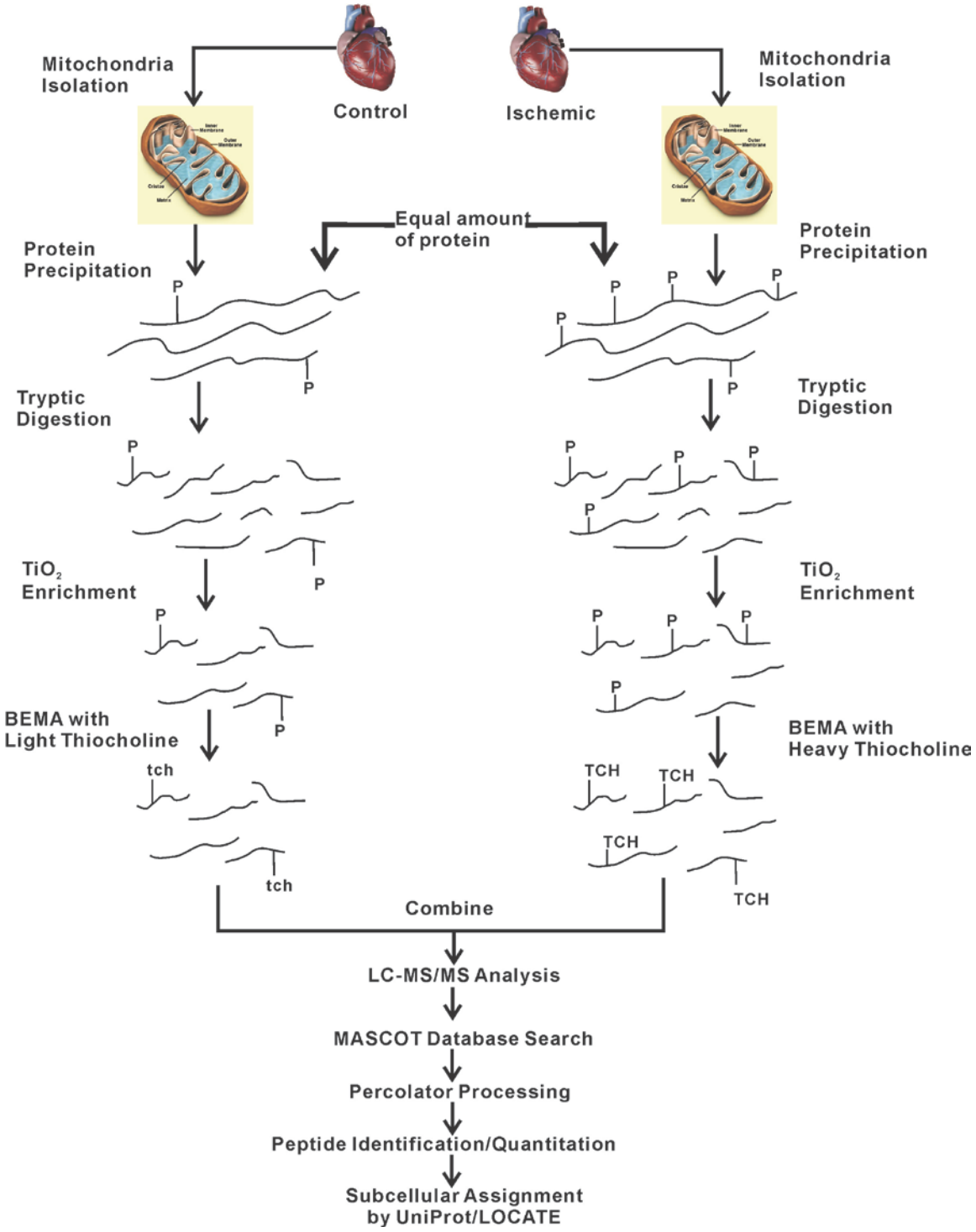
Mitochondria Isolation
Control
Ischemic
Mitochondria Isolation
Equal amount of protein
Protein Precipitation
Protein Precipitation
Tryptic Digestion
Tryptic Digestion
TiO2 Enrichment
TiO2 Enrichment
BEMA with Light Thiocholine
BEMA with Heavy Thiocholine
tch
TCH
Combine
LC-MS/MS Analysis
MASCOT Database Search
Percolator Processing
Peptide Identification/Quantitation
Subcellular Assignment by UniProt/LOCATE

Figure 4.2

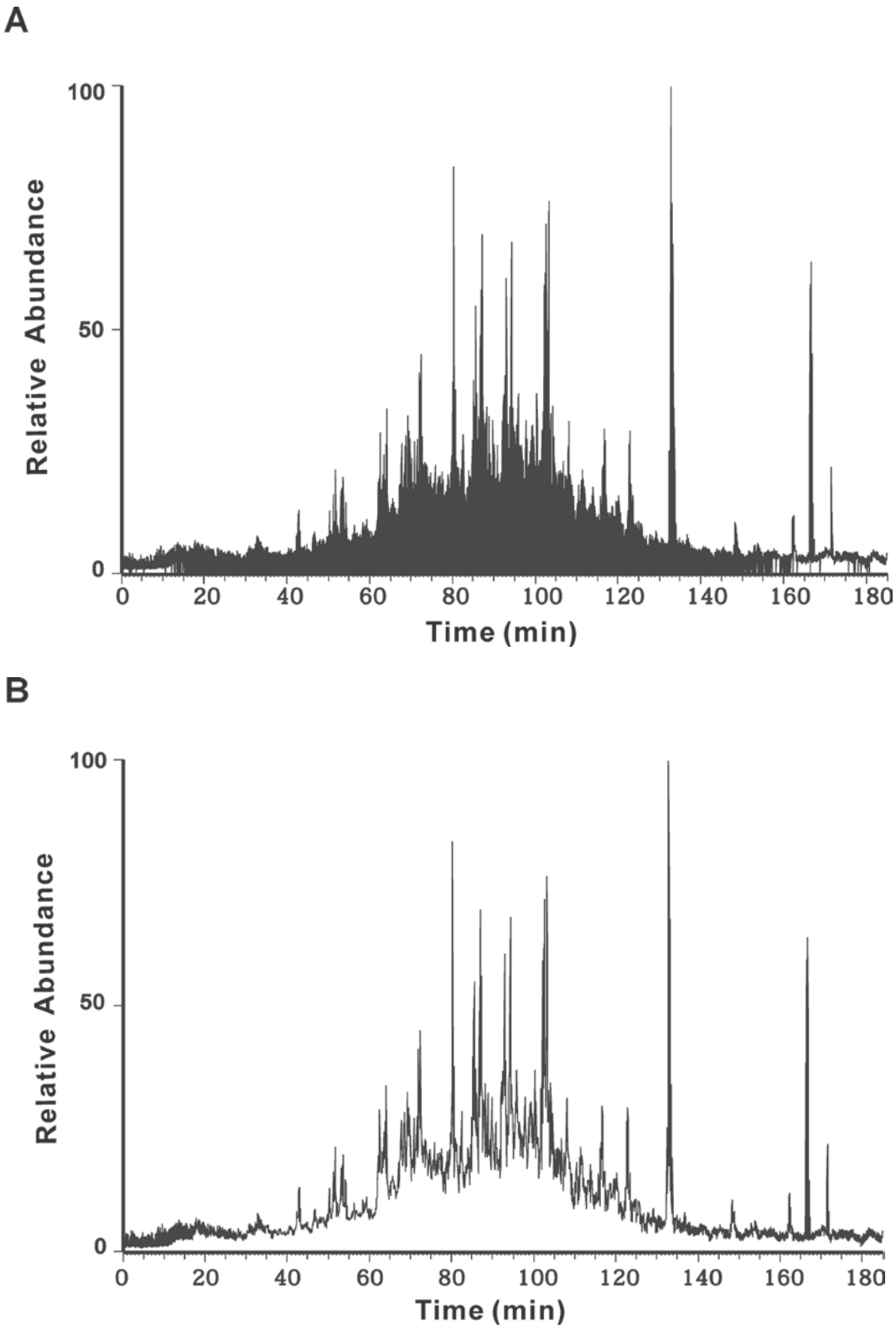
A
100
50
0
Relative Abundance
0
20
40
60
80
100
120
140
160
180
Time (min)
B
100
50
0
Relative Abundance
0
20
40
60
80
100
120
140
160
180
Time (min)

Figure 4.3

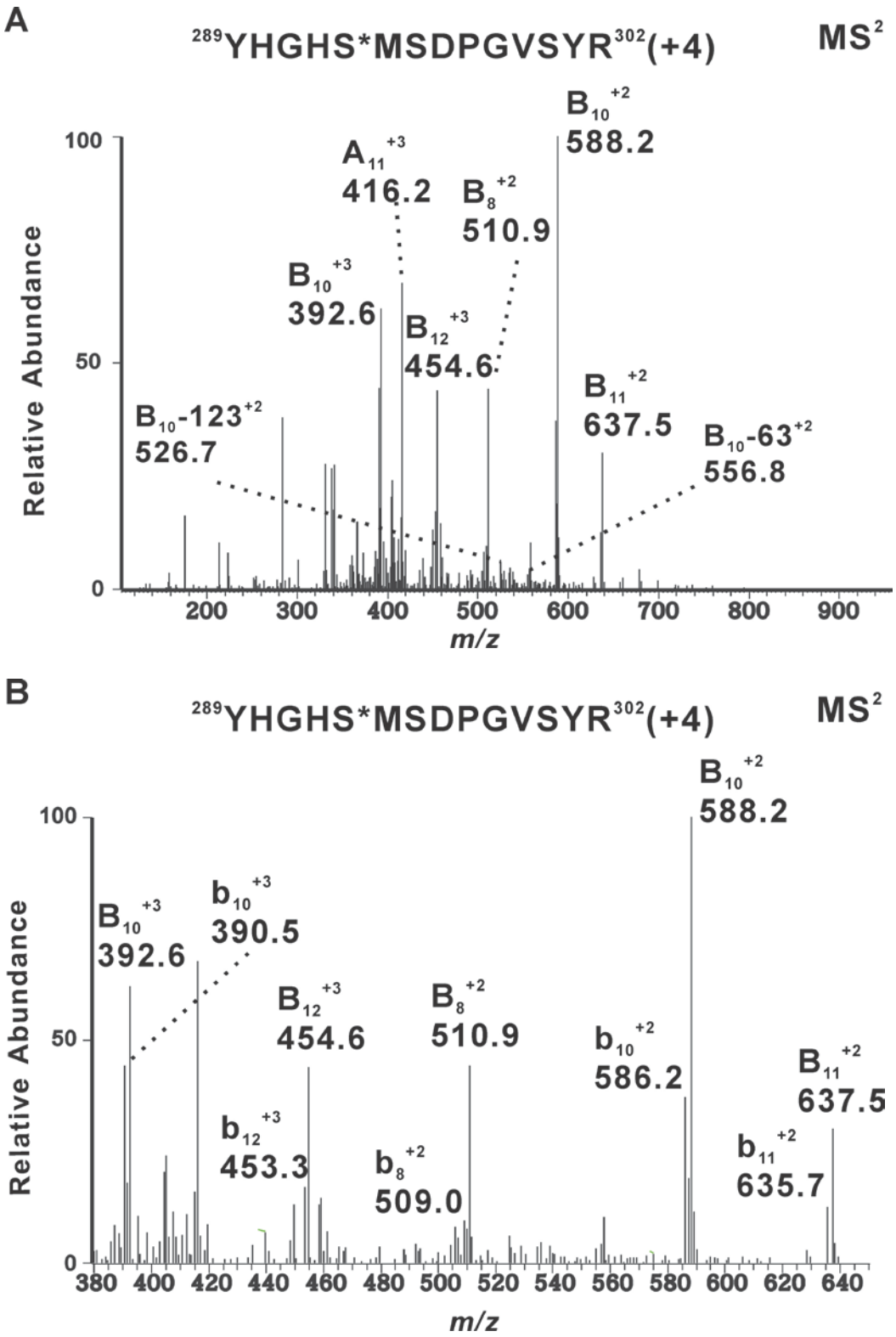
A
289YHGHS*MSDPGVSYR302(+4)
MS2
B10+2 588.2
A11+3 416.2
B8+2 510.9
B10+3 392.6
B12+3 454.6
B11+2 637.5
B10-123+2 526.7
B10-63+2 556.8
Relative Abundance
m/z
B
289YHGHS*MSDPGVSYR302(+4)
MS2
B10+2 588.2
B10+3 392.6
b10+3 390.5
B12+3 454.6
B8+2 510.9
b10+2 586.2
B11+2 637.5
b12+3 453.3
b8+2 509.0
b11+2 635.7
Relative Abundance
m/z

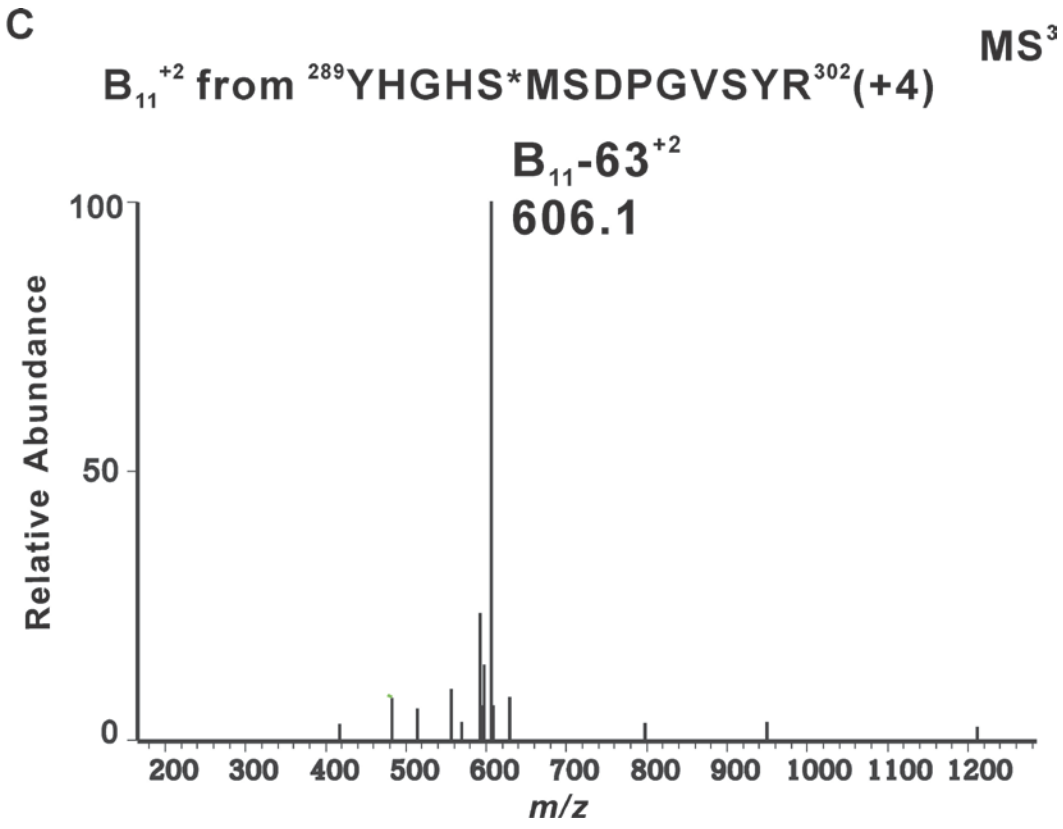
C
MS3
B11+2 from 289YHGHS*MSDPGVSYR302(+4)
B11-63+2
606.1
100
50
0
Relative Abundance
200 300 400 500 600 700 800 900 1000 1100 1200
m/z

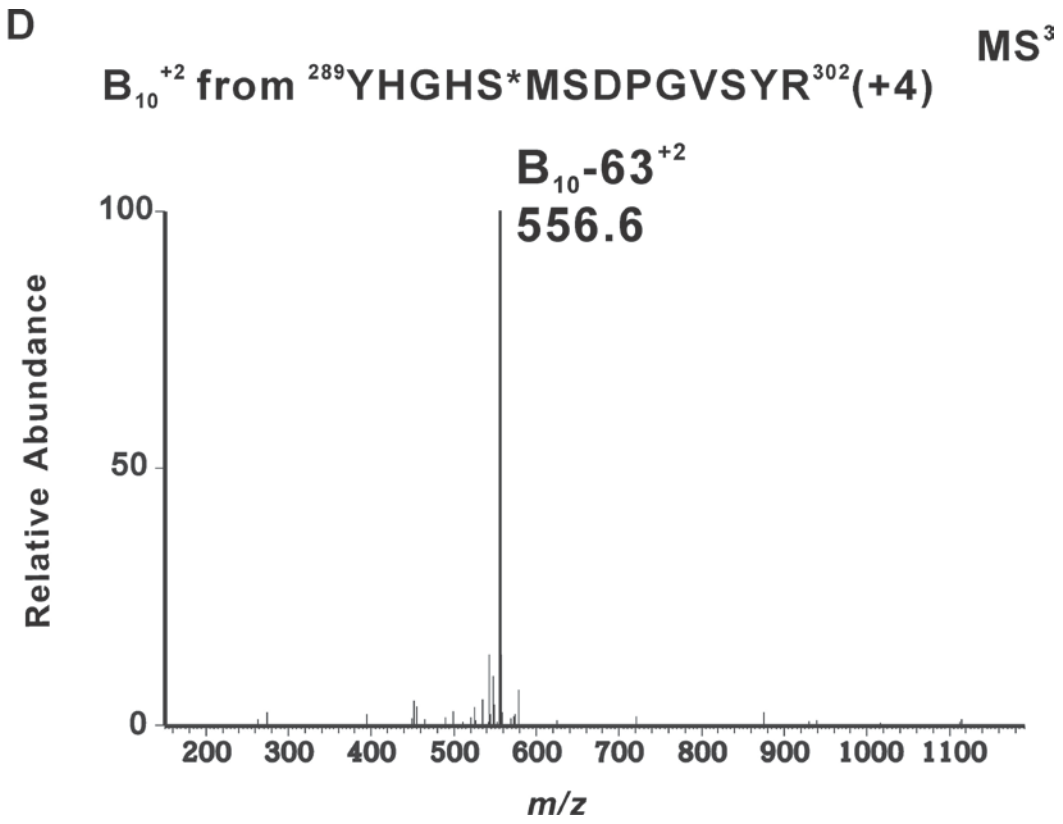
D
MS3
B10+2 from 289YHGHS*MSDPGVSYR302(+4)
B10-63+2
556.6
100
50
0
Relative Abundance
200 300 400 500 600 700 800 900 1000 1100
m/z

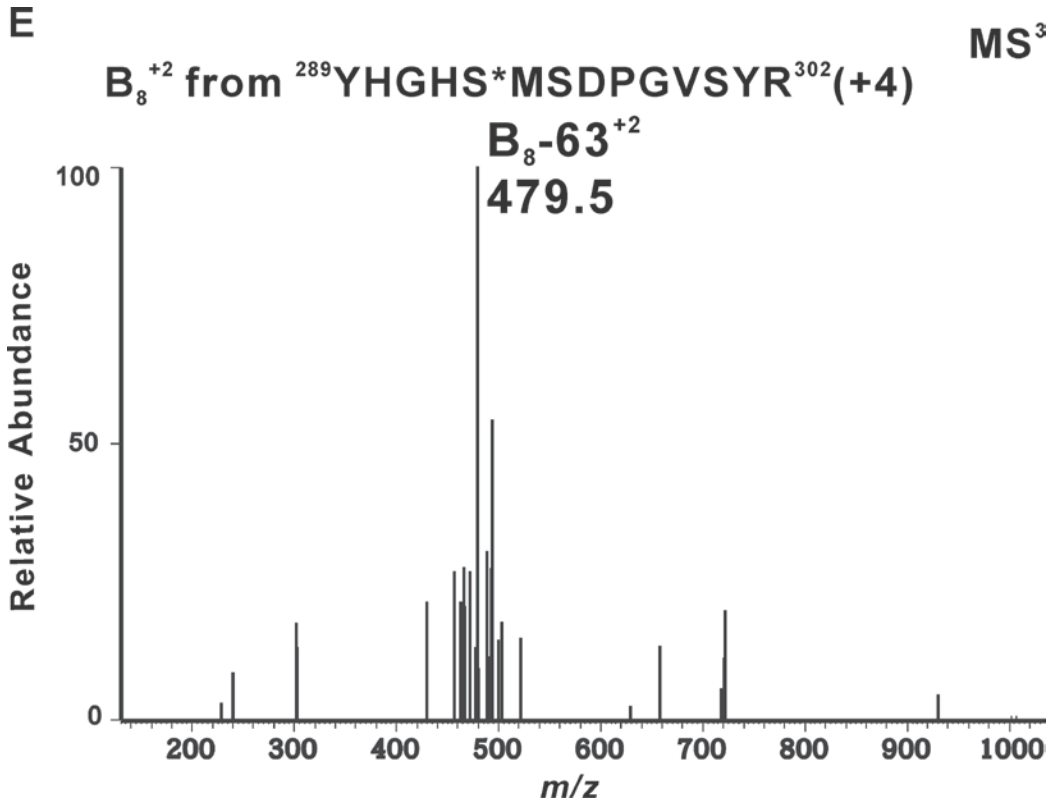
E
MS3
B8+2 from 289YHGHS*MSDPGVSYR302(+4)
B8-63+2
479.5
100
50
0
Relative Abundance
200
300
400
500
600
700
800
900
1000
m/z

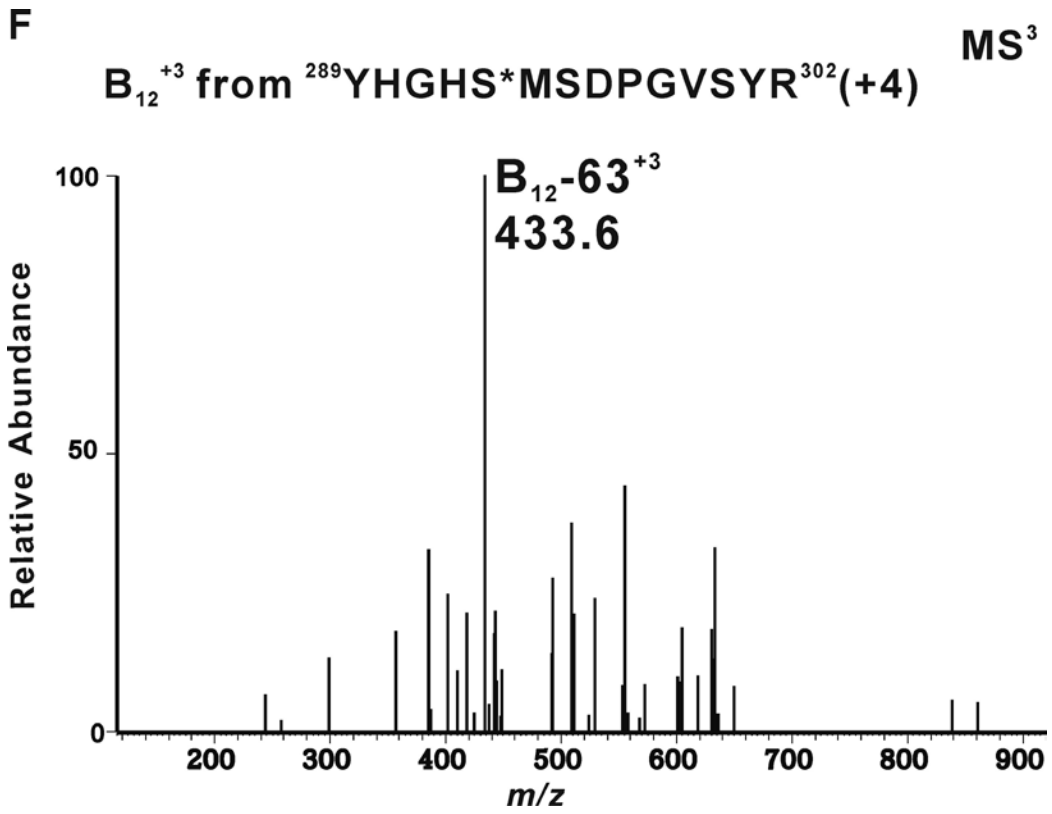
F
MS3
B12+3 from 289YHGHS*MSDPGVSYR302(+4)
B12-63+3
433.6
100
50
0
Relative Abundance
200
300
400
500
600
700
800
900
m/z

Figure 4.4

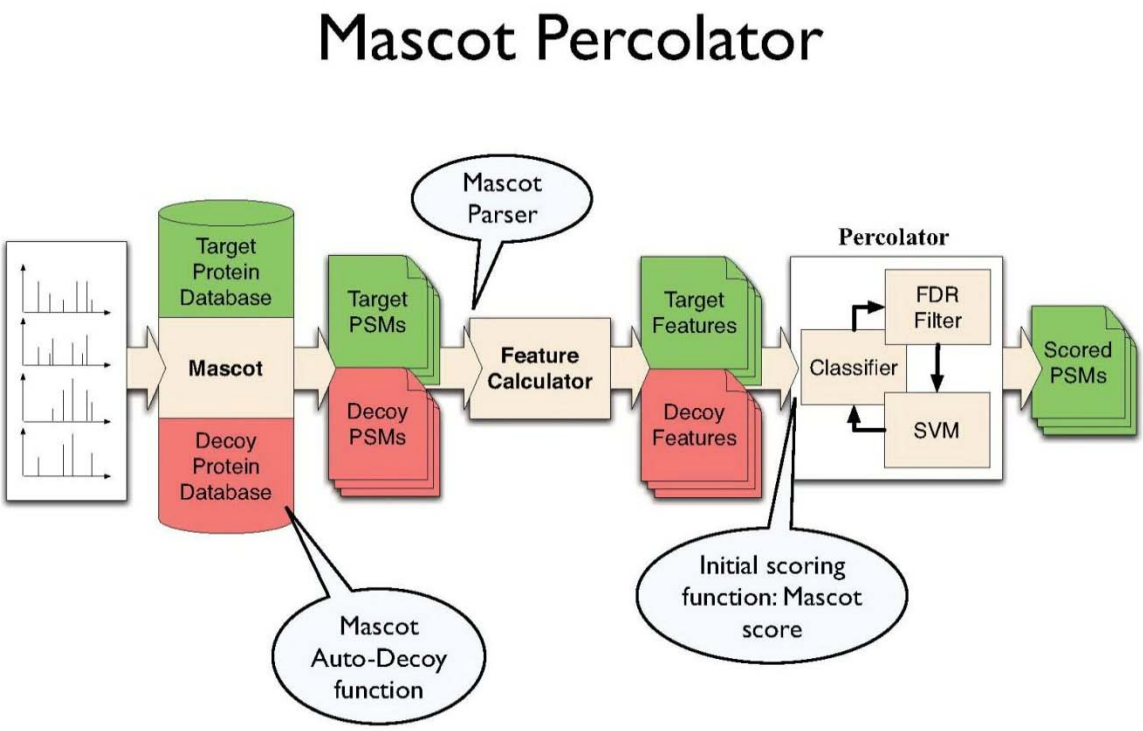

M. Brosch, L. Yu, T. Hubbard, J. Choudhary, *J Proteome Res* (2009).

Figure 4.5

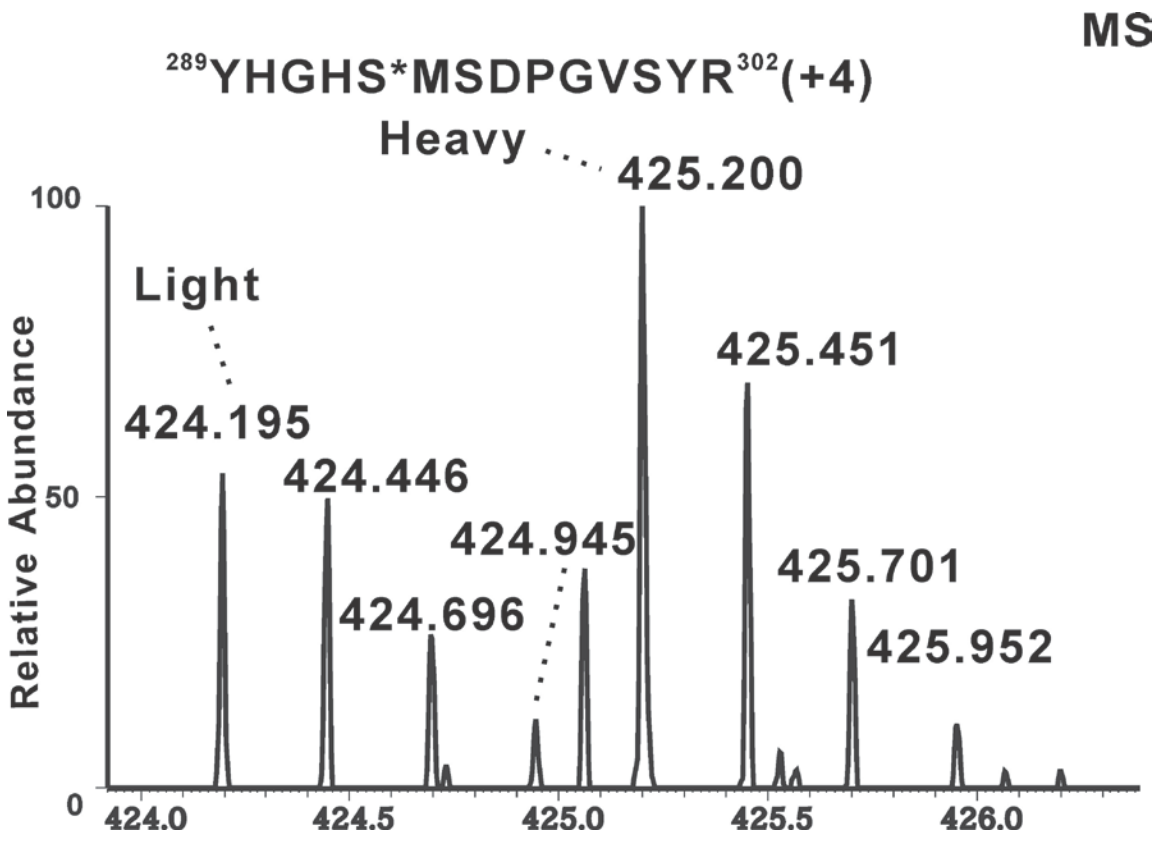
MS
289YHGHS*MSDPGVSYR302(+4)
Heavy
425.200
Light
425.451
424.195
424.446
424.945
425.701
424.696
425.952
Relative Abundance
100
50
0
424.0
424.5
425.0
425.5
426.0

Figure 4.6

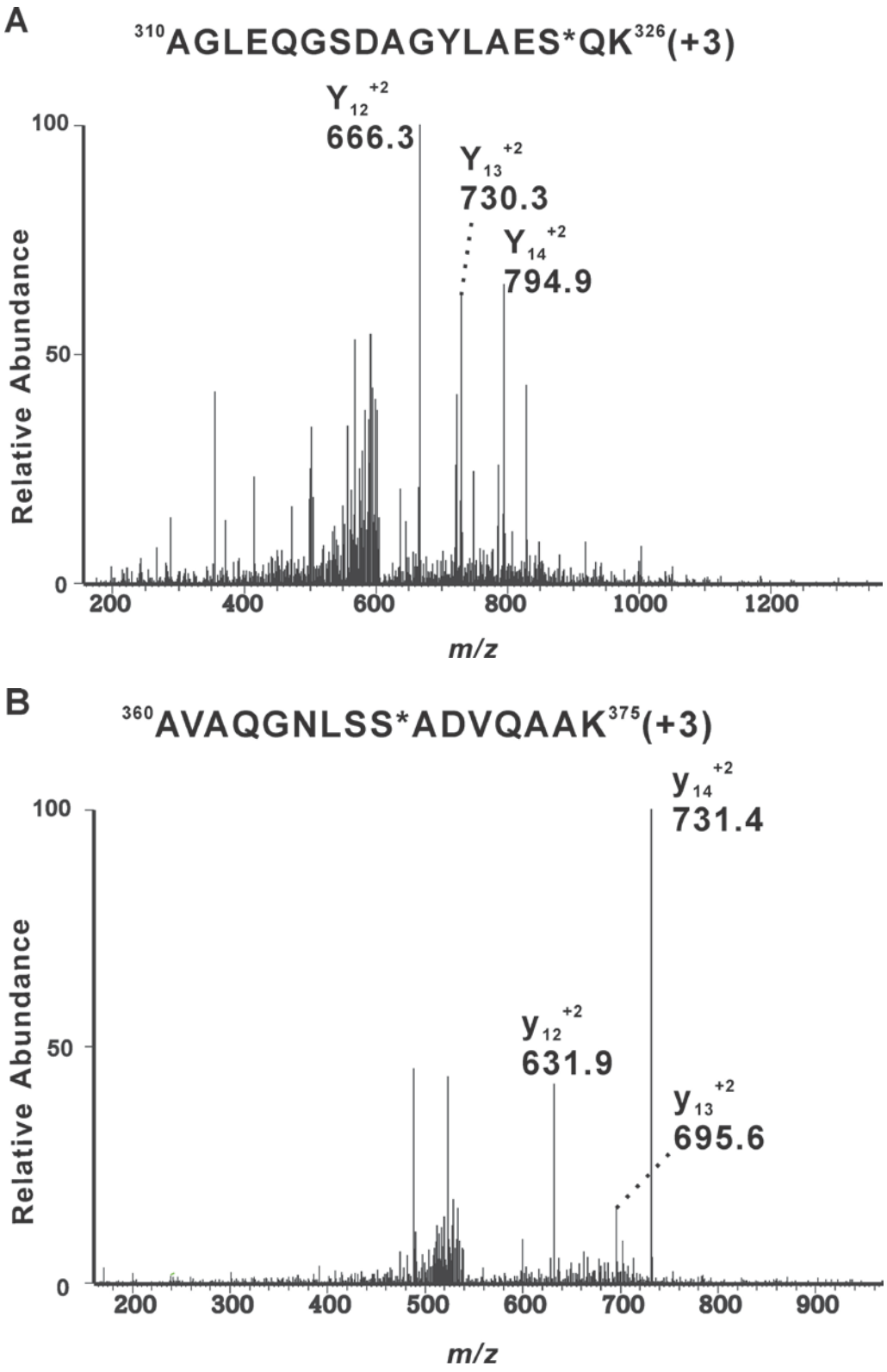
A
310AGLEQGSDAGYLAES*QK326(+3)
Y12+2
666.3
Y13+2
730.3
Y14+2
794.9
Relative Abundance
100
50
0
200
400
600
800
1000
1200
m/z
B
360AVAQGNLSS*ADVQAAK375(+3)
y14+2
731.4
y12+2
631.9
y13+2
695.6
Relative Abundance
100
50
0
200
300
400
500
600
700
800
900
m/z

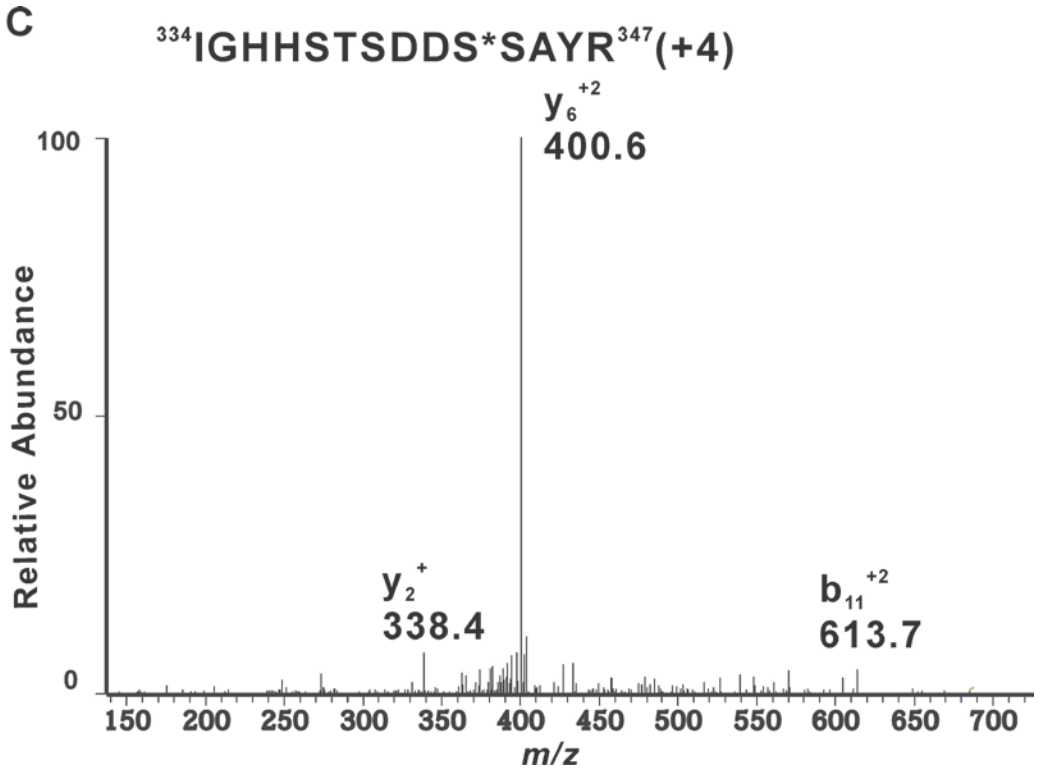
C
334IGHHSTSDDS*SAYR347(+4)
y6+2
400.6
y2+
338.4
b11+2
613.7
Relative Abundance
100
50
0
150 200 250 300 350 400 450 500 550 600 650 700
m/z

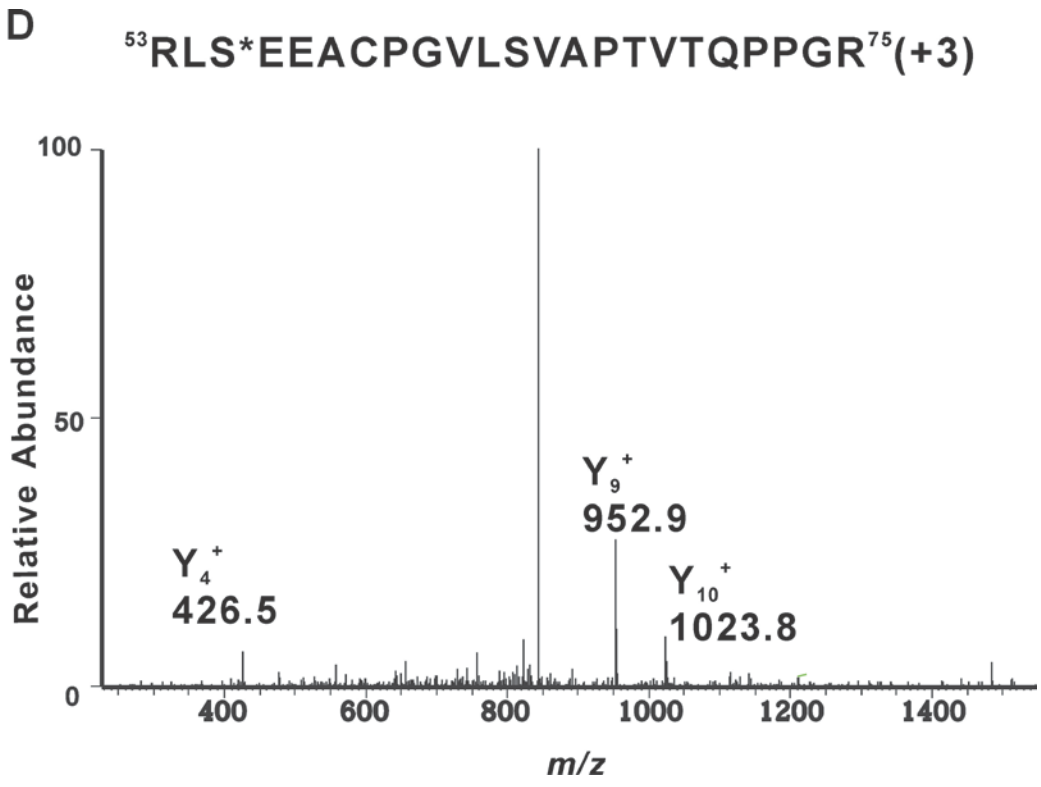
D
53RLS*EEACPGVLSVAPTVTQPPGR75(+3)
Y9+
952.9
Y4+
426.5
Y10+
1023.8
Relative Abundance
100
50
0
400 600 800 1000 1200 1400
m/z

CHAPTER 5

Conclusions and Future Directions

In this dissertation, we demonstrate a novel strategy employing alkaline β-elimination and Michael addition (BEMA) using natural abundance and stable isotope labeled thiocholine in conjunction with mass spectrometry for specific detection, identification and quantitation of phosphorylated serine/threonine containing peptides. This strategy exploits the transformation of negatively charged phosphate groups to endogenous positive charge bearing thiocholine moieties that resulted in a marked increase in ionization sensitivity during ESI accompanied by enhanced peptide sequence coverage during CID. The definitive localization of phosphorylated residues was greatly improved through the generation of diagnostic triads of fragmentation ions resulting from peptide bond cleavage and further neutral loss of either trimethylamine (-59 Da/-63 Da) or thiocholine thiolate (-119 Da/-123 Da) from the thiocholine side chain during CID in MS^2 and MS^3 experiments. The introduction of stable isotope labeled thiocholine enabled the quantitation of protein phosphorylation with high precision by ratiometric comparisons. The effectiveness of this developed technology was demonstrated in proteins isolated from both a living cell system and a perfused tissue system undergoing the pathologic alterations induced by myocardial ischemia. The endogenous

phosphorylations sites of iPLA$_2$β expressed in Sf-9 cells were identified. Comparison with convention methods demonstrated superior results in both identification phosphopeptides and localization of phosphosites. Moreover, quantitative analysis of the mitochondrial phosphoproteome following cardiac ischemia was performed resulting in the identification of 36 mitochondrial phosphopeptides with 37 new mitochondrial phosphosites.

The effectiveness of the developed BEMA strategy relies heavily on the reduction of sample complexity. In this thesis, a highly selective affinity enrichment resin, titanium dioxide (TiO_2), was utilized to eliminate the majority of the non-phosphorylated peptides before conducting the BEMA reactions. This greatly increased the specificity of the reactions and thus markedly improved reaction yields. Currently, a single reverse-phase (RP) column was used to separate the peptides before mass spectrometry. A two-dimensional (2-D) liquid chromatographic approach consisting of tandem strong cation exchange (SCX) and reversed-phase (RP) columns can be employed to greatly increase the sensitivity and the power of this approach [1-2].

Thiocholine possesses unique chemical properties that lead to the enhanced ionization and generation of a rich repertoire of signature fragment ions upon CID. This compound may also allow the affinity-purification of thiocholine containing peptides. It has been previously reported that cavitand-based host molecules formed stable host-guest complexes in water with quaternary amine containing small molecules [3]. The reversible non-covalent binding between the aromatic pocket of the cavitand and the quaternary

amine moiety of small targets is characterized by cation-pi interactions that have been well defined [4-5]. Chemical fixation of the cavitand-based host molecules on a resin can enable stationary phase extraction (SPE) of thiocholine-modified peptides for affinity enrichment. The enrichment step could be either placed offline prior to the LC-MS analysis or integrated as an additional dimension in the online HPLC separation.

As discussed in previous chapters, although the signature neutral loss of trimethylamine and thiocholine thiolate were incorporated in the MASCOT search engine, ions generated from neutral loss were not accounted for additional increase of probability/confidence levels for identification of the peptides in this study. The developed method is well-suited to be used with a weighted scoring algorithm that takes into account the intrinsic chemical properties of thiocholine-containing peptides that will likely enhance identification of phosphorylated peptides and phosphosites. Also the anticipated development of bioinformatics resulting from this approach will increase the utility of the current strategy. For example, a target MS^3 template can be added to the current options for the specific fragmentation of theoretical b and y ions instead of fragmenting ions based solely on their relative intensity in product-ion spectra. An automated quantitation program proceeding the validation of the peptide identification also would greatly improve the efficiency of the current strategy.

References

(1) Link, A. J.; Eng, J.; Schieltz, D. M.; Carmack, E.; Mize, G. J.; Morris, D. R.; Garvik, B. M.; Yates, J. R., 3rd *Nat Biotechnol* **1999**, *17*, 676-682.

(2) Washburn, M. P.; Wolters, D.; Yates, J. R., 3rd *Nat Biotechnol* **2001**, *19*, 242-247.

(3) Biros, S. M.; Ullrich, E. C.; Hof, F.; Trembleau, L.; Rebek, J., Jr. *J Am Chem Soc* **2004**, *126*, 2870-2876.

(4) Ma, J. C.; Dougherty, D. A. *Chem Rev* **1997**, *97*, 1303-1324.

(5) Monnaie, D.; Arosio, D.; Griffon, N.; Rose, T.; Rezaie, A. R.; Di Cera, E. *Biochemistry* **2000**, *39*, 5349-5354.

Appendix

A. ^{1}H NMR (D_2O) spectrum of natural abundance thiocholine

Figure A.

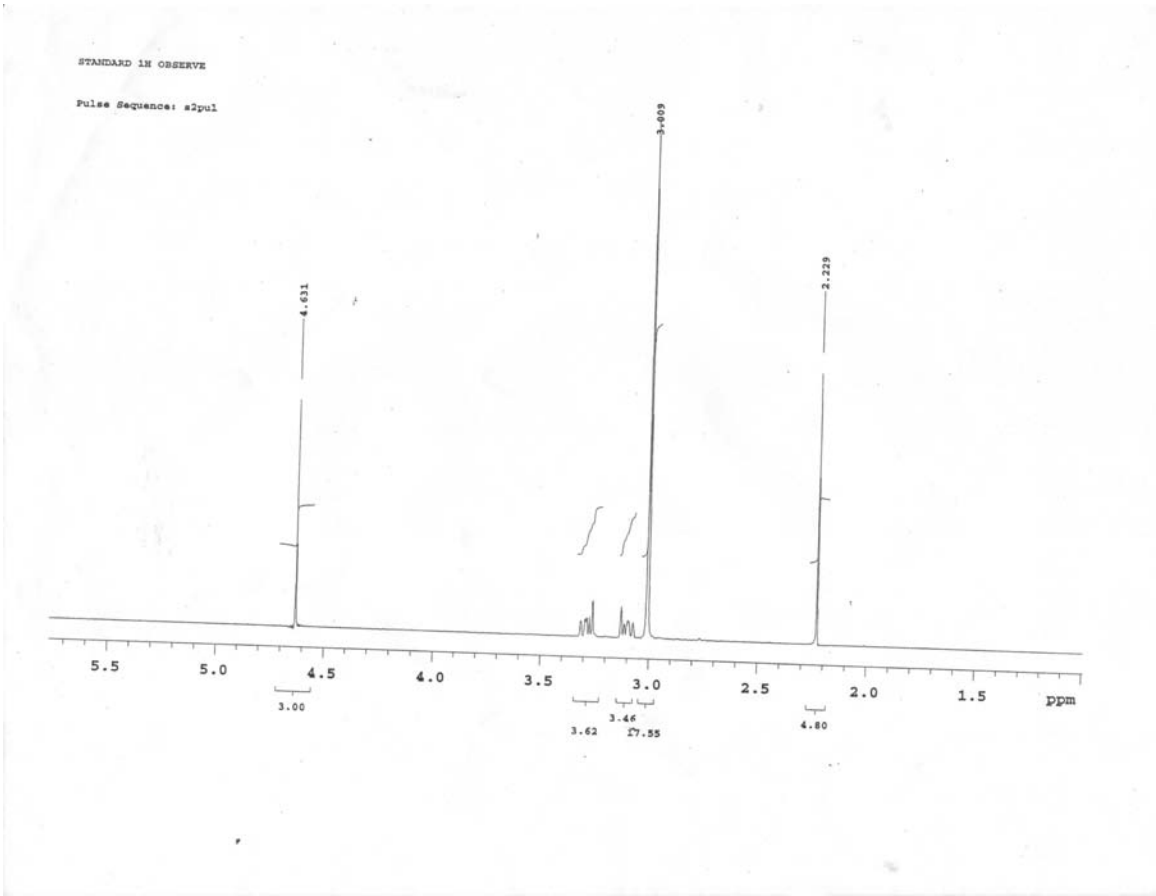

B. ^{1}H NMR (D_2O) spectrum of thiocholine-$^{13}C,d_3$

Figure B.

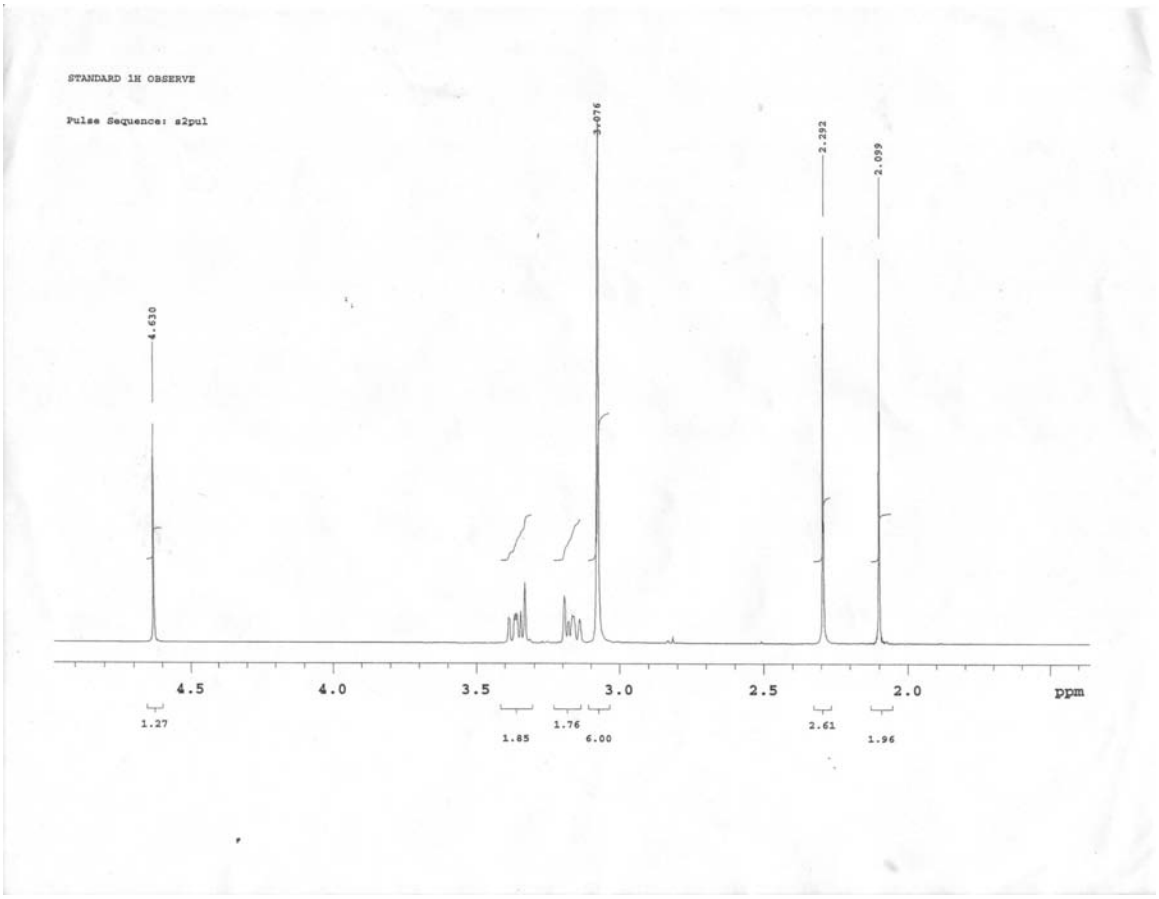

C. The scheme of the electron-donating effect of the β-methyl group of threonine affecting the reaction rates of β-elimination and Michael addition

Figure C.

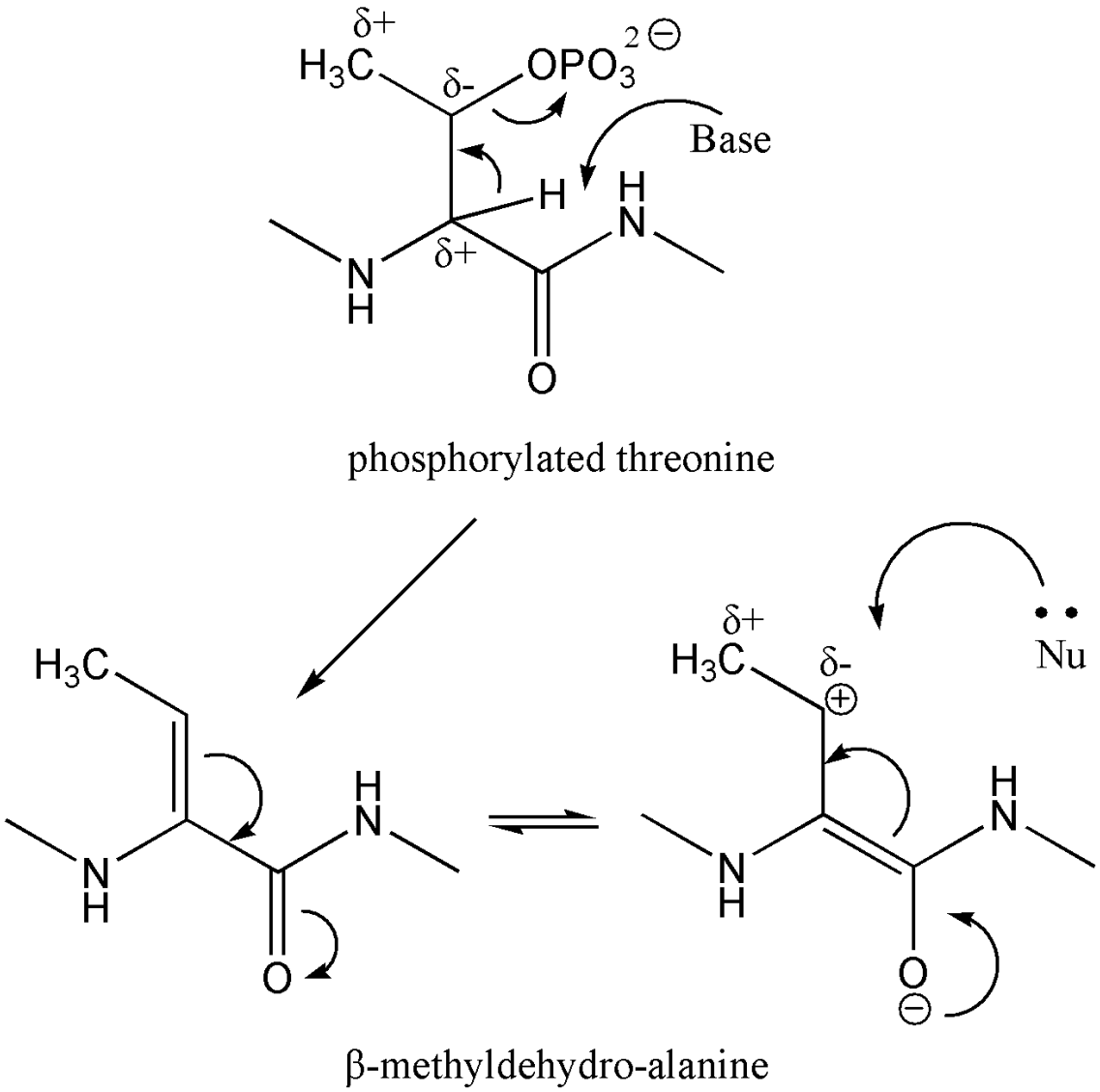

D. Nomenclature of peptide fragment ions

Figure D.